DISSERTATION

DEVELOPMENT OF LACTOBACILLUS ACIDOPHILUS AS AN ORAL VACCINE VECTOR AND EFFECTS OF RICE BRAN INGESTION ON THE MUCOSAL HEALTH OF MALIAN INFANTS

Submitted by

Allison C. Vilander

Department of Microbiology, Immunology, and Pathology

In partial fulfillment of the requirements

For the Degree of Doctor of Philosophy

Colorado State University

Fort Collins, Colorado

Summer 2020

Doctoral Committee:

Advisor: Gregg Dean

Zaid Abdo
Steven Dow
Amy MacNeill
Elizabeth Ryan

ABSTRACT

DEVELOPMENT OF LACTOBACILLUS ACIDOPHILUS AS AN ORAL VACCINE VECTOR AND EFFECTS OF RICE BRAN INGESTION ON THE MUCOSAL HEALTH OF MALIAN INFANTS

Most pathogens enter the body at the mucosa and induce innate and adaptive immune responses at these surfaces essential for protection against infection and disease. Induction of mucosal immune responses is best achieved locally but mucosal vaccines have been difficult to develop with few currently approved for use. Almost all are attenuated live vaccines which limits their use and efficacy in some populations. Strategies to enhance the mucosal immune response to vaccination and move away from attenuated live vaccines are needed. Prebiotics (nondigestible food ingredients that promotes growth of beneficial microorganisms) and probiotics (live microorganisms that are beneficial when ingested) are an active area of interest for improving mucosal health and increasing oral vaccine performance.

Here we present the development of the probiotic Gram-positive lactic acid bacteria *Lactobacillus acidophilu*s (LA) as a novel oral subunit vaccine. LA has many advantages as an oral vaccine vector including endogenous acid and bile resistance, heat tolerance, and numerous proteins that interact with the mucosal immune system. We show that LA can induce immune responses to weakly immunogenic neutralizing peptides from HIV-1 and rotavirus. To enhance the immune response, we developed the *E. coli* type I pilus protein, FimH, as a LA vaccine adjuvant. FimH increased the immune response to vaccination and increased LA trafficking by antigen presenting cells to the mesenteric lymph node, an important site of mucosal immune induction.

We also evaluate the effects of ingestion of the nutrient dense prebiotic rice bran on mucosal health in a cohort of healthy Malian infants at risk for malnutrition and the subclinical condition environmental enteric dysfunction. Rice bran ingestion was found to decrease episodes of diarrhea, decrease the age to elevated fecal microbiome α-diversity, and stabilize total fecal secretory IgA concentrations over time. These results indicate that rice bran protects from diarrhea and improves the mucosal environment.

ACKNOWLEDGMENTS

I would like to thank and recognize the people who worked on these projects and helped to support me through the many years of study and training necessary to complete my veterinary and PhD degrees. First, I would like to thank Dr. Wim Hol, Dr. Florian Hladik, and Dr. Kevin Lahmers for the opportunity to work in their labs and gain many of the skills necessary to be a successful scientist. I would like to thank all the pathologists at Colorado State University who took the time to train and prepare me for a career in pathology. Your encouragement and support of veterinary students and residents is essential to the success of the CSU veterinary program and I am excited to be a part of the team.

This dissertation would not have been possible without the support and mentorship of Dr. Gregg Dean. I thank you for giving me the opportunity to work in your lab and for your understanding of the challenges that come with navigating a dual training program. You allowed me the freedom to pursue projects of interest and understood the importance of my continued involvement in pathology and teaching. I know that these activities were essential to establishing my career at CSU and I look forward to our continued collaboration. I would like to recognize the work of current and former lab members and collaborators, specifically: Dr. Akinobu Kajikawa, Dr. Jonathan LeCureux, Alora LaVoy, Lin Zhang, Bridget Eklund, Dr. Kristopher Parker, Dr. Ousmane Koita, Dr. Ann Hess, Dr. Luis Zambrana, McKenzie Smith, Max Drummond, and Kimberly Shelton. I would also like to thank my committee members Dr. Zaid Abdo, Dr. Amy MacNeill, Dr. Steven Dow, and Dr. Elizabeth Ryan for their time and guidance. I would especially like to recognize Dr. Ryan for inviting me to be involved with the rice bran project and Dr. Abdo for his work on the rice bran microbiome analysis.

I would like to extend my gratitude and love to my parents who were the first to foster my interest in science and medicine, my wonderful and intelligent sisters, my entire extended family, and friends. Special thanks to my pathology resident-mates who have been essential in maintaining the mental and emotional stamina required to complete both pathology and PhD training. Finally, I would like to recognize my husband, Matt Vilander, for his endless love, support, and commitment.

TABLE OF CONTENTS

LIST OF TABLES

LIST OF FIGURES

CHAPTER 1: ADJUVANT STRATEGIES FOR LACTIC ACID BACTERIAL MUCOSAL VACCINES

1.1: Overview

Lactic acid bacteria (LAB) are Gram-positive, acid-tolerant bacteria that have long been used in food fermentation and are generally recognized as safe (GRAS). LAB are a part of a normal microbiome and act as probiotics, improving the gastrointestinal microbiome and health when consumed. An increasing body of research has shown the importance of the microbiome on both mucosal immune heath and immune response to pathogens and oral vaccines. Currently, there are few approved mucosal vaccines, and most are attenuated viruses or bacteria, which necessitates cold chain, carries the risk of reversion to virulence, and can have limited efficacy in individuals with poor mucosal health. On account of these limitations, new types of mucosal vaccine vectors are necessary. There has been increasing interest and success in developing recombinant LAB as next generation mucosal vaccine vectors due to their natural acid and bile resistance, stability at room temperature, endogenous activation of innate and adaptive immune responses, and the development of molecular techniques that allow for manipulation of their genomes. To enhance the immunogenicity of these LAB vaccines, numerous adjuvant strategies have been successfully employed. Here, we review these adjuvant strategies and their mechanisms of action which include: Toll-like receptor ligands, secretion of bacterial toxins, secretion of cytokines, direct delivery to antigen presenting cells, and enterocyte targeting. The ability to increase the immune response to LAB vaccines gives them the potential to be powerful mucosal vaccine vectors against mucosal pathogens.

1.2: Introduction

Lactic acid bacteria (LAB) are Gram-positive acid-tolerant bacteria that have long been used in food fermentation and are generally recognized as safe (GRAS). Additionally, they have been identified as probiotics, live organisms that improve health when consumed (1). LAB are a diverse group of bacteria that includes the genera *Lactobacillus* spp., *Lactococcus* spp., and *Streptococcus* spp. The effects of LAB on

mucosal health are diverse and have been most heavily studied in the gastrointestinal (GI) tract. General effects of LAB in the intestinal tract are known to include alteration of the intestinal microbiome composition, improved barrier function, niche competition with pathogens, and, germane to this review, modulation of the host immune system (2, 3).

Most pathogens enter the body at mucosal sites and protection of these barrier tissues is mediated by innate and adaptive immune responses. Mucus, peristalsis, gastric acid, bile, and antimicrobial peptides are examples of innate mucosal immune defense strategies while antigen-specific antibodies and cell-mediated responses are the workhorses of the adaptive response. Induction of both innate and adaptive mucosal immune responses is best achieved by direct immunization at the mucosa rather than through systemic routes (parenteral injection) (4, 5). Mucosal vaccines can also induce serum antibody and systemic cell-mediated responses. Mucosal delivery is an especially attractive mechanism of vaccination due to the ease of administration and the common-mucosal immune system, which allows for induction of immune responses at one mucosal surface followed by trafficking of immune cells to other distant mucosal sites (4).

Despite the inherent benefits of mucosal vaccines, there are few available for use worldwide. Of the currently licensed human mucosal delivered vaccines, all are live attenuated or inactivated viruses or bacteria. While these vaccines are effective at stimulating a strong mucosal immune response, the use of attenuated vaccines carries the risk of reversion to virulence and they cannot be used in immunologically sensitive populations (6). In addition, these mucosal vaccines can have varying efficacy depending on an individual's health, nutritional status, and microbiome (7, 8). Co-delivery of LAB with oral vaccines has shown the ability to increase the immune response in the face of low nutritional status or dysbiosis. For example, increased immune responses have been seen when probiotics are administered with oral rotavirus, polio, *Salmonella typhi*, and cholera vaccines (9).

Due to the limitations of the currently available mucosal vaccines and the benefits of probiotics on immune response to vaccination, development of LAB as mucosal vaccine vectors is attractive. LAB have several attributes as orally delivered mucosal vaccines including: Acid and bile resistance, stability at room temperature, endogenous activation of innate and adaptive immune responses, and the availability of

molecular techniques for genomic modification (10). Since the 1990s, the use of LAB as an oral vaccine platform has been explored against numerous viral and bacterial pathogens and toxins (11, 12). These vaccines have been shown to induce serum IgG and mucosal secretory (sIgA) as well as stimulate T cell responses. In addition to developing LAB for the delivery of antigens, numerous adjuvant strategies have been explored to enhance immune responses.

Adjuvants are used in conjunction with vaccines to increase the humoral and/or cellular response to a delivered antigen. Pairing the correct antigen and adjuvant can induce faster, more robust, and longer-lived (durable) immune responses, and may decrease the amount of antigen needed to induce protection (13). Adjuvants such as Alum, MF59, AS03, AF03, virosomes, and heat labile enterotoxin (LT) have long been used with systemic vaccines but adjuvant use has been more limited with mucosal vaccines. Only the intranasal influenza vaccine, Nasalflu, has been licensed for use with a mucosal adjuvant, *Escherichia coli* heat-labile toxin (LT), but it has since been removed from the market (14).

To realize the potential of LAB as mucosal vaccine vectors, an understanding of how to enhance the immunogenicity of these vaccines while preserving the inherent safety will be required. It is likely that despite the endogenous immune activating properties of LAB, one or multiple adjuvant strategies may be necessary to induce robust and long lasting protective immune responses. This may be especially true if the vaccine is expressing poorly immunogenic antigens or is used in sensitive populations such as individuals who are immune suppressed, nutrient compromised, have an altered microbiome, or have an increased mucosal disease burden. Here, we review the current strategies being investigated to adjuvant the immune response to mucosal delivered LAB vaccine vectors. As these studies are reviewed, it is important to recognize that the adjuvant effect on the immune response may be altered by the mucosal route of administration (intranasal, oral, or intravaginal), genus and species of LAB used as the delivery vehicle, the antigen per se, and the mechanism of antigen display (secreted, surface-display, or intracellular). Careful study and selection of each of these variables will likely be necessary to develop optimized LAB mucosal vaccines.

1.3: Lactic Acid Bacteria Mechanisms of Immune Interaction and Activation

To understand the effect that adjuvant strategies have on the immune response to a LAB mucosal vaccine, it is important to review the endogenous immune activating mechanisms possessed by LAB. A brief summary of typical LAB interactions with the mucosal immune system are depicted in Figure 1.1A.

Of note are the characteristics that make LAB especially attractive for use as a mucosal vaccine vector. LAB can stimulate innate immune response through the Gram-positive cell wall peptidoglycan and lipotechoic acid that activate the pattern-recognition receptors: Toll-like receptor (TLR) 2, nucleotide-binding oligomerization domain (NOD)-like receptor (NLR) family, and C-type lectin receptors (15-18). Various species of LAB can also activate TLR3, TLR6, TLR9, and stimulate interferon responses (19-21). Additionally, some LAB species can bind to intestinal mucus and the mucosal epithelium and/or microfold (M) cells resulting in mucosal colonization and increased uptake and transport into mucosal immune induction sites such as Peyer's patches in the small intestine or tonsillar crypts. LAB can interact with antigen-presenting cells (APCs) such as dendritic cells (DC) and induce sIgA and IgG. The mechanism of DC activation and the resulting immune responses are highly dependent on the LAB strain. For example, it has been shown that murine DCs can have different responses depending on the strain of LAB and this is further complicated by the fact that these responses can be different even between DC subtypes (22, 23). This illustrates the complexity in selecting an appropriate LAB strain as a candidate vaccine vector.

(A)

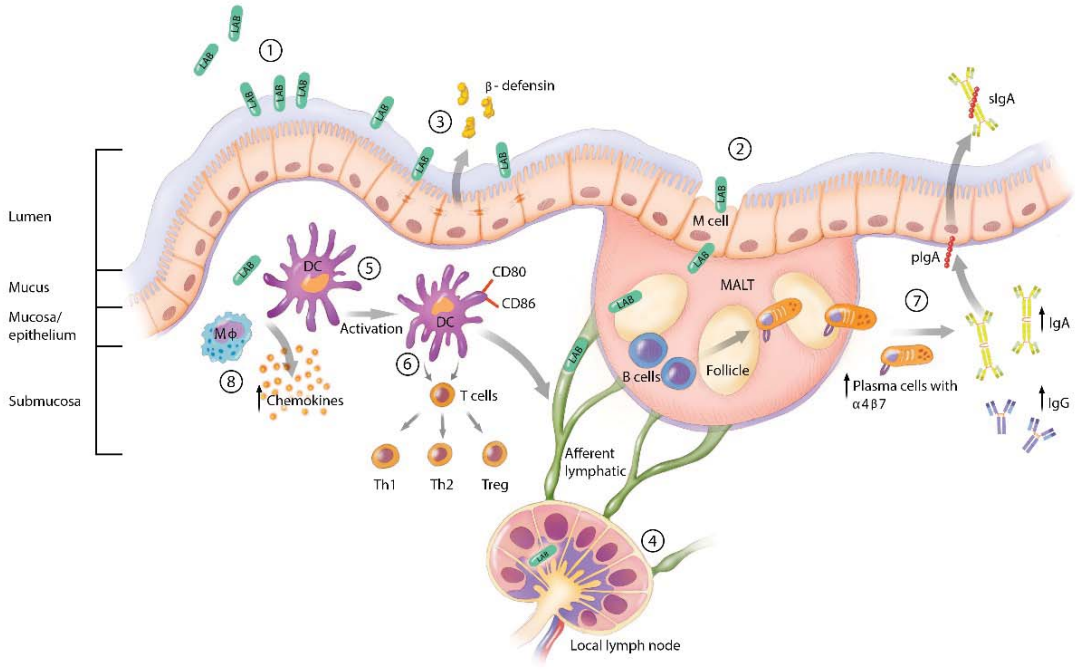
Lumen
Mucus
Mucosa/
epithelium
Submucosa
LAB
β - defensin
sIgA
M cell
DC
Activation
CD80
CD86
MALT
pIgA
Mϕ
Chemokines
T cells
B cells
Follicle
Plasma cells with
α4β7
IgA
IgG
Th1
Th2
Treg
Afferent
lymphatic
Local lymph node

(B)

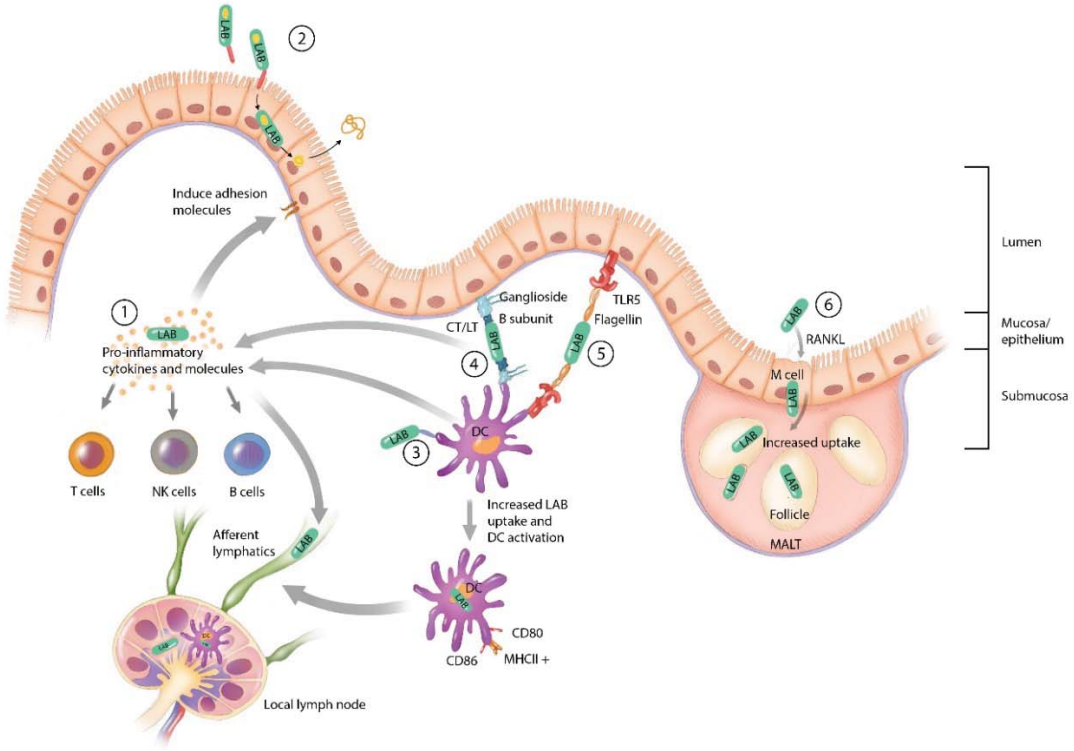
LAB
Induce adhesion
molecules
Pro-inflammatory
cytokines and molecules
Ganglioside
CT/LT
B subunit
TLR5
Flagellin
RANKL
M cell
Increased uptake
Follicle
MALT
Lumen
Mucosa/
epithelium
Submucosa
T cells
NK cells
B cells
DC
Increased LAB
uptake and
DC activation
Afferent
lymphatics
CD80
CD86
MHCII +
Local lymph node

(C)

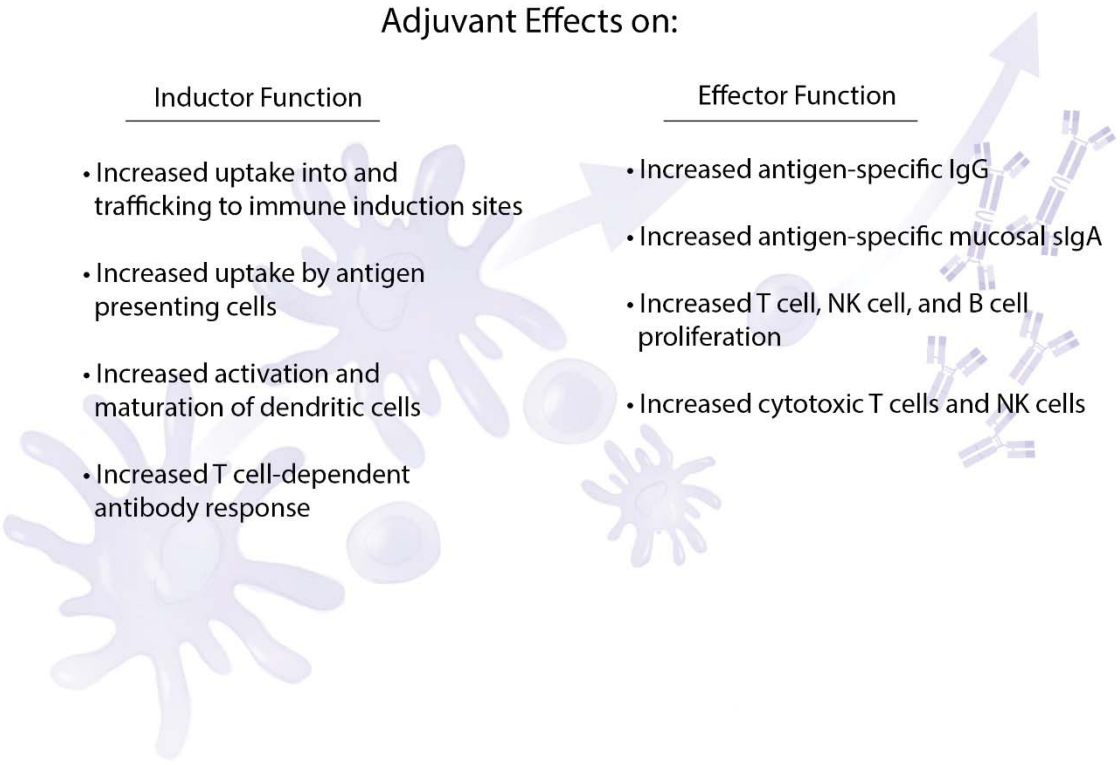

Figure 1.1. Lactic acid bacteria (LAB) interactions with the mucosa and mucosal immune system. (**A**) Endogenous LAB mucosal interactions. LAB possess the ability to bind to mucus (**1**), epithelial cells, and microfold (M) cells (**2**) allowing for uptake into mucosal associated lymphoid tissue (MALT) and trafficking to local lymph nodes (**4**) (24-26). The interactions of LAB with the epithelium can induce epithelial defenses such as the secretion of β-defensin (**3**) (27, 28). LAB can activate macrophages (**8**) and dendritic cells (DCs) (**5**), which can traffic phagocytosed LAB to local immune induction sites (**4**) (29-32). LAB also induce effector immune responses such as polarization of naïve T cells to Th1, Th2, and Treg cells (**6**) and humoral responses such as B cell proliferation, class switching to IgG and IgA, induction of long-lived plasma cells, and induction of the mucosal homing integrin α4β7 (**7**) (33, 34). (**B**) LAB mucosal adjuvant strategies. (**1**) LAB secretion of pro-inflammatory cytokines such as IL-12, IL-1β, and IL-2 activates T cells, NK cells, and B cells, induces epithelial cell adhesion molecule expression, and promotes trafficking of LAB to local lymph nodes. (**2**) LAB surface expression of the epithelial cell adhesion molecules InlA and/or FnBPA promotes binding and uptake of LAB by epithelial cells, delivery of eukaryotic expression plasmid, and secretion of protein. (**3**) LAB surface expression of DC-binding peptides results in targeting, increased uptake, and activation of DCs as well as trafficking to local immune induction sites. (**4**) Surface expression of LT or CT B subunit results in LAB binding to gangliosides on the surface of epithelial cells and DCs. Co-delivery of full toxins or CT/LT A subunit results in a pro-inflammatory response. (**5**) Surface-expressed flagellin, a TLR5 ligand, induces cytokine production by epithelial cells and direct activation of DCs. (**6**) LAB secretion of RANKL results in increased M cells and

uptake of LAB into MALT. (**C**) Review of the effects of adjuvants on the immune response to LAB mucosal vaccination. LAB: Lactic acid bacteria; DC: Dendritic cell; Mϕ: Macrophage; MALT: Mucosal-associated lymphoid tissue; pIgA: Polymeric immunoglobulin receptor; sIgA: Secretory IgA; NK cells: Natural killer cells; M cells: Microfold cells; TLR: Toll-like receptor; RANKL: Receptor activator of nuclear factor kappa-B ligand; InlA: *Listeria monocytogenes* internalin A; FnBPA: Fibronectin-binding protein A; CT: Cholera toxin; LT: *E. coli* heat-labile toxin

1.4: Mucosal Vaccine Adjuvant Strategies

Robust immune responses to mucosal vaccines have been difficult to achieve. In general, mucosal-delivered vaccines stimulate lower responses compared to systemic vaccines. To overcome this attenuated response, multiple mucosal adjuvants have been identified. Adjuvants of interest include: LAB expression of proteins that stimulate innate immune responses such as pathogen-associated molecular patterns (PAMPs), TLRs, NLRs, retinoic acid-inducible gene-like receptors (RLRs), and C-type lectins, targeting of professional APCs, immune modulating molecules (chemokines, cytokines), and bacterial toxins (35, 36). Molecular tools have been developed to allow for genetic manipulation of LAB making it possible to express adjuvants in multiple ways such as cell-surface display, secretion, and cytoplasmic (37). The method of display should be carefully considered depending on the adjuvant, its mechanism of action, and the mode of LAB delivery. For instance, an adjuvant could be co-administered with a LAB vaccine that is delivered intranasally or intravaginally while an orally delivered LAB vaccine would encounter the harsh environment of the stomach, making co-administration inappropriate.

The majority of studies reviewed here used LAB to co-express antigen and adjuvant as opposed to co-administration of a separately produced adjuvant. This method of antigen/adjuvant LAB delivery is not only convenient but is also superior for oral delivery. LAB co-expression of antigen and adjuvant promotes survival of the adjuvant through the stomach and duodenum, enhances interaction with the mucosal surface including delivery to APCs and mucosal immune induction sites, and through colonization of the GI tract, prolonged delivery of the immune stimulating compound. Additionally, through their endogenous immune activation (Figure 1.1C), LAB can act in concert with the adjuvant to enhance immune responses.

The adjuvant strategies that have been employed with LAB vaccine vectors act through diverse mechanisms (Figure 1.1B) and evaluation of the adjuvant must be reviewed in the context of the route of delivery, specific LAB vector, and the expression strategy. These factors and the antigen and adjuvant employed, alterations in immune response, and protection against challenge are summarized in Section 1.5, Tables 1.1–1.5, and Figure 1.1B, C.

1.5: Lactic Acid Bacteria Adjuvant Strategies

1.5.1: Cytokine Secretion

Cytokines act to stimulate and attract immune cells. The selection of a cytokine for use as an adjuvant can be based on the desired immune response to vaccination and its known influence on immune cells. Three cytokines: IL-12, IL-1β, and IL-2 have been investigated for use as adjuvants with LAB vaccines. They have all been utilized as secreted molecules with the exception of one study by Li et al. where IL-12 was delivered as cDNA (38). Cytokine expression strategies, as described below, have generally been successful and there are certainly other cytokines that could be explored. The challenge may be how to express the cytokine adjuvant in such a way that it does not add function to the bacterial vector and does not depend on antibiotic resistance to maintain expression from a plasmid. Cytokine expression could prove to be a challenge in the regulatory approval process.

1.5.1.1: IL-12

The major sources of IL-12 are monocytes, macrophages, DCs, and neutrophils. The actions of this cytokine are to induce T cell and natural killer (NK) cell proliferation, increase IFN-γ, polarize $CD4^+$ T cells to a Th1 phenotypes, and increase cytotoxicity (39). LAB vaccines supplied with IL-12 have been used against viral induced neoplasia (human papilloma virus) and the intracellular pathogens *Leishmania major* and *Mycobacterium tuberculosis*. Immune responses were greater for the LAB administered with an IL-12 adjuvant as measured by IgG and sIgA (from bronchoalveolar lavage and intestinal wash).

Additionally, there was elevated IFN-γ and IL-2 (to a lesser extent). IFN-γ polarizes T cells to a Th1 phenotype, important in responding to these intracellular pathogens, and IL-2 is important for T cell proliferation. This Th1 polarization is observed in other adjuvant studies reviewed here.

1.5.1.2: IL-1β

IL-1β is secreted by monocytes and macrophages in response to TLR stimulation. It is secreted in an inactive form and cleaved by activated caspase-1 following assembly of the inflammasome (40). Intracellular activation without secretion of IL-1β can also occur (41, 42). IL-1β is a pro-inflammatory cytokine and has been shown to act as a mucosal adjuvant (43). It is important in T cell-mediated adaptive immune responses, induces adhesion molecules on mesenchymal and endothelial cells, and is an inducer of the B cell proliferation cytokine IL-6 (44, 45). The role of IL-1β on T cell-mediated antibody responses is important as T-dependent B cell responses often generate higher-affinity antibodies and increased memory. Secretion of IL-1β has been studied with both *L. casei* and *L. acidophilus*. In both, IL-1β increased IgG and mucosal sIgA when co-expressed with an antigen or delivered with an attenuated antigen (*Salmonella enterica*) (46, 47). Activated T cells and DCs resulted in increases in the inflammatory cytokines TNF-α, TNF-β, IL-6, and IL-4. The use of IL-1β as an adjuvant may have disadvantages as its pro-inflammatory effects may result in unintended consequences, although none were reported in the studies reviewed here.

1.5.1.3: IL-2

IL-2 has been used as an adjuvant with *L. lactis* and *L. rhamnosus* GG. IL-2 plays a role in induction of immune responses, specifically proliferation and differentiation of $CD4^+$ and $CD8^+$ T cells, T regulatory (Treg) cells, and NK cells (48). IL-2 also induces proliferation of intestinal epithelial cells at low concentrations while at high concentrations it can induce epithelial apoptosis. Secreted IL-2 resulted in increased IgG and sIgA and increased trafficking of LAB to mesenteric lymph nodes, an important site for sIgA induction (49, 50). While increased immune responses were observed using IL-2 as an adjuvant,

altered levels of IL-2 have been found in inflammatory bowel disease patients and the complex interaction IL-2 has between inducing tolerance versus inflammation may be problematic for its use as a mucosal adjuvant (51-53).

Table 1.1. Cytokine adjuvant strategies for lactic acid bacteria.

Adjuvant	LAB	Expression	Antigen	Immune Response	Delivery	Species	Study
			IL-12				
IL-12	*L. lactis*	Secreted	Human Papilloma Virus (E7)	Increased BAL IgG and sIgA Increased IFN-γ $CD4^+$ and 8^+ T cells	Intranasal	Murine C57BL/6	Bermudez-Humaran et al. 2005 (31)
IL-12	*L. lactis* *L. plantarum*	Secreted	Human Papilloma Virus (E7)	*L. lactis*, Intranasal Delivery Increased Serum and GAL IgG; Increased GAL IgA Increased IFN-γ *L. plantarum*, Intranasal Delivery Increased IFN-γ Decreased Tumor Burden	Intranasal Oral	Murine C57BL/6	Cortes-Perez et al. 2007 (54)
IL-12	*L. lactis*	Secreted	*Leishmania major* *Leishmania* (Homologue of Activated C Kinase)	Subcutaneous Increased IgG1 and IgG2a Increased IFN-γ Decreased Parasite Load Oral Decreased Parasite Load Increased Intestinal sIgA Increased IFN-γ, IL-2	Subcutaneous Oral	Murine BALB/c	Hugentobler et al. 2012 (55) Hugentobler et al. 2012 (56)
IL-12	*L. lactis*	Cytoplasmic (DNA)	Human Papilloma Virus (E7)	Increased IFN-γ Decreased Tumor Volume	Intranasal	Murine C57BL/6	Li et al. 2014 (38)

IL-12	*L. lactis* *L. plantarum*	Secreted (by *L. lactis* with *L. plantarum* Expressing the Antigen)	*Mycobacterium tuberculosis* (Subunit Epitopes: Ag85B, CFP-10, ESAT-6, Rv0475, Rv2031c)	Increased IgG Increased IFN-γ, IL-2	Oral	Murine BALB/c	Mustafa et al. 2018 (57)
IL-1β							
IL-1β	*L. casei*	Secreted	*Salmonella enterica* (SE)	Increased IL-6, TNF-α, TGF-β Increased IgG and Intestinal sIgA when Co-Delivered with SE	Oral	Murine C3H/HeJ	Kajikawa et al. 2010 (46)
IL-1β	*L. acidophilus*	Secreted	HIV-1 (Membrane Subunit Epitope)	Increased IgG, Intestinal and Vaginal sIgA Increased Intestinal and Vaginal Epitope-Specific IgA B cells Increased IL-4	Oral	Murine BALB/c	Kajikawa et al. 2015 (47)
IL-2							
IL-2	*L. rhamnosus* GG	Secreted	Green Florescent Protein (GFP)	Increased Trafficking to MLN and Spleen. Increased MLN T Cells, IgA B Cells, DCs Increased GFP-Specific IgG and Fecal sIgA Increased IFN-γ, IFN-α, IL-12	Oral	Murine C57BL/6 and BALB/c	Kandasamy et al. 2011 (49)
IL-2	*L. lactis*	Secreted	Avian Influenza (Haemagglutinin 5)	Increased IgG and Serum IgA	Oral	Murine BALB/c	Szatraj et al. 2014 (58)

BAL: Bronchoalveolar lavage; GAL: Gastrointestinal lavage; MLN: Mesenteric lymph node.

1.5.2: Dendritic Cell (DC) Targeting Adjuvants

DCs are professional APCs critical for induction of adaptive immune responses and as such are enticing targets to enhance LAB immunogenicity. In the mucosa, DCs play a central role in inducing T and

B cells and maintaining the balance of inflammation and tolerance. DCs take up antigens at mucosal surfaces in multiple ways. In the GI tract, DCs sample antigens through M cells or goblet cells, luminal sampling, binding to the neonatal Fc receptor, and apoptotic enterocytes (59). The immune response generated by DCs depends on the method of antigen up-take and pro-inflammatory signals and can result in IgA class switching of B cells, increased sIgA, Th1 and cytotoxic lymphocyte induction, and induction of the mucosal homing integrin α4β7. Due to their importance in inducing mucosal immune responses, adjuvants that target DCs are attractive for use in mucosal delivered vaccines.

The most common method of targeting DCs with LAB is the surface expression of a DC-peptide attached to an antigen. 12-mer peptides were discovered through screening of a peptide phage display library for binding to the DC cell surface (60). The peptides do not change the function of the DCs but target bound antigens for DCs resulting in the priming of T cells. This has been an active area of investigation with 10 publications evaluating peptide adjuvant qualities. In all these studies, the vaccines were delivered orally with the exception of one intranasal vaccine against avian influenza in chickens (61). Delivery of LAB expressing antigen fused to a DC-peptide resulted in increased DC activation as determined by expression of MHCII, CD80, CD40, and CD86, increased serum IgG and mucosal sIgA, an increased Th1 T cell response, and protection from disease following challenge. DC-peptides seem to induce strong cell-mediated responses in addition to a robust antibody response. One study did report on possible tolerance induction with an increase in the Treg-associated cytokine TGF-β following vaccination and challenge with porcine epidemic diarrhea virus (62). While TGF-β can be associated with Tregs, it can act in concert with IL-6 to induce Th17 cells. Thus, the significance of this finding is unknown, and more studies would be necessary to understand the mechanisms involved in this case.

Additional strategies have been reported for targeting of LAB mucosal vaccines to DCs, including surface expression of complement C3d3, anti-CD205, and the neonatal Fc receptor (FcRn) (63-65). Of these three methods, only anti-CD205 acts solely by binding to DC cells. C3d3 can also target B cells and FcRn can bind to mucosal epithelial cells and other immune cells (66). These approaches showed similar immune stimulating effects as compared to the DC-peptide adjuvant. Additionally, anti-CD205 was shown to be an

effective adjuvant for delivery of a DNA plasmid to DCs and C3d3 acted to increase antibody responses and T and B cell proliferation to an intravaginal contraceptive vaccine. Taken together, DC targeting of LAB is a promising strategy that may also allow tuning of the immune outcome.

Table 1.2. Dendritic cell (DC) adjuvant strategies for lactic acid bacteria.

Adjuvant	LAB	Expression	Antigen	Immune Response	Delivery	Species	Study
DC-peptide							
DC-pep	*L. acidophilus*	Surface-Display	*Bacillus anthracis* (Protective Antigen)	Increased IL-12, IL-10, TNFα, MCP-1 Increased Survival to Challenge	Oral	Murine A/J	Mohamadzadeh et al. 2009 (67)
DC-pep	*L. gasseri*	Surface-Display	*Bacillus anthracis* (Protective Antigen)	Increased IgG Increased IL6, MCP-1, IFN-γ, IL-12 Increased Survival to Challenge Increased T Cell Stimulation Following Challenge	Oral	Murine A/J	Mohamadzadeh et al. 2010 (68)
DC-pep	*L. plantarum*	Surface-Display	Newcastle Disease Virus (Hemagglutinin-Neuraminidase)	Increased Intestinal sIgA Increased Splenic and Peripheral Blood $CD4^+$ T Cells Increased Survival to Challenge	Oral	Chicken	Jiang et al. 2015 (69)
DC-pep	*L. plantarum*	Surface-Display	Avian Influenza (Hemagglutinin)	Murine Increased MLN and PP DC Activation ($CD80^+$, $CD86^+$) Increased IFN-γ Increased Survival to Challenge with Decreased Lung Viral Titer Chicken Increased $CD3^+$ T Cell Proliferation and Increased $CD3^+CD4^+/8^+$ PBMC Percentages Increased IFN-γ Increased BAL sIgA and Serum IgG Decreased Lung Viral Titer	Oral	Murine BALB/c Chicken	Shi et al. 2016 (70)
DC-pep	*L. plantarum*	Surface-Display	Avian influenza (Nucleoprotein and Matrix Protein)	Increased PP and LP DC Activation ($CD80^+$, $CD86^+$, $CD40^+$, $MHCII^+$) Increased PP IgA^+ B Cells Increased Fecal and BAL sIgA Titer Increased IFN-γ, TNF-α Increased T Cell Proliferation	Oral	Murine BALB/c, C57BL/6	Yang et al. 2016 (71)

				Increased Survival Rate to Challenge and Decreased Lesions and Virus in Lung			
DC-pep	*L. casei*	Surface-Display	Porcine Epidemic Diarrhea Virus (Core Neutralizing Epitope)	Increased MLN and PP DC Activation ($CD80^+$, $CD86^+$, $MHCII^+$) Increased IgG, Viral Neutralization, and Genital Tract and Intestinal Mucus sIgA Titer Increased Lymphocyte Proliferation Increased IFN-γ, IL-4	Oral	Murine BALB/c	Wang et al. 2017 (72)
DC-pep	*L. plantarum*	Surface-Display	Enterotoxigenic *E. coli* (ETEC) (FaeG of K88 Fimbriae)	Increased Adhesion to Porcine Intestinal Cells and Decreased Attachment of ETEC (In Vitro) Increased IgG and Intestinal sIgA Increased Splenic and MLN B Cells and DCs Increased TNF-α, IL-12, IL-4 Decreased Intestinal Lesions and Weight Loss Following Challenge	Oral	Murine BALB/c	Yang et al. 2017 (73)
DC-pep	*L. plantarum*	Surface-Display	Avian Influenza (Nucleoprotein and Matrix Protein)	Oral Increased Splenic $CD4^+$ and $CD8^+$ T Cells and T Cell Proliferation Increased IgG and BAL sIgA Decreased Disease and Lung Virus Intranasal Increased Splenic $CD8^+$ T Cells and T Cell Proliferation Increased BAL sIgA Decreased Disease and Lung Virus	Oral Intranasal	Chicken	Yang et al. 2017 (61)
DC-pep	*L. plantarum*	Surface-Display	*Eimeria tenella* (SO7)	Increased IgG and Intestinal sIgA Decreased Oocyst Shedding and Cecum Lesion Scores Following Challenge	Oral	Chicken	Yang et al. 2017 (74)
DC-pep	*L. acidophilus*	Surface-Display	*Clostridium botulinum* (Botulinum Toxin Serotype A)	Approximately 70% Protection to Challenge (Protection B cell-Mediated)	Oral	Murine BALB/c	Sahay et al. 2018 (75)
DC-pep	*L. casei*	Surface-Display	Porcine Epidemic	Increased IgG and Intestinal sIgA	Oral	Porcine	

			Diarrhea Virus (Collagenase-Digested Fragment of S Protein)	Increased Th1/Th2 (IFN-γ/IL-4) $CD4^+$ T Cells Increased MLN TLR4, TLR9, and TGF-β and Decreased TNF-α Expression After Challenge Increased Survival and Decreased Viral RNA After Challenge			Hou et al. 2018 (62)
DC-pep	*L. plantarum*	Surface-Display	Porcine Epidemic Diarrhea Virus (S Protein)	Increased DC Activation ($CD40/CD80^+$) Increased PP IgA^+ B Cells Increased Serum IgG, Intestinal sIgA, and Neutralizing Antibodies (IgG/sIgA) Increased MLN IFN-γ and IL-17	Oral	Murine BALB/c	Huang et al. 2018 (76)
DC-pep and M cell targeting peptide (Col)	*L. casei*	Surface-Display	Porcine Epidemic Diarrhea Virus (Core Neutralizing Epitope)	Increased IgG and Vaginal, Intestinal Mucus, and Fecal sIgA Increased Splenic Lymphocyte Proliferation Increased IFN-γ, IL-4 Increased Antibody-Mediated Virus Neutralization	Oral	Murine BALB/c	Ma et al. 2018 (77)
DC-pep	*L. casei*	Surface-Display	Bovine Viral Diarrhea Virus Glycoprotein E2	Increased PP DC Activation ($CD40^+$) Increased IgG and Intestinal sIgA Increased Neutralizing IgG and sIgA Increased IFN-γ, IL-4 Increased Splenic $CD4^+/CD8^+$ T Cells and T Cell Stimulation	Oral	Murine BALB/c	Wang et at. 2019 (78)
				Other			
Complement (C3d3)	*L. casei*	Surface-Display	Human Chorionic Gonadotropin (hCG)	Increased Serum/Vaginal IgG and IgA with Increased Longevity of Response Increased T and B Cell Proliferation	Vaginal	Murine BALB/c and C57BL/6	Yao et al. 2007 (63)
Anti-CD205	*L. plantarum*	Surface-Display	DNA (Plasmid)	Increased LAB DC Internalization Increased Delivery of Plasmid to DCs	Oral	Murine BALB/c	Michon et al. 2015 (64)
Neonatal Fc receptor (FcRn)	*L. plantarum*	Surface-Display	Influenza (Ectodomain of Matrix 2 Protein)	Increased DC Activation ($CD86^+/CD80^+$) Increased Splenic and MLN IFN-γ Increased Intestinal sIgA Increased MLN and PP IgA^+ B cells Increased Survival and Decreased Viral Load Following Challenge	Oral	Murine BALB/c	Yang et al. 2017 (65)

BAL: Bronchoalveolar lavage; PP: Peyer's patch; MLN: Mesenteric lymph node; DC: Dendritic cell; LP: Lamina propria.

1.5.3: Secretion of Bacterial Toxins

Cholera toxin (CT) and the *E. coli* heat labile enterotoxin (LT) are well-studied mucosal adjuvants that have been used to enhance immune response to antigen delivered by LAB. CT activates DCs and promotes Th2 T cells and B cell isotype switching, while LT promotes antigen presentation and APC-T cell interactions (79). The toxins are composed of two subunits: Active (A) and binding (B) (35, 80). The use of individual subunits is attractive as it can avoid the unwanted side effects associated with use of the whole toxin (81). The specific mechanisms of cellular and immune system interaction are known for each subunit. The A subunit acts intracellularly to increase cAMP through ADP-ribosylating activity, and the B subunit binds to ganglioside on the surface of most cells. Importantly, the A subunit possesses the toxigenic effects but only when paired with the B subunit (82, 83). Meanwhile, the B subunit is generally considered non-toxic and enhances antigen-specific immune response through direct binding of immune cells and enhancement of antigen delivery. In the LAB studies reviewed here, CT and LT were delivered as full toxins co-administered with LAB or as individual subunits either surface-displayed or secreted.

CT and LT LAB adjuvants increased immune responses when compared to LAB mucosal (intranasal or oral) delivered vaccines alone. Outcomes included an increase in IgG and mucosal sIgA, increased protection against pathogen challenge, increased T cell responses ($CD4^+$ and $CD8^+$), and an increase in IFN-γ, IL-4, and IL-17. Of interest, studies utilizing CT subunits showed an immune response that was more Th1 polarized (increased IFN-γ) while studies using LT as an adjuvant resulted in both Th1 and Th2 responses (increased IFN-γ and IL-4) (84-88).

The use of CT and LT adjuvants is appealing due to the robust mucosal immune stimulating effects, but in vivo safety remains a serious concern. An example of the toxic effects of CT and LT was demonstrated by the intranasal influenza vaccine, Nasalflu. This vaccine showed increased immune response when delivered with whole LT and no toxicity was observed in clinical trials. Following approval, it was removed from the market after one year of clinical use due to increased incidence of facial paralysis (89). It is possible that this unintended side effect could have been avoided with use of a single LT subunit

or if administered through a different mucosal route (orally, for example). No toxicity was reported in the studies reviewed here but, regardless, further toxicity studies are necessary.

Table 1.3. Bacterial toxin adjuvant strategies for lactic acid bacteria.

Adjuvant	LAB	Expression	Antigen	Immune Response	Delivery	Species	Study
Cholera Toxin (CT)							
CT subunit B	*L. casei*	Co-administered	*Bordetella pertussis* (Filamentous Haemagglutinin Adhesin)	Increased IgG	Subcutaneous	Murine BALB/c	Colombi et al. 2006 (90)
CT subunit B	*L. lactis*	Co-administered	Avian Influenza (Hemagglutinin Antigen)	Increased IgG and Intestinal sIgA Increased IFN-γ Increased Survival to Challenge	Oral	Murine BALB/c	Lei et al. 2011 (84)
CT subunit B	*L. casei*	Secreted	None	Increased IgG	Intranasal	Murine BALB/c	Okuno et al. 2013 (91)
CT subunit A1	*L. casei*	Surface-Display	Influenza (Matrix Protein 2)	Increased IgG and BAL sIgA Increased IFN-γ (Intranasal) Increased Protection and Decreased Lung Viral Titer Following Challenge	Oral Intranasal	Murine BALB/c	Chowdhury et al. 2014 (85)
CT subunit A1	*L. casei*	Surface-Display	Influenza (Matrix Protein 2 and Hemagglutinin)	Increased IgG and BAL and Intestinal sIgA Increased IFN-γ (Intranasal and Oral) and IL-4 (Intranasal) Increased protection and decreased lung viral titer Following challenge Longer Lasting Immune Response	Oral Intranasal	Murine BALB/c	Li et al. 2015 (86)
***E. coli* Heat-Liable Toxin (LT)**							
LT subunit B	*L. casei*	Surface-Display	Porcine rotavirus (VP4 capsid protein)	Increased Ocular, Vaginal, and Intestinal sIgA	Oral	Murine BALB/c	Qiao et al. 2009 (92)
LT subunit B	*L. casei*	Surface-Display Secreted	Porcine Epidemic Diarrhea Virus (Core Neutralizing Epitope)	Increased Intestinal, Vaginal, Nasal, Ocular, and Serum sIgA/IgA (Secreted Induced Highest Levels) Increased Neutralizing Antibodies Increased IFN-γ and IL-4	Oral	Murine BALB/c	Ge et al. 2012 (87)

LT subunit B and A (LTAK63)	*L. casei*	Surface-display	Enterotoxigenic *E. coli* (F4 (K88) fimbrial adhesion FaeG)	Increased IgG and Intestinal, Vaginal, and Nasal sIgA Increased Splenic Lymphocyte Proliferation Increased Protection to Challenge	Oral	Murine BALB/c	Yu et al. 2017 (93)
LT subunit B	*L. plantarum*	Surface-display	Avian influenza (hemagglutinin antigen)	Increased Intestinal sIgA Increased $CD4^+$ T Cell IFN-γ (MLN), IL-4 (MLN, Splenic), IL-17 (MLN, Splenic) and $CD8^+$ T Cell IFN-γ (MLN, Splenic) Increased PP IgA^+ B Cells Increased Protection to Challenge	Oral	Murine BALB/c	Jiang et al. 2017 (88)

BAL: Bronchoalveolar lavage; MLN: Mesenteric lymph node; PP: Peyer's patch.

1.5.4: Bacterial Derived Adjuvants

Numerous bacterial proteins have been explored for use with LAB mucosal vaccines. These strategies take advantage of immune activating and invasive proteins that are utilized by pathogenic bacteria, and our considerable knowledge regarding host-bacteria interactions at the molecular level. In many cases the binding domains of bacterial proteins are well-characterized and relatively small, making incorporation of these peptides or short proteins easier to express in a LAB vaccine platform. This provides the opportunity to expand the PRR-activating repertoire and/or enhance interactions between the LAB construct and host.

1.5.4.1: Toll-like Receptor (TLR) 5 Ligand

TLRs are expressed on many cell types and are an important activator of the innate immune response. TLR5 recognizes flagellin, a component of bacterial flagella, which stimulates production of chemokines and cytokines through myeloid differentiation factor 88 (MyD88) signaling (15). In addition to TLR5 activation, flagellin binds to the cytosolic nucleotide binding oligomerization domain-like receptors (NLR) NLRC4, which leads to caspase-1 inflammasome activation (94). There has been much

interest in flagellin as a vaccine adjuvant due to its ease of expression, stability, and robust activation of immune response (35, 95). There is high expression of TLR5 in the lung, intestinal epithelial cells, monocytes/macrophages, and DCs. Due to this expression pattern, the use of flagellin as a mucosal adjuvant could result in immune activation as well as delivery of an antigen to APCs. Flagellin has been surface-expressed with multiple LAB including: *L. casei*, *L. gasseri*, and *L. acidophilus* (96-98). Oral delivery of LAB expressing antigen and flagellin resulted in increased DC maturation, IgG and mucosal sIgA titers, and increases in both Th1 and Th2 cytokines. While the studies reviewed here only evaluated oral administration, flagellin could be a potent adjuvant for vaccines delivered through other mucosal routes. It has been shown to produce robust immune responses following intranasal delivery and TLR5 is expressed highly in numerous locations of the female reproductive tract, making it attractive for use with intravaginal delivered vaccines (99, 100)

1.5.4.2: Enterocyte Cell Targeting

Targeting LAB though surface expression of enterocyte binding proteins has been explored with the non-invasive LAB, *L. lactis*, through the use of *Listeria monocytogenes* internalin A (InIA) and/or *Staphylococcus aureus* fibronectin binding protein A (FnBPA) (101-105). InlA is a cell wall protein that allows *L. monocytogenes* to bind and be internalized by epithelial cells (106). FnBPA is also an epithelial cell binding protein that can bind to fibrinogen, elastin, and fibronectin allowing for internalization of *S. aureus* into non-phagocytic cells (107). *L. lactis* with cell surface expression of InlA and/or FnBPA has been used to deliver DNA plasmids to intestinal epithelial cells. Delivery of β-lactoglobulin antigen DNA resulted in an increase of β-lactoglobulin within the intestinal lumen, increased Th1 and Th2 cytokine responses, and increased serum and bronchoalveolar fluid IgG and serum IgA (after intranasal delivery of DNA coding for *Mycobacterium tuberculosis* Ag85A) (102-105). The use of InlA and FnBPA to deliver antigens to epithelial cells may be an effective mucosal vaccine strategy, especially if the desire is to deliver antigen via a eukaryotic expression plasmid (DNA vaccine).

1.5.4.3: Additional Bacterial Derived Adjuvants

Other bacterial proteins and messengers have been explored as LAB adjuvants. These include: Muramyl dipeptide, *Neisseria meningitidis* PorA, c-di-AMP, and Salmonella resistance to complement killing (108-111). Addition of these adjuvants to LAB mucosal vaccines resulted in an increased immune response and/or protection to challenge. The mechanism, if known, is described below.

Muramyl dipeptide (MDP) is a part of the bacterial cell wall and was delivered as a dipeptide with tuftsin, another biologically active compound. As mentioned above, LAB activate NOD2 and this is mediated through MDP breakdown products of the bacterial peptidoglycan. The exact mechanism of immune enhancement by MDP in combination with tuftsin is not fully elucidated but has been shown to activate APCs (112).

PorA is an outer membrane protein from the Gram-negative bacteria *Neisseria meningitidis*. This protein is immunodominant and, while using this protein as a vaccine antigen against *N. meningitidis* has not been successful, it has the potential to act as an adjuvant when conjugated to an antigen. For example, PorA increased the immune response to HpaA antigen from *Helicobacter pylori* (109). The exact mechanism of action of PorA is still under investigation.

The bacterial second messenger c-di-AMP was evaluated as an intracytoplasmic adjuvant. c-di-AMP has numerous effects on the immune system including type I interferon responses, promotion of Th1 and Th2 responses, increased lymphocyte proliferation, and activation of APCs (113). Delivery of c-di-AMP with an antigen against *Trypanosoma cruzi* resulted in a *T. cruzi*-specific immune response and is proof of concept that LAB can deliver biologically active c-di-AMP.

Finally, the use of Salmonella resistance to complement killing (RCK) protein was evaluated. This protein is important in interfering with complement killing and invasion into cells, including epithelial cells and APCs (114, 115). The use of RCK as a mucosal adjuvant was successful in increasing immune responses. The complete mechanism of immune activation is still unknown.

Table 1.4. Bacterial derived adjuvant strategies for lactic acid bacteria.

Adjuvant	LAB	Expression	Antigen	Immune Response	Delivery	Species	Study
Toll-like receptor 5 ligand							
Salmonella flagellin	*L. casei*	Surface-Display	*Salmonella enterica* (SipC)	Increased IL-8 Increased IgG Increased IL-2, GM-CSF, IFN-γ	Oral	Murine C3H/HeJ	Kajikawa et al. 2010 (98)
Salmonella flagellin	*L. gasseri*	Surface-Display	None	Increased TLR5 Stimulation Increased DC Maturation ($MHCII^+CD80^+CD86^-$) Increased $IL17^+$ Lymphocytes Increased Lamina Propria Plasma Cells	Oral	Murine BALB/c	Stoeker et al. 2011 (97)
Salmonella flagellin	*L. acidophilus*	Surface-Display	HIV-1 (Gag)	Increased IL-1β, IL-6 Increased IgA-Secreting B Cells in FRT and LI Decreased IFN-γ after HIV-1 In Vitro Exposure	Oral	Murine BALB/c	Kajikawa et al. 2012 (96)
Enterocyte targeting							
Listeria monocytogenes Internalin A	*L. lactis*	Surface-Display	DNA (GFP)	Increased Entry into Epithelial Cells and Delivery of GFP Plasmid	Oral	Guinea pigs Hartley	Guimaraes et al. 2005 (101)
Internalin A	*L. lactis*	Surface-Display	DNA (β-Lactoglobulin Antigen)	Increased β-Lactoglobulin in Intestinal Lumen	Oral	Murine BALB/c	de Azevedo et al. 2012 (102)
Fibronectic-Binding Protein A	*L. lactis*	Surface-Display	DNA (β-Lactoglobulin Antigen)	Increased β-Lactoglobulin in Intestinal Lumen	Oral	Murine BALB/c	Pontes et al. 2012 (103)
Fibronectic-Binding Protein A and Internalin A	*L. lactis*	Surface-Display	DNA (β-Lactoglobulin Antigen)	Intranasal Increased IL-4, IL-5, Decreased IFN-γ Oral Increased IL-5, Decreased IFN-γ	Oral Intranasal	Murine BALB/c	Pontes et al. 2014 (104)
Fibronectic-Binding Protein A	*L. lactis*	Surface-Display	DNA (*Mycobacterium tuberculosis* Ag85A)	Increased IFN-γ, TNF-α, IL-6 Increased Serum IgG, IgA, and BAL IgG	Intranasal	Murine C57BL/6	Mancha-Agresti et al. 2017 (105)
Additional bacterial derived adjuvants							
Muramyl Dipeptide and Tuftsin	*L. casei*	Secreted	Transmissible Gastroenteritis Virus (D Antigenic Site of the	Increased Intestinal, Serum, Nasal, Ocular, and Vaginal sIgA Increased Splenic T Cell Proliferation Increased Antibody-Mediated Viral Neutralization	Oral	Murine BALB/c	Jiang et al. 2014 (108)

			Spike Protein)	Increased IL-10, TGF-β Increased Th17 Cells and Decreased Treg Cells			
Neisseria meningitidis PorA	*L. lactis*	Cytoplasmic	Helicobacter pylori (HpaA)	Increased IgG	Oral	Murine BALB/c	Vasquez et al. 2015 (109)
c-di-AMP	*L. lactis*	Cytoplasmic	*Trypanosoma cruzi* (Trans-Sialidase Enzyme)	Increased Immune Response to *T. cruzi* Challenge	Oral	Murine BALB/c	Quintana et al. 2018 (110)
Salmonella Resistance to Complement Killing	*L. lactis*	Surface-display	Infectious Bursal Disease (VP2)	Increased Survival and Decreased Bursal Atrophy, Following Challenge (Intramuscular > Oral) Increased Neutralizing Antibody (Intramuscular > Oral)	Oral Intramuscular	Chicken	Wang et al. 2019 (111)

DC: Dendritic cell; FRT: Female reproductive tract; LI: Large intestine; BAL: Bronchoalveolar lavage; TLR: Toll-like receptor.

1.5.4.3: Other Adjuvant Strategies

There were three LAB adjuvant studies that did not fit into the above categories: Japanese herbal medicines (Juzen-taiho-to (JTT) and Hochi-ekki-to (HEY)), receptor activator of nuclear factor kappa-B ligand (RANKL), and thymosin α-1 (116-118). They are briefly reviewed in Table 1.5 and their mechanisms of action described here.

The ability of the Japanese herbal medicines JTT and HEY to enhance immune response when co-administered with a *L. casei* oral human papilloma vaccine was evaluated (116). These medicines have been shown to improve immune responses when delivered as an oral or intranasal adjuvant, but the exact mechanism of action is poorly described (119, 120). When delivered with *L. casei*, there was an increase in Th1 and Th2 cytokines. Other effects on the immune response following vaccination were not reported.

A study by Kim et al. aimed to increase the immune response to an oral *L. lactis* vaccine against the bacterium *Brachyspira hyodysenteriae* through the secretion of the M cell-inducing protein RANKL (117). M cells are important for pathogen uptake from the intestinal lumen and transport into the Peyer's patches (121). *L. lactis* RANKL secretion increased M cell development, serum IgG, and fecal sIgA. This is an

interesting adjuvant strategy as it acts through increased transport of the vaccine strain into Peyer's patches and not through a pro-inflammatory or DC targeting method.

Surface-display of the immune-modifier peptide hormone, thymosin α-1, was evaluated as an adjuvant for an orally delivered *L. plantarum* vaccine against classical swine fever (118). This peptide is secreted by the thymus and its use as a vaccine adjuvant has been shown to affect T cell maturation, cytotoxicity, Th1 and Th2 cytokine production, and increase antibody production (122, 123). Thymosin α-1 as a LAB adjuvant resulted in increased immune responses and protection from viral challenge in pigs.

Table 1.5. Other adjuvant strategies for lactic acid bacteria.

Adjuvant	LAB	Expression	Antigen	Immune Response	Delivery	Species	Study
Herbal Medicine (JTT, HET)	*L. casei*	Co-administered	Human Papilloma Virus (E7)	Increased IFN-γ, IL-2 Secretion	Oral	Murine C57/BL6	Taguchi et al. 2012 (116)
RANKL	*L. lactis*	Secreted	*Brachyspira hyodysenteriae* (Membrane Protein B)	Increased M Cell Development Increased IgG and Fecal sIgA	Oral	Murine BALB/c	Kim et al. 2015 (117)
Thymosin α-1	*L. plantarum*	Surface-Display	Classical Swine Fever (E2 Protein)	Increased IgG and Intestinal sIgA Increased Virus Neutralizing Antibodies Increased Cytotoxic Cells Increased IFN-γ, IL-2, TNF-α Increased Protection to Challenge	Oral	Porcine	Xu et al. 2015 (118)

RANKL: Receptor activator of nuclear factor kappa-B ligand; M cell: Microfold cell.

1.6: Discussion

LAB have been investigated as potential mucosal vaccine platforms for nearly three decades (124, 125). Significant progress has been made to explore the inherent immunogenicity of various LAB, develop strategies to express recombinant proteins, and test antigen and adjuvant concepts (126). To date, there is no licensed LAB-based vaccine primarily because necessary immunogenicity, efficacy, and durability have

not been achieved. The desperate need for mucosal vaccine platforms continues, as does the promise of approaches that employ LAB. Success will depend on exploiting our current knowledge and emerging technologies. A thoughtful choice of LAB species and strain, antigens, and adjuvant will be required to generate immune protection in the target host. Adjuvants provide tremendous flexibility to direct the nature of the adaptive immune response by supplementing the inherent attributes of LAB. They can target the vaccine construct to a specific cell type, activate particular innate immune pathways, or be selected to drive a desired arm of the adaptive response.

Highly immunogenic mucosal adjuvants with appropriate safety profiles have been identified and here we reviewed many of these adjuvants in the context of a LAB vaccine vector (35, 127). LAB were able to produce and display or secrete these adjuvant cytokines, immune targeting peptides, bacterial toxins, and other immune stimulating bacterial proteins. Immune responses after mucosal administration were generally increased in all studies. Specific outcomes included: Increased humoral immune responses (increased IgG and sIgA), increased immune cell proliferation and activation, increased uptake of LAB into immune induction sites, and decreased morbidity and mortality following challenge with bacterial, viral, and parasitic pathogens. Additionally, these adjuvant strategies showed the ability to induce both Th1 and Th2 responses and increase sIgA titers at mucosal sites distant to the site of administration.

There were other interesting observations in the reviewed studies. The surface display of enterocyte-targeting bacterial proteins by *L. lactis* resulted in delivery of DNA plasmids to enterocytes and protein secretion into the intestinal lumen. This is a potential alternative strategy of protein antigen delivery and could also be utilized to deliver DNA to promote secretion of anti-viral or bacterial peptides (102-105). Another reported benefit of these bacterial vectors is the ability to outcompete pathogens at mucosal surfaces. An example is a LAB vaccine against Enterotoxigenic *E. coli* (ETEC) with surface display of DC-peptide and ETEC fimbriae. The vector induced increased protective immune responses to ETEC infection and provided immediate protection from pathogen invasion by interfering with attachment of ETEC to intestinal cells (73).

As engineered LAB mucosal vaccines with enhanced immunogenicity are tested in vivo, further investigation is needed into the safety of these strategies. The addition of adjuvants to a vaccine should not cause long-lasting or debilitating local or systemic reactions or induce hypersensitivity reactions, autoimmunity, or neoplasia (128). While LAB are regarded as safe and are used in numerous food products and health supplements, it is unknown if the inclusion of adjuvants would affect their safety profile. No adverse effects were reported in the studies reviewed here despite the use of CT and LT subunits or secretion of pro-inflammatory cytokines. Additionally, it is unknown if repeated exposure to genetically modified LAB would result in unintended immune responses as wild type probiotics are already known to induce and enhance mucosal antibody responses (129, 130). Whether off-target effects might result in anti-LAB (or other commensal) immune responses should be explored by analyzing the microbial community structure in vaccinated subjects.

1.7: Conclusions

The adjuvant strategies reviewed here are diverse and all resulted in increased immune responses. Next-generation LAB have the potential to be powerful mucosal vaccine vectors. Facile techniques that enable multiple genetic modifications, such as CRISPR/Cas, will likely usher in a new era of innovation that may enable the realization of a commercially viable LAB-based mucosal vaccine (37, 131, 132).

CHAPTER 2: LACTOBACILLUS ACIDOPHILUS AS AN ORAL VACCINE VECTOR

2.1: Overview

As reviewed in sections 1.2 and 1.3, lactic acid bacteria (LAB) have many advantages as oral vaccine vectors including: gastric acid and bile resistance, oral administration, and heat stability. The genus and species utilized as the vector is important as each LAB has different innate characteristics and interactions with the immune system. In Chapter 2, the focus is on the further development of the lactic acid bacteria *Lactobacillus acidophilus* (LA) strain NCFM as a vaccine vector. In addition to the aforementioned advantages, LA has many endogenous proteins that can activate the immune system including lipoteichoic acid, peptidoglycan, muramyl dipeptide, and dendritic cell (DC)-specific intercellular adhesion molecule 3 (ICAM-3)-grabbing nonintegrin (DC-SIGN). LA also possesses mucus-binding proteins, a microfold (M) cell binding protein, and is amenable to genetic manipulation; accommodating plasmid expression systems and genomic integration of foreign DNA sequences (16, 18, 25, 133-136). These characteristics make LA attractive for oral vaccine development. LA has been extensively studied as a vaccine vector against numerous pathogens including: chicken anemia virus, foot-and-mouth disease, human immunodeficiency virus (HIV), influenza, rotavirus, *Bacillus anthracis*, *Clostridium botulinum*, *E. coli* EHEC O157:H7 and ETEC, and *Helicobacter pylori* (47, 68, 96, 137-144).

Important for LA vaccine development is the availably of molecular tools for genetic modification. These tools have been developed by Klaenhammer et al. (136). The methods for LA modification include plasmid-based expression systems and an uracil phosphoribosyltransferase (upp) gene knock-out (Δupp) strain of LA NCFM that allows for genomic integration of foreign DNA (Figure 2.1). This method can be used to target specific areas of the genome by designing homologous flanking DNA segments that promote double crossover recombination. Proof of concept was shown by Goh et al. who first used this method to knock-out a LA surface layer protein and O'Flaherty et al. who utilized this system for stable chromosomal integration of epitopes from the *Clostridium botulinum* neurotoxin and anthrax protective antigen (140, 145).

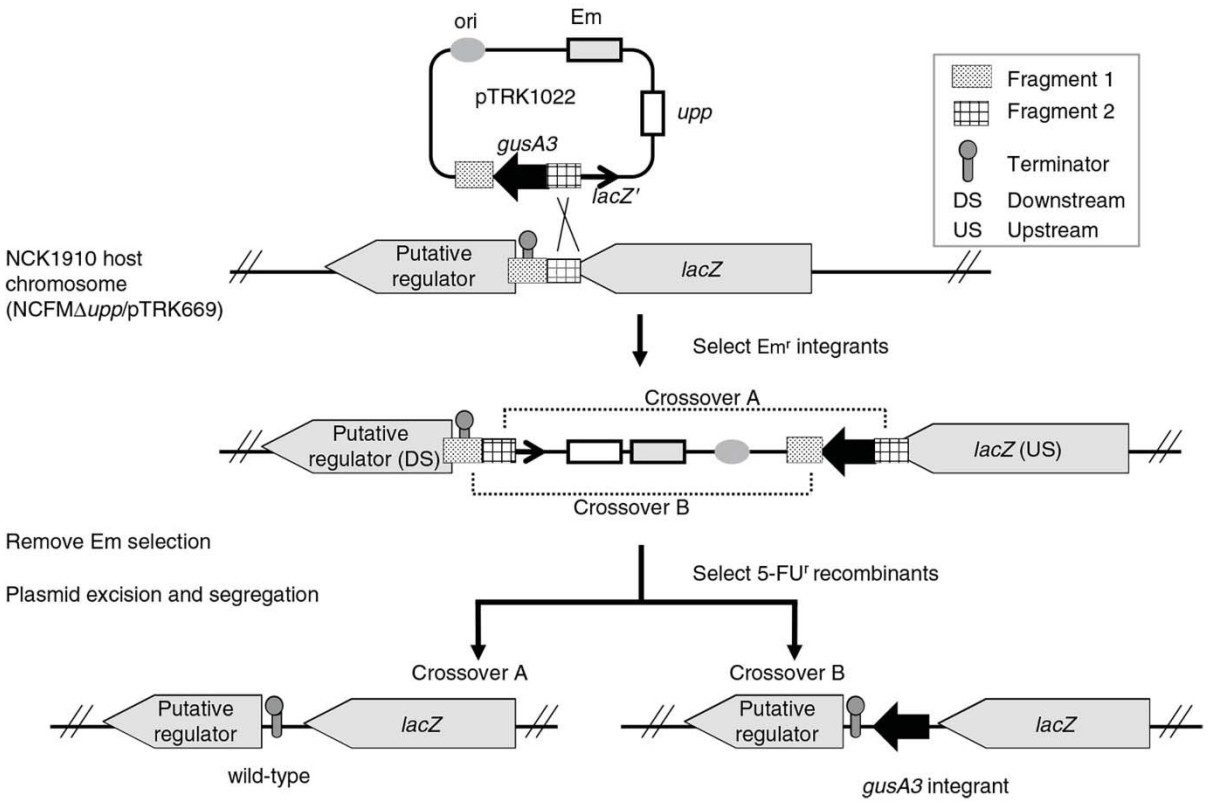

Figure 2.1. Lactobacillus acidophilus NCFM Δupp double-crossover method for genetic recombination. A plasmid containing the genomic insert of interest flanked by homologous genomic DNA fragments, erythromycin (Em) resistance, and upp gene making the LA sensitive to 5-fluorouracil (5-FU). The plasmid is transformed into NCFM Δupp LA mutants (1) resulting in single cross-over and plasmid integration into the genome (2). Single cross-over mutants are selected by Em resistance (3) and then the plasmid sequence is lost under pressure of 5-FU (6). Loss of the plasmid sequence either results in "Crossover A" (4) and reversion to wildtype LA or "Crossover B" (double crossover) (5) and stable genomic integration of the insert. Figure revised, courtesy of Douglas et al. (136).

Plasmid based expression and the LA Δupp double-crossover methods have been utilized in the Dean Lab to develop a variety of recombinant LA oral vaccines against HIV-1 (47, 98, 146, 147). One of these developed LA strains (GAD31) expresses a 16-amino acid linear epitope from the membrane proximal external region (MPER) of HIV-1 within the highly expressed LA surface protein, SlpA. The MPER epitope (NEQELLELDKWASLWN) is from the HIV glycoprotein (GP) 41 envelope protein, and several human monoclonal antibodies against this region have been found to be broadly neutralizing against HIV (148-150). The MPER epitope has proven to be poorly immunogenic and LA MPER surface expression results in little to no measurable serum IgG and mucosal IgA immune responses in mice (47).

This makes GAD31 a good strain for studying the immune modifying effects of various LA adjuvants. To date, two adjuvant strategies have been tested: secretion of inflammasome product and proinflammatory cytokine IL-1β (GAD19) and surface expression of the Toll-like receptor (TLR) 5 ligand *Salmonella enterica* serovar Typhimurium flagellin (FliC) via two surface anchoring systems (electrostatic linker PrtP: C-terminal protein fragment of the surface proteinase and covalent anchor Mub: mucus binding protein binding domain) (47, 96, 146). All adjuvant strategies are expressed from plasmids and maintained by antibiotic resistance. Both FliC and IL-1β adjuvanted LA-MPER result in increased serum and mucosal antibody responses in mice when compared to GAD31 (47, 151).

Sections 2.2 and 2.3 describe work performed to further develop LA as a vaccine vector by developing: 1) the *E. coli* type 1 pilus fimbrial adhesin, FimH, as a LA-MPER vaccine adjuvant and 2) LA NCFM as a next generation oral vaccine for rotavirus. Table 2.1 lists vaccine stains described here and developed in sections 2.2 and 2.3.

Table 2.1. LA bacterial strains utilized in Chapter 2. Summary of LA strains including SlpA epitopes and adjuvants used in Chapter 2.

LA Strain	SlpA Epitope Expression	Adjuvant
LA170	None	None
GAD31	HIV-1 MPER: NEQELLELDKWASLWN	None
GAD19	HIV-1 MPER: NEQELLELDKWASLWN	Mouse IL-1β
GAD12	HIV-1 MPER: NEQELLELDKWASLWN	FliC-PrtP
GAD10	HIV-1 MPER: NEQELLELDKWASLWN	FliC-Mub
GAD40	HIV-1 MPER: NEQELLELDKWASLWN	FimH-Mub
GAD41	HIV-1 MPER: NEQELLELDKWASLWN	5'flag tag-FimH-Mub
GAD42	HIV-1 MPER: NEQELLELDKWASLWN	FimH-3'flag tag-Mub
GAD80	RV VP8: MASLIYRQLL	None
GAD81	RV VP8: MASLIYRQLL	Mouse IL-1β
GAD82	RV VP8: MASLIYRQLL	FliC-PrtP
GAD83	RV VP8: MASLIYRQLL	FimH-Mub

MPER: membrane proximal external region; RV: rotavirus

2.2: *Escherichia coli* Type 1 Pilus Fimbrial Adhesin FimH as a *Lactobacillus acidophilus* Vaccine Adjuvant

2.2.1: Introduction

Discovery and evaluation of novel vaccine adjuvants to enhance immune response to delivered antigen is an important step in vaccine development. This is especially important for mucosal delivered vaccines where the immune response to vaccination is generally more difficult to achieve than with parenteral vaccines. Current adjuvant strategies for mucosal vaccines are reviewed in section 1.4.

We have developed a *Lactobacillus acidophilus* (LA) vaccine platform that has been evaluated as an oral vaccine against HIV-1 (summarized in section 2.1). While LA possesses many endogenous mechanisms for activating the immune system, the systemic and local (mucosal) immune response to vaccination with LA expressing the MPER epitope within the surface layer protein, SlpA, (GAD31) has been low. This contrasts with immune responses measured to oral vaccination with LA expressing a known class II MHC-peptide binding peptide from ovalbumin (unpublished data). These results indicate that MPER is a weak immunogen making GAD31 an excellent vector for the evaluation of LA adjuvants. Immune responses in mice orally dosed with LA strains either secreting the inflammasome product and proinflammatory cytokine IL-1β or surface expressing the TLR5 ligand FliC result in increased systemic and mucosal immune responses when compared to GAD31 (47, 151). This increase in immune response indicates that one or more adjuvant strategies will likely be necessary for an effective oral LA vaccine platform.

FimH is a type 1 fimbriae adhesion protein present on certain pathogenic *E. coli* and *Salmonella* spp. It is an especially important virulence factor for uropathogenic *E. coli* where it facilitates urogenital colonization via adhesion to Tamm-Horsfall proteins (152). Based on the structural similarity of Tamm-Horsfall proteins to the M cell specific protein glycoprotein (GP) 2, it was found that *E. coli* and *Salmonella* spp. expressing FimH can bind to M cells resulting in increased uptake into Peyer's patches (PP). PP are specialized sites of immune induction in the intestines and entry through PP has been shown to be important

for the induction of fecal IgA (153). Because of the potential to increase IgA production, M cell targeting has been an active area of mucosal vaccine adjuvant development making FimH an attractive protein for use in an oral vaccine (154-156). In addition to M cell targeting, FimH possesses other attractive immune activating characteristics including binding to TLR4 and macrophages by the CD48 receptor (157, 158). Proof of concept for the use of FimH as a vaccine adjuvant was shown by Fan et al. who used FimH to increase PP uptake of a vaccine against coxsackievirus B3. FimH increased antigen-specific IgA and mucosal IgA secreting cells (159).

Here we evaluate the ability of LA surface expressed FimH to enhance the immune response to the MPER epitope. LA FimH expression was confirmed via western blot and flow cytometry and immune response assessed by ELISA and ELISPOT following oral delivery to mice. The interaction of LA-MPER expressing FimH with M cells and TLR4 was assessed to confirm the mechanism of immune interaction and activation.

2.2.2: Materials and Methods

2.2.2.1: LA-MPER FimH (GAD40) Construction

Three FimH expression plasmids were constructed by restriction digest and ligation into plasmid pTRK1033 containing the MUB LA surface anchor, secretion signal, origin of replication, and erythromycin resistance gene (146). The N-terminal domain (amino acids (AA) 22-181) of *E. coli* FimH (Uniport Knowledgebase (UniPortKB) P08191) DNA sequence was ordered as a gene block from Integrated DNA Technologies (Coralville, IA, USA). Table 2.2 lists the FimH protein sequence, gene block sequences, and primers used for PCR amplification.

Table 2.2. FimH protein sequence, gene block sequences, primers, and constructed plasmids.

N-terminal FimH sequence	FACKTANGTAIPIGGGSANVYVNLAPVVNVGQNLVVDLSTQIFCHNDYPETIDYVT LQSAYGGVLSNFSGTVKYSGSSYPFPTTSETPRVVYNSRTDKPWPVALYLTPVSSAG GVAIKAGSLIAVLILRQTNNYNSDDFQFVWNIYANNDVVVPTGG		
FimH 5'-flag tag gene block	CTGTAAAGGCAGATGAAGTTGATGATGCTAGCCGGCCGGACTACAAAGATGAC GATGATAATTTGCATGCAAAACCGCTAATGGAACCGCCATTCCAATTGGTGGTG GCAGTGCAAATGTCTATGTAAACTTGGCCCCAGTTGTCAATGTCGGACAAAATC TTGTAGTAGATTTAAGCACTCAAATTTTTTGTCATAACGACTATCCAGAGACCAT CACTGATTACGTTACCTTACAACGCGGTTCAGCATACGGAGGTGTCTTATCTAAC TTCTCAGGAACTGTAAAGTATAGTGGTTCAAGTTACCCATTCCCAACCACTTCAG AGACACCTCGTGTCGTTTACAATAGCAGAACAGATAAACCTTGGCCTGTCGCCT TATACCTTACCCCTGTAAGCTCAGCAGGTGGAGTCGCCATCAAAGCAGGCTCAT TAATCGCTGTATTAATTTTACGCCAGACTAATAACTATAACTCTGATGACTTTCA ATTCGTCTGGAATATCTATGCCAACAATGACGTAGTCGTACCAACAGGCGGCGG TACCGTGCCAACAGTTACTCCAAC		
FimH 3'-flag tag gene block	CTGTAAAGGCAGATGAAGTTGATGATGCTAGCCGGCCGTTTGCATGTAAAACTG CCAACGGAACAGCCATCCCTATTGGTGGTGGTTCTGCTAATGTTTATGTAAATTT AGCCCCTGTAGTAAATGTCGGCCAGAACTTGGTCGTAGATCTTAGTACTCAGAT CTTTTGTCATAACGATTATCCTGAGACCATCACTGATTATGTCACATTACAGCGA GGCTCAGCCTACGGTGGTGTTTTATCAAACTTCTCTGGAACTGTAAAGTATAGC GGAAGCTCTTATCCTTTTCCAACTACCAGTGAAACTCCACGTGTAGTCTACAATA GCCGAACTGATAAGCCATGGCCTGTTGCTCTTTATCTTACTCCTGTAAGTAGCGC CGGTGGTGTAGCAATTAAAGCCGGAAGCTTGATCGCTGTCTTGATTTTAAGACA GACAAATAACTATAATTCAGACGATTTCCAGTTTGTATGGAACATCTACGCAAA TAATGATGTCGTCGTCCCAACTGGCGGCGATTACAAGGACGATGATGACAAAGG TACCGTGCCAACAGTTACTCCAAC		
Primers			
AV-09	ctg taa agg cag atg aag ttg atg		
AV-10	gtt gga gta act gtt ggc agc g		
AV-29	gcc gcc agt tgg gac gac gac at		
AV-30	gtt gga gta act gtt ggc acg gta ccg ccg cca gtt ggg acg acg aca t		
AV-11	ttt cgc cca gcg cta tga aaa gga tgg tgg gtt gt		
AV-12	agc ggg ttt aaa ctc aat ggt gat ggt gat gat gtg tag tgt ggg gag tcc c		
Plasmids			
Name	**Surface Expressed Protein**	**Tag**	**Surface Anchor**
pTRK-AV40	FimH	No tag	Mub
pTRK-AV41	FimH	5'-flag tag	Mub
pTRK-AV42	FimH	3'-flag tag	Mub

FimH sequences for plasmid construction were amplified by PCR with the following primers: 5'-flag tag-FimH: 5' flag tag gene block with AV-09 and AV-10, 3'-flag tag-FimH: 3' flag tag gene block with AV-09 and AV-10, and no tag-FimH: 3' flag tag G block with AV-09 and AV-29, the PCR product was then further amplified with primers AV-09 and AV-30. The plasmid, pTRK1033, was restriction digested with NheI and Kpn, the digested plasmid and FimH PCR amplicon assembled via Gibson

Assembly (New England Biolabs, Ipswich, MA, USA), and then transformed into α-5 competent *E. coli*. The resulting plasmids pTRK-AV40, pTRK-AV41, and pTRK-AV42 were screened by PCR, confirmed by sequencing, and transformed into GAD31 based on a previously described protocol (136, 160). Briefly, GAD31 was serially cultured in antibiotic-free MRS media (Becton Dickinson/BD Biosciences, San Jose, CA) to remove the erythromycin resistance plasmid and then grown until exponential growth phase was achieved. LA were washed with an isosmotic buffer (1M sucrose and 2.5mM $MgCl_2$) and concentrated 100-fold. Concentrated LA was mixed with approximately 500 ng of plasmid, transferred to a 2-mm-gap electroporation cuvette, and supplied with 2.5kV, 400 Ω, 25μF electrical pulse. Transformants were selected on LB agar plus erythromycin plates.

2.2.2.2: GAD40 FimH Western Blot and Flow Cytometry

Anti-flag western blotting was used to confirm surface expression of FimH for GAD41 and GAD42 constructs. LA were grown to exponential phase in MRS plus erythromycin and washed with phosphate-buffered saline (PBS) plus 1X protease inhibitor (ProteaseArrest, G Biosciences, St. Louis, MO, USA). Washed LA were incubated overnight at 4°C in PBS plus 1X protease inhibitor and mutanolysin (Sigma-Aldrich, Darmstadt, DEU). Washes were repeated and LA homogenized by beating with 0.1 mm zirconia/silica beads (BioSpec, Bartlesville, OK, USA). The homogenized LA was incubated with benzonase (Millipore-Sigma, Burlington, MA, USA), mixed with Pierce lane marker sample loading buffer (Thermo Scientific, Waltham, MA, USA), and proteins separated by sodium dodecyl sulfate-polyacrylamide gel electrophoresis (SDS-PAGE) on a 4-20% Mini-PROTEAN TGX precast protein gel (Bio-Rad, Hercules, CA, USA) run with Precision Plus Protein WesternC blotting standard (Bio-Rad, Hercules, CA, USA). Proteins were transferred to a polyvinylidene difluoride (PVDF) membrane using the Bio-Rad Trans-Blot Turbo Transfer System (Hercules, CA, USA). The membrane was blocked with 1% non-fat dry milk in PBS + 0.05% Tween20 (PBST) and protein labeled using rat anti-flag primary (Ebioscience, San Diego, CA, USA) and goat anti-rat IgG HRP (SeraCare, Milford, MA, USA) secondary.

Chemiluminescence was detected using Bio-Rad Clarity enhanced chemiluminescence western blotting substrate on a ChemiDoc XRS+ System (Hercules, CA, USA).

GAD40 FimH and MPER expression was detected by flow cytometry. GAD31 and GAD40 were grown to exponential phase from overnight cultures and washed with PBS. LA was resuspended in PBS and colony forming units (CFU) calculated based on the optical density at 600nm. $1x10^7$ CFU LA were suspended in staining buffer (PBS + 1% fetal bovine serum (FBS)) plus mouse anti-FimH mAb824 (a gift from Dr. Svgeni V. Sorurenko, University of Washington, Seattle, WA) or with human-anti-HIV MPER IgG (NIH AIDS Reagent Program, Germantown, MD, USA) and incubated on ice. LA were washed with PBS and then the primary antibody detected with either goat anti-mouse PE (Invitrogen, Waltham, MA, USA) or mouse anti-human IgG Alexa488 (Molecular Probes, Eugene, OR, USA). Following incubation with the secondary antibody, LA were washed twice, resuspended in PBS, and flow cytometry was performed using a Gallios flow cytometer (Beckman Coulter, Indianapolis, IN, USA). Analysis was performed using FlowJo software (Ashland, OR, USA). Gates were set using LA labeled only with the secondary antibodies.

2.2.2.3: Mouse GP2 Expression and Purification

A plasmid containing mouse glycoprotein 2 (mGP2) was purchased from OriGene (Rockville, MD, USA). mGP2 was amplified from the plasmid using primers AV-11 and AV-12 to add a 3'-His tag (Table 2.2). The amplified fragment was cloned into the pND14 eukaryotic expression plasmid (a gift from Dr. Gary Rhodes, University of California, Davis, CA) by restriction digest (AfeI and PmeI) and ligation and then transformed into NEF5α competent cells by heat-shock. Positive transformants were selected by antibiotic resistance and the pND14-mGP2-His plasmid confirmed by PCR and DNA sequencing.

pND14-mGP2-His plasmid was transfected into 293T cells using TransIT-LT1 transfection reagent (Mirus, Madison, WI, USA) based on the manufacturers recommended protocol. 24 hours after transfection the media was replaced with Opti-MEM reduced serum media (Gibco, San Diego, CA, USA), cells were incubated for 48 hours, media collected, and mGP2-His protein purified by Capturem His-Tagged

purification miniprep kit (Takara Bio USA, Mountain View, CA, USA). mGp2-His was confirmed by SDS-PAGE gel and western blot. Western blot was performed similar to the FimH anti-flag western blot protocol described in section 2.2.2.2. The protein was detected on western blot with mouse anti-His tag HRP (Bio-Rad, Hercules, CA, USA).

2.2.2.4: GAD40 FimH-Mouse GP2 Binding Assay

mGP2-His binding to FimH was confirmed by indirect ELISA using a modified protocol based on the method by Stoeker et al. (97). GAD31, GAD40, GAD41, and GAD42 were grown in MRS plus erythromycin overnight. LA were washed with PBS and CFU were calculated by the optical density at 600nm. LA were suspended in PBS at a concentration of $1x10^8$ CFU/ml and 100 µl of each LA strain was added to 5 wells of a Maxisorp 96-well plate (Nunc, Rochester, NY, USA). Plates were incubated at 45°C overnight to evaporate PBS. Wells were washed with PBST and blocked with blocking buffer (1% bovine serum albumin (BSA) in PBS) for 2 hours at room temperature. Wells were washed with PBST and 100 µl purified mGP2-His diluted to 0.2 µg/ml in sample diluent (PBST + 1% BSA) was added to each well. The plates were incubated for 1 hour at room temperature, washed with PBST, and GP2 binding detected by adding 100 µl mouse anti-His tag HRP (Bio-Rad, Hercules, CA, USA) diluted in PBST. After 1-hour incubation at room temperature, the wells were washed with PBST and incubated for 15 minutes with 100 µl with SureBlue Reserve TMB Peroxidase Substrate (SeraCare, Milford, MA, USA). The color development was stopped with 1N HCl and the absorbance measured at 450 nm – 570 nm on a plate reader. Absorbance levels are reported as the average of the five wells coated with the same strain of LA.

2.2.2.5: Ethics Statement and Mouse Usage

All experiments involving the use of animal complied with all relevant regulations and with the guidelines and approval of Colorado State University's Institutional Animal Care and Use Committee (IACUC 14-5332A). Animals were monitored daily and all animals were euthanized at the end of studies by either carbon dioxide inhalation or overdose of Isoflurane followed by cervical dislocation.

All mice were wild type female Balb/cJ obtained from Jackson Laboratories (Bar Harbor, ME, USA). Mice were maintained in specific pathogen-free conditions, housed socially (2-5 mice per cage) in commercially available individually ventilated cages, and provided with autoclaved bedding and enrichment. Animals were fed ad libitum commercially irradiated rodent chow (Teklad Global, Envigo, Indianapolis, IN, USA) (unless specially stated for approved procedures) and tap water filtered via reverse osmosis in autoclaved water bottles. Animals were tracked and monitored daily for any signs of stress or illness.

2.2.2.6: Intestinal Loop Peyer's Patch LA Uptake and Mesenteric Lymph Node Trafficking

GAD31and GAD40 were grown overnight at 37°C in MRS plus erythromycin. LA were washed with PBS and CFU were calculated based on the optical density at 600nm. $5x10^9$ CFU LA were suspended in 1 ml PBS plus 5 mM cell trace violet (Invitrogen, Waltham, MA, USA) and incubated on ice. Labeling was stopped with 10% FBS in PBS and then LA were diluted to $5x10^9$ CFU/ml in doing buffer (100 mM sodium bicarbonate buffer and 1 M trypsin inhibitor (Sigma-aldrich, Darmstadt, DEU)). Twelve 8-12-week-old female Balb/cJ mice were held without food for 16 hours and anesthetized via isoflurane inhalation. LA were injected into an isolated segment of the small intestine based on the intestinal loop method described by Fukuda et al. (161). Briefly, the abdomen of anesthetized mice was prepped via repeated scrubbing with 70% ethanol and the fur removed by clippers. The small intestine was isolated by encircling ligatures at the pyloric and ileo-cecal junction (Figure 2.2A). 200 µl LA in dosing buffer (corresponding to $1x10^9$ CFU LA) was delivered into the isolated small intestine through a 22 G needle resulting in intestinal distention (Figure 2.2B). The abdomen was closed with skin clamps and the mice maintained under anesthesia for 1-hour post-LA delivery. Mice were euthanized by over-dose of isoflurane followed by cervical dislocation. The small intestine and mesenteric lymph node (MLN) collected into RPMI (Corning, Tewksbury, MA, USA) supplemented with glutamine and HEPES (collection media).

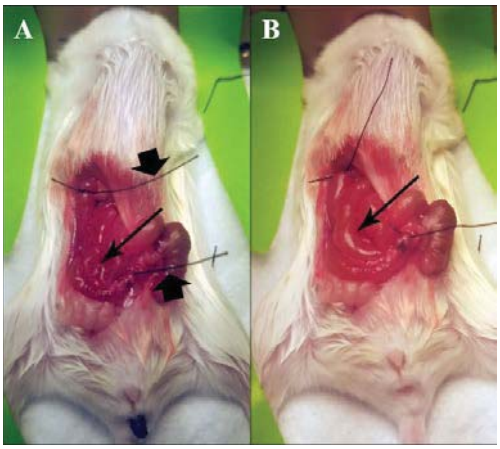

Figure 2.2. Intestinal loop LA small intestine delivery. Abdomen of female Balb/c mice maintained under anesthesia. (For orientation, the head is located at top of image.) (A) The small intestine (thin arrow) is isolated by encircling ligatures (thick arrows). (B) $1x10^9$ CFU LA suspended in dosing buffer was injected via a 22G needle into the isolated section of small intestine. Thin arrow shows dilation of small intestine following LA delivery.

The small intestine was washed with cold PBS, reclosed with suture, the lumen infused with 1 ml cold 10% n-acetyl-L-cysteine pH 7.4 (Sigma-Aldrich, Darmstadt, HR), and incubated for 10 minutes on ice to digest intestinal mucus. The intestine was washed with cold PBS and PP collected by dissection into cold collection media. PP and MLN were incubated for 30 min at 37°C in RPMI supplemented with 10% FBS, glutamine, HEPES, MEM non-essential and essential amino acids, sodium pyruvate, 2-mercaptoethanol, and gentamycin to kill any remaining surface bacteria. PP and MLN were processed into a single cell suspension by physical disruption, filtered, and live cells counted using a Cellometer Auto200 (Nexcelom Bioscience, Lawrence MA, USA). Cells were suspended in 1X RIPA buffer (Thermo Scientific, Waltham, MA, USA) at $5x10^6$ cells/ml and incubated for 5 minutes on ice to lyse mammalian cells. The cellular lysate was plated on MRS agar plus erythromycin to select for LA. Plates were incubated under anaerobic conditions for 48 hours and colonies counted.

2.2.2.7: Peyer's Patch and Mesenteric Lymph Node Antigen Presenting Cell Flow Cytometry

GAD31, GAD19, and GAD40 were grown, labeled with cell trace violet, and suspended at $5x10^9$ CFU/ml in dosing buffer as described in section 2.2.2.6. 10-12-weeks-old female Balb/cJ mice were held

without food for 16 hours and then orally dosed with 200 µl LA for a total of $1x10^9$ CFU delivered. 1 hour after oral delivery, mice were euthanized by CO_2 asphyxiation followed by cervical dislocation and mesenteric lymph nodes collected into collection buffer. MLN were processed into single cell suspensions and counted as described in section 2.2.2.6. Cells were blocked with anti-mouse CD16/32 (Biolegend, San Diego, CA, USA) and labeled in staining buffer with a cocktail of 7-AAD viability staining solution (Biolegend, San Diego, CA, USA), PE anti-mouse CD64 (Biolegend), PE/Cy7 anti-mouse I-A/I-E (Biolegend), Alexa Fluor 647 anti-mouse CD103 (Biolegend), APC/Cy7 anti-mouse/human CD11b (Biolegend), biotin hamster anti-mouse CD11c (BD Pharmingen, San Jose, CA, USA), and FITC streptavidin (Biolegend). Cells were washed, suspended in PBS, and flow cytometry was performed using a Gallios flow cytometer (Beckman Coulter, Indianapolis, IN, USA). Analysis was performed using FlowJo software (Ashland, OR, USA). Gates were set using fluorescence minus one (FMO) controls after gating for live cells.

2.2.2.8: GAD40 TLR4 Activation Assay

HEK-Blue human TLR4 and HEK-Blue Null2 control cell lines (InvivoGen, San Diego, CA, USA) were grown in cell culture treated flasks (Corning, Tewksbury, MA, USA) to confluency in DMEM media plus 10% heat-inactivated FBS, glutamine, penicillin, streptomycin, and normocin (cell culture media) (Gibco, San Diego, CA, USA). After two passages, media was supplemented with selection antibiotics (TLR4: HEK-Blue selection and Null2: zeocin (InvivoGen, San Diego, CA, USA)). 25,000 cells were plated on 96-well cell culture coated plates (Greiner Bio-One, Monroe, NC, USA) in cell culture media. Plates were maintained at 37°C and 5% CO_2 for 4 hours prior to the addition of LA.

GAD31 and GAD40 were grown at 37°C overnight, diluted 1:10, and grown to exponential phase in MRS plus erythromycin. LA were washed with endotoxin-free PBS and CFUs were calculated based on the optical density at 600nm. LA were diluted in PBS and $4x10^7$ to $2.5x10^6$ CFU (correlates to multiplicity of infection of 50-1.56) of either GAD31 or GAD40 were added in duplicate to the HEK-Blue human TLR4 and HEK-Blue Null2 plated cells. 100ng and 10 ng of LPS were added as a positive control and PBS was

used as a negative control. LA and cells were incubated at 37°C and 5% CO_2 overnight. 20 µl supernatant from each well was collected and added to 180 µl QUANTI-Blue Detect reagent (InvivoGen, San Diego, CA, USA) and incubated at 37°C for 4 hours. Colorimetric change was detected by absorbance measured at 620 nm – 655 nm on a plate reader.

2.2.2.9: GAD19 and GAD40 Mouse Dosing Experiment and Tissue Collection and Processing

GAD19 and GAD40 were grown for 12-16 hours at 37°C in MRS plus erythromycin and washed with PBS. CFUs were calculated based on the optical density at 600nm and LA suspended at $5x10^9$ CFU/ml in dosing buffer as described in section 2.2.2.6. 10-12-weeks-old female Balb/cJ mice were orally dosed with 200 µl LA for a total of $1x10^9$ CFU delivered on three sequential days, every other week for 12 weeks. Prior to the first day of dosing, samples were collected for antibody analysis. Serum was collected by tail vein bleed, vaginal samples collected by vaginal wash with 100 µl PBS, and fecal supernatant collected following centrifugation of fecal samples homogenized in PBS plus 1X protease inhibitor. All samples were held at -80°C until analysis.

Two weeks following the final oral LA dose, mice were euthanized by CO_2 asphyxiation followed by cervical dislocation and spleen, PP, MLN, colon, and female reproductive tract (FRT) collected in RPMI supplemented with glutamine, HEPES, penicillin, and streptomycin. Tissues were processed into single cell suspensions. PP and spleen were mechanically disrupted using a GentleMACS dissociator (Miltenyi Biotec, Auburn, CA, USA) and MLN mechanically disrupted by mashing the lymph tissue through a 100 µm cell strainer. The colon and FRT were processed based on the method described by Stoeker et al. (97). Briefly, the colon and FRT had fat/mesentery removed by careful dissection, tissues were suspended in PBS with 1 mM dithiothreitol (DTT) and 5 mM ethylenediaminetetraacetic acid (EDTA), and lumens gently brushed to remove debris and mucus. Using scissors, the tissues were cut into less than 1 mm pieces which were suspended in culture media (RPMI supplemented with 10% FBS, glutamine, HEPES, 2-mercaptoethanol, sodium pyruvate, essential and non-essential amino acids, penicillin, and streptomycin) plus 125 µg/ml Liberase TM (Sigma-Aldrich, Darmstadt, DEU) and 100 µg/ml DNase I (Sigma-Aldrich, Darmstadt, DEU)

followed by agitation using a GentleMACS dissociator. Tissues were incubated at 37°C for 30 (colon) or 60 (FRT) minutes with gentle rocking. Suspensions were filtered and cells isolated by Percoll gradient.

All processed samples were filtered, and live cells counted using a Cellometer Auto200 (Nexcelom Bioscience, Lawrence MA, USA). Cells were stored on ice in culture media until ELISPOT plate set-up and flow analysis.

2.2.2.10: MPER Antigen Specific ELISPOT

Twenty-four hours prior to tissue collection and processing, ELISPOT plates (MAIPSWU, EMD Millipore, Burlington, MA, USA) were prepared according to the manufacturer's recommendations, coated with 10 µg/ml anti-IgA antibody (ELISpot^{Plus} Kit, Mabtech, Nacka Strand, SWE), and incubated at 4˚C overnight. On the day of tissue collection and processing, plates were washed with PBS and blocked with culture medium for at least 1 hour at 37˚C. Cell suspensions from spleen, PP, MLN, colon, and FRT in culture media were added to wells in duplicate. Spleen, PP, and MLN were added at 250,000 cells/well. Due to the limited number of cells isolated from the FRT and colon, cells from two mice were combined and plated at 100,000 cells/well. Plates were incubated at 37˚C and 5% CO_2 for 18 hours. Following incubation, cells were discarded, wells washed with PBST, and 100 µl/ml of MPER-biotin peptide (GNEQELLELDKWASLWN-biotin, Bio-Synthesis Inc., Lewisville, TX, USA) at 1 µg/ml added to wells and incubated for 2 hours at room temperature. Wells were washed with PBST and then 100 µL/well of Streptavidin-HRP (Thermo Scientific, Rockford, IL, USA) was added and incubated for 1 hour at room temperature. Wells were washed 3x with PBST and then 3x with PBS and 100 µL/well of 0.44 µm filtered room temperature TMB for ELISPOT (Mabtech, Nacka Strand, SWE) added. Plates were incubated for 10 minutes at room temperature and the reaction stopped by washing wells with ultrapure water. Plates were dried overnight and spots counted using Cellular Technology Limited Immunospot analyzer and software (Cleveland, OH, USA).

Fifty-thousand cells from the spleen, PP, MLN, colon, and FRT were washed with staining buffer plus 1 mM EDTA, blocked with anti-mouse CD16/32 (Biolegend), and labeled with a cocktail of 7-AAD

viability staining solution (Biolegend), FITC anti-mouse CD45 (Biolegend), and Pacific Blue anti-mouse CD19 (Biolegend). Flow cytometry was performed using a Gallios flow cytometer (Beckman Coulter, Indianapolis, IN, USA). Analysis was performed using FlowJo software (Ashland, OR, USA). Gates were set using fluorescence minus one (FMO) controls after gating for live cells. $CD45^{+}CD19^{+}$ B cell percentages determined from flow cytometry analysis were used to calculate the MPER-specific IgA secreting cells per $1x10^{6}$ B cells based on the following calculation:

$$\text{spots per well} * \left(\frac{(1 * 10^{6})}{\text{cells per well} * \%\ \text{B cells}}\right)$$

2.2.2.11: MPER Antigen Specific Serum, Vaginal Wash, and Fecal Supernatant ELISA

Nunc MaxiSorp 96-well plates (Rochester, NY, USA) were coated overnight with 1 µg/ml of MPER peptide (GNEQELLELDKWASLWN, Bio-Synthesis Inc., Lewisville, TX, USA) in 15 mM Na_2CO_3 and 35 mM $NaHCO_3$ carbonate buffer at pH 9.6. The next day, wells were blocked with blocking buffer for 1 hour at room temperature, washed with PBST, and then 100 µl serum, vaginal wash, or fecal supernatant serially diluted in sample diluent added. Serum samples and fecal supernatants started at a dilution of 1:100 and vaginal wash started at a dilution of 1:1000. Plates were incubated with samples for 2 hours at room temperature, washed with PBST, and 100 µl anti-mouse IgG-HRP (serum) (Cell Signaling, Beverly, MA, USA) or anti-mouse IgA-HRP (vaginal wash or fecal supernatant) (Bethyl, Montgomery, TX, USA) in sample diluent added and incubated for 1 hour at room temperature. Wells were washed with PBST and 100 µl SureBlue Reserve TMB (Seracare, Milford, MA, USA) added for 15 min. Colorimetric reaction was stopped with 1N HCl and the absorbance measured at 450 nm – 570 nm on a plate reader.

Endpoint titers were determined using samples collected prior to LA delivery as negative controls. Titer cut offs were calculated as follows:

$$\text{average absorbance of negative samples} + (\text{standard deviation} * 99\%\ \text{confidence level multiplier})$$

Where the 99% confidence level multiplier was determined from the chart published by Frey et al. (162). Titers were considered positive if the sample value was greater than the calculated cut off.

2.2.2.12: Statistics

Significant differences between groups were determined by one-way ANOVA followed by an uncorrected Dunn's multiple comparisons test (Kruskal-Wallis test) using GraphPad Prism 8.1.0 for windows (GraphPad software, San Diego, CA, USA).

2.2.3: Results

2.2.3.1: LA-MPER FimH Construction, Surface Expression Validation, and GP2 Binding

FimH is the ligand binding domain of the type 1 *E. coli* and *Salmonella enterica* serovar Typhimurium Type I fimbriae. As a mature protein, it consists of 279 AA that form two domains: a N-terminal ligand binding domain (AA 1-156) and a C-terminal domain (AA 160-279) that complexes with the fimbriae protein FimC (163, 164). Full-length FimH has been shown to have decreased solubility without expression as a FimH-FimC complex. The N-terminal domain is readily expressible and soluble while maintaining the biologically active ligand (GP2) binding domain. Based on the solubility constraints of using full length FimH, the FimH N-terminal ligand binding domain with and without a flag-tag was cloned into plasmid pTRK1033 (146). Three plasmids were constructed and then transformed into GAD31 creating: GAD40 (FimH), GAD41 (FimH + 5'-flag tag), and GAD42 (FimH + 3'-flag tag).

Surface expression of FimH was confirmed by anti-flag western blot (GAD41 and GAD42) (Figure 2.3A) and flow cytometry (GAD40) (Figure 2.3C). MPER expression was also confirmed by flow cytometry (Figure 2.3B). All constructs showed robust expression of MPER and FimH.

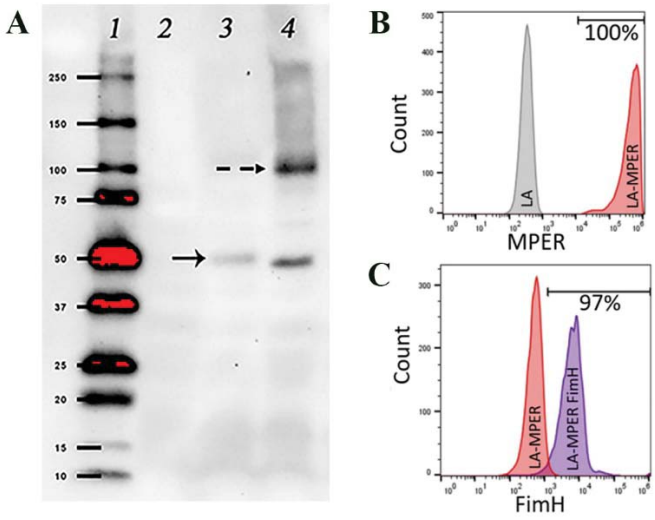

Figure 2.3. GAD40 FimH surface expression. (A) FimH surface expression was confirmed by western blot using an anti-flag antibody to detect FimH-flag on extractions of LA surface layer proteins. There is a positive band (solid arrow) that correlates to the molecular weight 44KD for both GAD41 (lane 3) and GAD42 (lane 4) compared to GAD30 (lane 2). There is an additional band (dashed arrow) present for GAD42 that corresponds to a FimH dimer. (B) MPER expression is confirmed by flow cytometry using an anti-MPER antibody. Histogram shown is LA170 (LA) versus LA-MPER (GAD31). Results are representative of all MPER expressing constructs. (C) FimH expression is confirmed by flow cytometry using an antibody specific for the FimH ligand binding domain.

While the anti-FimH antibody provided by Dr. Sorurenko is specific for the FimH ligand binding domain, it was important to evaluate the ability of the LA constructs expressing FimH to bind to GP2. Binding was assessed by an in vitro ELISA binding assay using mouse GP2 (mGP2) expressed in 293T cells and purified by His-tag. mGP2 was readily able to bind to GAD40 and GAD42 coated onto 96-well ELISA plates. mGP2 binding was significantly higher for GAD40 and GAD42 than GAD30 or PBS-only confirming that FimH surface expressed by LA retains its GP2 binding activity (Figure 2.4). The GAD41 strain did not bind mGP2 significantly higher than GAD30. It is hypothesized that the 5'-flag tag present on this construct blocked binding to mGP2. All further experiments were performed with GAD40 only.

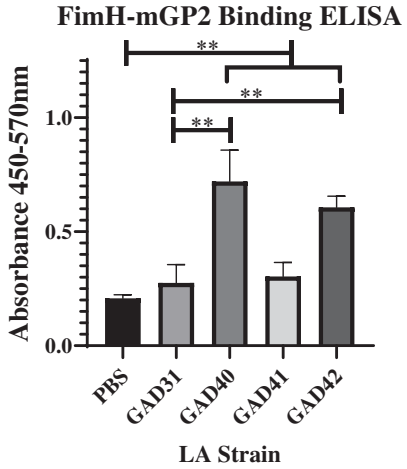

Figure 2.4. In vitro FimH LA-MPER mGP2 binding. mGP2 binding to Maxisorp plates coated overnight with GAD31, GAD40, GAD41, and GAD42 as measured by 450-570nm absorbance. mGP2 binding was significantly higher for GAD40 and GAD42 than GAD31. **p<0.05 based on a Kruskal-Wallis one-way ANOVA.
mGP2: mouse glycoprotein 2

2.2.3.2: In Vivo Mechanism of FimH Immune System Interaction

The uptake of GAD40 into PPs and trafficking to MLNs was assessed by direct delivery of GAD40 and GAD31 into an isolated section of the small intestine of Balb/cJ mice under general anesthesia utilizing the intestinal loop method. This method allows for evaluation of LA uptake and trafficking while avoiding the gastric acid and bile present in the orad gastrointestinal system which could cleave surface proteins (161). Results from the intestinal loop showed that there was no difference between uptake of GAD31 and GAD40 into PPs with robust uptake of both LA strains (Figure 2.5B). This is likely because LA possess an endogenous M-cell binding protein, uromodulin, and therefore FimH expression did not increase LA M-cell bindings and PP uptake (25). Surprisingly, FimH resulted in a significant increase in GAD40 trafficking to MLNs compared to GAD31 (Figure 2.5A). Other lactic acid bacteria have been reported to traffic to the MLN through both phagocytes and local lymphatics (49). This is the first report of LA trafficking to MLN. We hypothesize that FimH activates APCs resulting in increased GAD40 trafficking to the MLN.

To test this hypothesis, Balb/cJ mice were gavaged with cell trace violet labeled GAD31, GAD19, and GAD40. GAD19 was included as an adjuvant control to assess if the MLN trafficking was specific to FimH-expression on GAD40. MLNs were collected, processed into a single cell suspension, and analyzed

by flow cytometry. Samples were analyzed for cell trace positive (LA) events and association with $MHCII^{+}CD64^{+}$ macrophages and $MHCII^{+}CD64^{-}CD11c^{+}CD103^{+/-}$ DCs (165, 166). Flow cytometry showed that like the intestinal loop results, CD40 trafficked to MLN in larger number than CD31 (Figure 2.5C). Similar MLN trafficking was observed for GAD19 indicating that the LA trafficking to the MLN was mediated by immune activation and is not FimH specific. APC analysis showed that GAD19 and GAD40 were more likely to be associated with macrophages and DCs, especially $CD103^{+}$ DCs which are important in regulating T cell responses and adaptive immunity (Figure 2.5D).

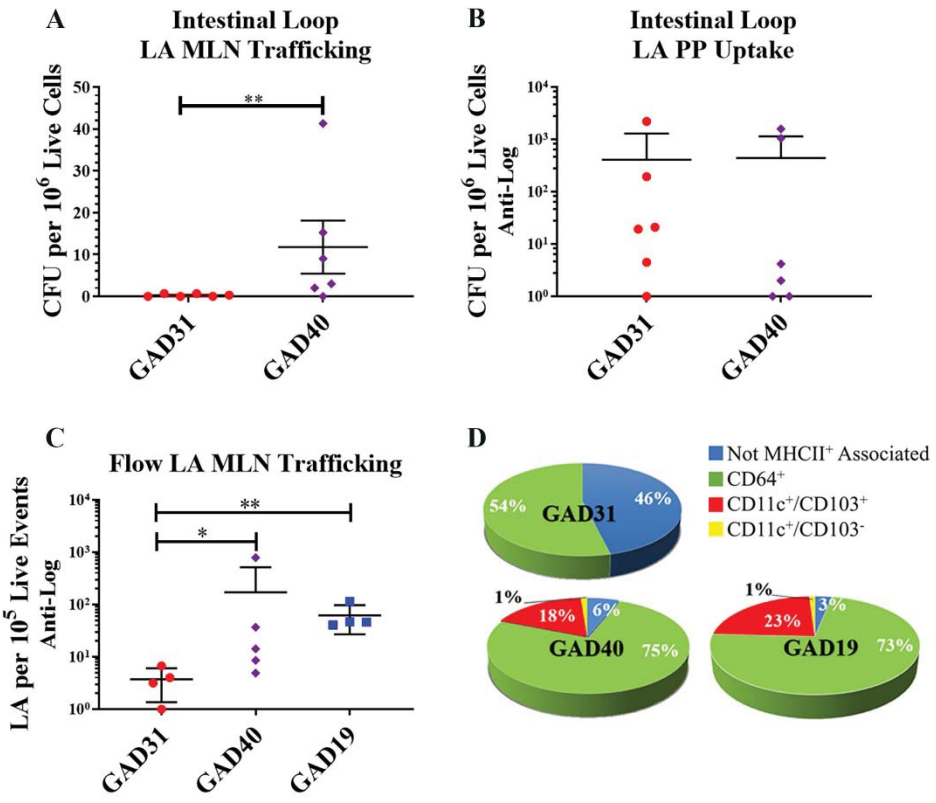

Figure 2.5. LA PP uptake and MLN trafficking. PP LA uptake and MLN LA trafficking was assessed by intestinal loop (A and B). GAD31 or GAD40 were directly inoculated into an isolated section of small intestine in anesthetized Balb/cJ mice. PP and MLN were collected and processed into single cell suspensions and plated on erythromycin resistance plates. CFU per 10^6 live cells were calculated. There was no difference in PP LA uptake between GAD31 and GAD40 (B) but a significant increase in GAD40 MLN trafficking compared to GAD31 (A). Similar increase in MLN trafficking was observed following oral delivery of cell trace violet labeled LA with adjuvanted strains (GAD40 and GAD19) compared to GAD31 (C). Analysis of APC associated with cell trace violet labeled LA showed that GAD40 and GAD19 were more likely to be associated with $MHCII^+$ cells than GAD 31 especially $CD103^+$ DCs (D). **p<0.05; *p<0.1 based on a Kruskal-Wallis one-way ANOVA.
Macrophages: $MHCII^+CD64^+$; dendritic cells (DC): $MHCII^+CD64^-CD11c^+CD103^{+/-}$
CFU: colony forming units; PP: Peyer's patch; MLN: mesenteric lymph node; LA: *Lactobacillus acidophilus*

2.2.3.3: FimH TLR4 Activation

The MLN trafficking results indicate that FimH is activating the immune system. FimH has been identified as a TLR4 ligand (157). To determine if TLR4 binding was the mechanism of GAD40 immune

activation, GAD40 was incubated with HEK-Blue TLR4 reporter cell line. TLR4 activation by GAD40 could not be detected. Control cells incubated with the TLR4 ligand, LPS, activated appropriately.

2.2.3.4: MPER-Specific Immune Response to Oral Dosing with GAD19 and GAD40

Female Balb/cJ mice were orally dosed six times over 12 weeks with $5x10^9$ CFU of GAD19 and GAD40. Immune response to vaccination was assessed by MPER-specific serum IgG and fecal supernatant and vaginal wash IgA (ELISA) as well as anti-MPER IgA-secreting $CD19^+$ B cells collected from spleen, PP, MLN, colon, and FRT (ELISPOT). FRT B-cells and vaginal wash IgA were used to assess induction of immune cell homing to mucosal sites distant from the site of immune induction (intestines). The ability of mucosal immune cells to be activated in one location and then take up residence in distant mucosal sites is known as the "common mucosal immune system." This system allows for mucosal dissemination of immune cells regardless of the site of antigen exposure and immune activation (4, 167). ELISA and ELISPOT results were compared to previously obtained GAD31 dosing results provided by Dr. Jonathan LeCureux. Dr. LeCureux's results are representative of GAD31 immune responses obtained from previous dosing experiments (151). The results show that FimH induced immune responses that were similar to those of GAD19 (Figure 2.6). GAD40 induced significantly elevated systemic and local immune responses with increased MPER-specific serum IgG and IgA-secreting MPER-specific B cells compared to GAD31.

MPER-specific IgA from fecal supernatant and vaginal wash were not significantly elevated from GAD31 for either GAD19 or GAD40 despite an increase in antigen-specific B cells at these sites. It is possible that the lack of a measurable IgA response at mucosal sites is the result of dilution that occurs in the process of collecting fecal supernatants and collecting vaginal washes. Development of assays with increased sensitivity would likely result in increased detection of MPER-specific antibodies.

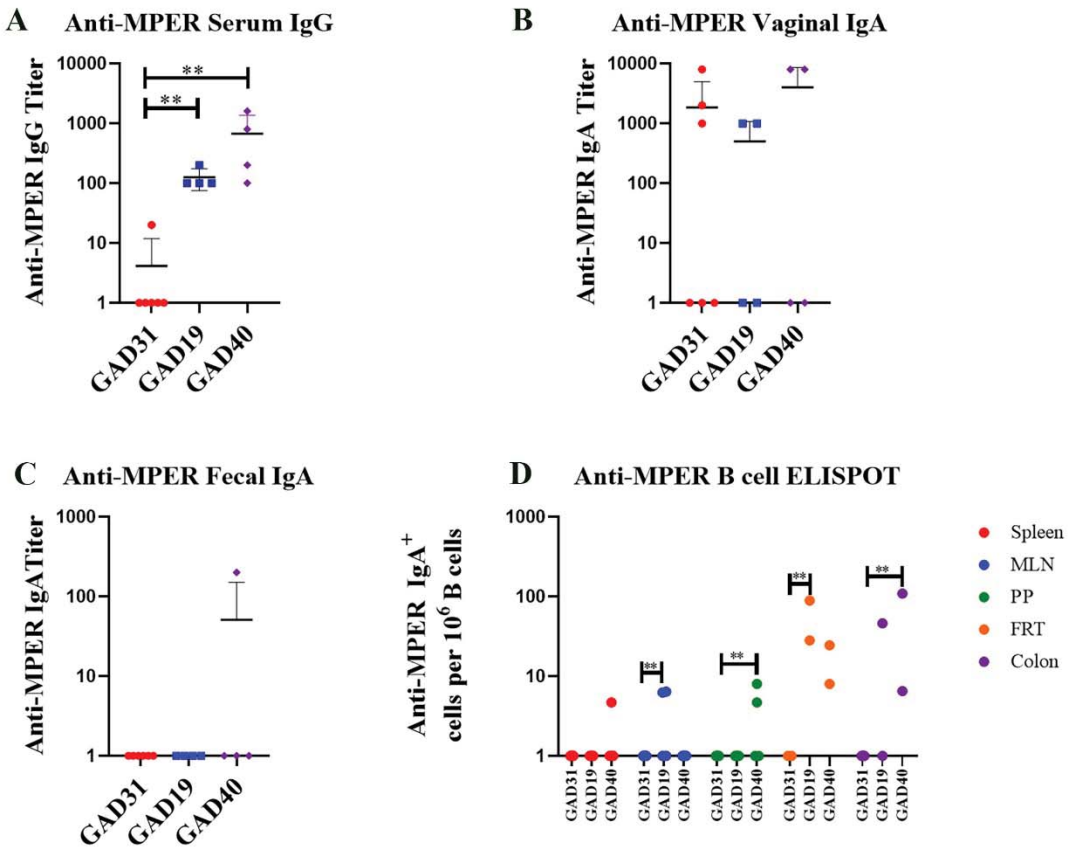

Figure 2.6. MPER-specific immune response following oral dosing. Anti-MPER immune responses in Balb/cJ mice after 6 oral doses of $5x10^9$ CFU of GAD19 and GAD40. Results are compared to previously obtained GAD31 immune responses (151). Both adjuvanted LA strains (GAD19 and GAD40) resulted in statistically increased anti-MPER serum IgG antibody responses (A) compared to GAD31. Average fecal (C) and vaginal (B) anti-MPER IgA were increased for GAD40 versus GAD31 and GAD19 (results not significant). There was a statistically significant increase in MLN and colonic MPER-specific $CD19^+$ B cells for GAD40 versus GAD31 (D). *$p<0.1$ and **$p<0.05$ based on a Kruskal-Wallis one-way ANOVA. Y-axis shown in anti-log.
MLN: mesenteric lymph node; PP: Peyer's patch; FRT: female reproductive tract

2.2.4: Discussion

The identification and development of vaccine platforms that induce robust mucosal and systemic immune responses is a high priority for the next generation of vaccines. Induction of protective mucosal immune responses are critical for preventing transmission of pathogens at mucosal sites and are best

induced locally (4). Oral vaccines are easy to deliver requiring no special training or equipment and can induce mucosal immune responses at sites such as gastrointestinal lymphoid tissue (GALT), PPs, and MLNs. Additionally, trafficking of immune cells via the "common mucosal immune system" results in protection of distant mucosal sites such as the lungs and urogenital tract. Mucosal delivered vaccines are currently available for only 6 mucosal pathogens (168). The approved vaccines are primarily modified-live or recombinant pathogens which limit use in immune sensitive populations and carry the risk of reversion to virulence. Our goal is to develop a safe and effective, orally delivered, vaccine platform that could be employed against a wide variety of mucosal pathogens.

LA as an oral vaccine vector has advantages such as endogenous gastric acid and bile resistance, mucus binding proteins, and the ability to activate innate immune responses. Additionally, the availability of tools for LA genetic modification allows for its development as a stable, sub-unit vaccine vector against numerous pathogens (47, 68, 96, 137-144). Here LA is evaluated as an oral vaccine against HIV-1 which is intriguing due to the reported protection from infection conferred by anti-envelope mucosal IgA (169, 170). Previous LA studies have shown that oral delivery of LA expressing MPER does induce local (mucosal IgA) and systemic (IgG) immune responses in mice. Anti-MPER antibodies have proven difficult to induce through peptide expression alone but the addition of adjuvants (IL-1β and FliC) have increased immune response to vaccination and show the importance of identifying and evaluating adjuvants for LA oral vaccines (47, 96).

Here we evaluated the use of the *E. coli* Type I fimbriae protein, FimH, as a LA vaccine adjuvant. Expression of the FimH N-terminal ligand binding domain on the LA surface induced anti-MPER serum IgG and mucosal IgA B cells following oral dosing in mice. The immune response was similar to those achieved with other adjuvant strains (IL-1β secretion). Of note is that the GAD40 construct showed an increased number of mice with anti-MPER specific fecal IgA and IgA secreting colonic B cells when compared to GAD19. These results suggest that FimH enhances the local (gastrointestinal) immune response. Due to the small number of animals used in this study, a larger dosing experiment would need to be performed to confirm this finding.

The lack of measurable IgA responses in some mice is a perplexing problem in this and previous studies. Prior to this study, it was hypothesized that the lack of IgA response in some mice was due to deficient PP LA uptake. The intestinal loop experiment showed that all LA strains are readily taken up into PPs. The decreased local IgA response may instead be limited by the detection method because of the dilution that occurs with collect of the vaginal and fecal samples. Methods of IgA detection with increased sensitivity could help to alleviate this issue. Functional assessment of the immune response via virus challenge following oral vaccination would provide important information about the nature of the immune response generated. Ultimately, challenge studies are needed to determine efficacy and the full potential of the LA oral vaccine.

The mechanism of increased immune response by the FimH adjuvant remains to be elucidated. Based on previously published mechanistic studies, it was predicted that the increased immune response would be due to increased uptake into PPs and/or TLR4 activation. Here we show similar levels of PP uptake for LA with and without FimH and no TLR4 activation as measured using a HEK-Blue human TLR4 cell line. The lack of TLR4 activation is surprising as it conflicts with previous studies using multiple methods to evaluate TLR4 activation (FimH-TLR4 binding ELISA, luciferase assay performed with 293 T cells expressing human TLR4, and TLR4 -/- knockout mice) (157, 171). In these FimH-TLR4 experiments, either full length FimH or bacteria expressing full length FimH were used. Protein modeling studies evaluating the TLR4 binding domain of FimH have shown that the FimH C-terminal domain has the strongest interaction with TLR4 (172). There is FimH N-terminal-TLR4 binding, but it is predicted to be weak. It is possible that the FimH N-terminal domain expressed on the surface of GAD40 is weakly activating TLR4 but at a level too low to be detected by our in vitro methods.

It is clear from the intestinal loop uptake experiment and flow cytometry analysis that FimH surface expression and IL-1β secretion results in significant increases in LA trafficking to the MLN by APCs. The increased number of GAD40 associated with APCs in the MLN is likely responsible for the increased immune response as MLNs are important sites for IgA class switching and induction of the mucosal homing integrin, α4β7 (50). The exact mechanism of APC-FimH interaction is unknown. That GAD40 and GAD19

had similar trafficking to MLN indicates that FimH is activating the innate immune system. FimH has been shown to bind to CD48 on macrophages and enhance FimH expressing bacterial survival in phagosomes (158). The interaction of GAD40 with CD48 requires further investigation.

In conclusion, FimH expressed on the surface of LA acts as a mucosal adjuvant increasing mucosal and systemic immune responses to the poorly immunogenic peptide HIV-1 MPER. FimH can be added to the growing list of proteins that can increase the immune response induced by a LA oral vaccine. The ability to modify LA to induce more robust immune responses to oral vaccination shows the potential of LA as a powerful mucosal vaccine vector.

2.3: *Lactobacillus acidophilus* as an Oral Vaccine Against Rotavirus

2.3.1: Introduction

Diarrheal illness is the second leading cause of death in children age 5 and under worldwide and rotavirus is responsible for 40 percent of hospitalizations due to diarrheal illness. It is estimated that rotavirus killed approximately 215,000 children in 2013 (173). The World Health Organization recommends including a rotavirus vaccine in all global vaccination protocols but only two vaccines are licensed worldwide, both are attenuated live (174).

In addition to the inherent risks of attenuated vaccines which include reversion to virulence, recombination with circulating viruses, and safety in immune sensitive populations, both vaccines have limited efficacy (50-60%) in developing countries leaving millions of children at risk for rotavirus infection and diarrheal illness (175). The cause of the decrease response to attenuated live rotavirus vaccines in developing countries is unknown. Factors such as mal/undernutrition, differences in microbiome, co-infection with enteric pathogens, increased incidence of the subclinical condition environmental enteric dysfunction (EED), and material antibody interference are believed to play a role (176, 177). It is acknowledged that a new generation of vaccines is needed to overcome these many obstacles and provide protection for at risk populations.

IgA plays a key role in mucosal protection against rotavirus infection in humans and animal models. Mucosal immunization by orally delivered vaccines is the most effective means to induce mucosal IgA, however there is a paucity of vaccine platforms that have been prove to be safe and immunogenic (178-183). We have developed an orally delivered mucosal vaccine platform that employs the commensal probiotic bacterium *Lactobacillus acidophilus* (LA). This platform offers several important feasibility advantages as a rotavirus vaccine since LA is a commensal designated as GRAS (generally regarded as safe) by the FDA, is relatively inexpensive to produce, does not require cold-chain, and is needleless. Additionally, probiotic ingestion has been shown to improve immune response to the current rotavirus vaccinates and decrease disease associated diarrhea (184-186). These characteristics make a subunit

rotavirus vaccine based on the LA platform a strong candidate to address the current gaps in global rotavirus vaccination.

As described in section 2.1, our LA mucosal vaccine vector can induce both local and systemic immune responses to poorly immunogenic linear epitopes expressed within the LA surface layer protein, SlpA. We also have LA strains that express mucosal adjuvants to enhance the immune response to vaccination including: the inflammasome product and proinflammatory cytokine IL-1β, the Toll-like receptor (TLR) 5 ligand *Salmonella enterica* serovar Typhimurium flagellin (FliC), and the *E. coli* type I pilus microfold (M) cell targeting protein FimH (47, 96). Rotavirus LA vaccine development is well informed by known correlates of protection attributed to antibody responses against specific rotavirus peptides/proteins (187-189). Many peptide targets of protective antibodies are from the VP4 capsid trypsin cleavage fragment, VP8. Indeed, protection by the current attenuated live RV vaccines is primarily attributed to antibody responses against VP8 (190).

Here we report the results of the construction of a LA rotavirus vaccine incorporating a 10 amino acid (AA) epitope from the N-terminus of the VP8 capsid protein (VP8pep). This epitope is highly conserved among type A rotavirus and can neutralize rotavirus providing protecting from infection and disease (187). Systemic and local (mucosal) anti-VP8pep immune responses were evaluated following oral dosing in Balb/cJ mice utilizing LA strains with and without mucosal adjuvants. To assess differences in immune activation and response to our mucosal adjuvants, cytokine responses at the local immune induction sites were also evaluated.

2.3.2: Materials and Methods

2.3.2.1: LA VP8pep Strain Construction

LA with a 10 AA epitope from the RV capsid protein VP8 (VP8pep) inserted into the slpA protein was constructed based on the published double crossover method (47, 136, 145). Briefly, the 10 AA epitope (MASLIYRQLL) was constructed with the primer pairs: AK_63 and AV_49 or AV_50 and AK_64 (Table

2.3) using the previously constructed plasmid pTRK1053 as template DNA (47). The PCR products were gel purified and then further amplified using primers AK_63 and AK_64. The PCR product and pTRK1053 were restriction digested with the enzymes *Bam*HI and *Hind*III and then ligated to form plasmid pTRK-AV05. pTRK-AV05 was transformed into α-5 competent *E. coli*, positive transformants selected via antibiotic resistance, and plasmid confirmed by PCR and sequencing. Following plasmid confirmation, pTRK-AV05 was transformed into *L. acidophilus* NCK1910 Δupp mutant by electroporation. The slpA gene was replaced by double crossover as described in Figure 2.1. 5-fluorouracil resistant LA were confirmed for slpA-VP8pep recombinants by PCR and sequencing. The confirmed mutant strain is referred to as GAD80 (Table 2.1).

Table 2.3. VP8pep primers.

Primer	Sequence	Reference
AK_63	TTT TAA GCT TCA TCT GAG GAT AAA GTT GTT TGA T	(47)
AV_49	CAA GAA GCT GTC TAT AAA TCA AAC TGG CCA TAC CGG TGA ATT TTA CAT TT	Here
AK_64	TTT TGG ATC CGA ATC GAA GTA TCA GAA GAT CC	(47)
AV_50	GCT TCT TGC AAA CAG TGA TAA TCA AAC	Here

GAD80 was further used to create strains GAD81 (secretion of mouse IL-1β), GAD82 (prt-FliC), and GAD83 (mub-FimH) by electroporation of plasmids pGAD17, pTRK1034, and pTRK-AV40 (47, 146). Positive transformants were selected by antibiotic resistance and confirmed by PCR.

2.3.2.2: VP8pep, FliC, and FimH Flow Cytometry

GAD80, GAD81, GAD82, and GAD83 expression of RV VP8pep, FliC, and FimH surface expression was confirmed by flow cytometry. Wild type (WT) LA and GAD80-83 were grown to exponential phase from overnight cultures and washed with PBS. LA was resuspended in PBS and colony

forming units (CFU) calculated based on the optical density at 600nm. $1x10^7$ CFU LA were suspended in staining buffer (PBS + 1% fetal bovine serum (FBS)) plus the primary antibody (listed on Table 2.4) and incubated on ice. LA were washed with PBS, the primary antibody detected with the appropriate secondary antibody (listed on Table 2.4) and incubated on ice, LA were washed twice, resuspended in PBS, and flow cytometry was performed using a Gallios flow cytometer (Beckman Coulter, Indianapolis, IN, USA). Analysis was performed using FlowJo software (Ashland, OR, USA). Gates were set using LA labeled only with the secondary antibodies.

Table 2.4. Primary and secondary antibodies for LA surface expression detection.

Strain	Primary	Manufacturer	Secondary	Manufacturer
GAD80, 81, 82, 83	Rabbit anti-VP8pep	Genscript (Piscataway, NJ, USA)	Donkey anti-rabbit FITC	Bioledgend (San Diego, CA, USA)
GAD82	Mouse anti-Salmonella FliC	Bioledgend (San Diego, CA, USA)	Goat anti-mouse PE	Invitrogen (Waltham, MA, USA)
GAD83	Mouse anti-FimH	Gift from Dr. Svgeni V. Sorurenko (University of Washington, Seattle, WA)	Goat anti-mouse PE	Invitrogen (Waltham, MA, USA)

2.3.2.3: Mouse IL-1β Cytokine ELISA

Mouse IL-1β secretion by GAD81 was confirmed by commercial mouse IL-1 beta uncoated ELISA (Invitrogen, Waltham, MA, USA). GAD80 and GAD81 were grown overnight at 37°C in MRS broth plus erythromycin. Overnight growth media was mixed with the provided ELISA/ELISPOT diluent at a 1:500, 1:1000, and 1:2000 dilution and 100 µl added to Nunc MaxiSorp 96-well plates (Rochester, NY, USA) coated overnight with the provided anti-IL-1β antibody in duplicate. The plate was prepared and developed according to the manufacturers recommended protocol. IL-1β concentration was calculated based on the kit standard diluted at a range of 2300 to 17.97 pg/ml.

2.3.2.4: Ethics Statement and Mouse Usage

All experiments involving the use of animal complied with all relevant regulations and the guidelines and approval of Colorado State University's Institutional Animal Care and Use Committee

(IACUC 18-8061A). Animals were monitored daily and all animals were euthanized at the end of studies by either carbon dioxide inhalation followed by cervical dislocation.

All mice were wild type male and female Balb/cJ obtained from Jackson Laboratories (Bar Harbor, ME, USA). Mice were maintained in specific pathogen-free conditions, housed socially in single sex groups (2-5 mice per cage) in commercially available individually ventilated cages, and provided with autoclaved bedding and enrichment. Animals were fed ad libitum commercially irradiated rodent chow (Teklad Global, Envigo, Indianapolis, IN, USA) and tap water filtered via reverse osmosis in autoclaved water bottles. Animals were tracked and monitored daily for any signs of stress or illness.

2.3.2.5: Mouse Dosing Experiment and Tissue Collection and Processing

LA were grown for 16-18 hours at 37°C in MRS plus erythromycin and washed with PBS. CFUs were calculated based on the optical density at 600nm and LA suspended at $5x10^9$ CFU/ml in dosing buffer (100 mM sodium bicarbonate buffer and 1 M trypsin inhibitor (Sigma-aldrich, Darmstadt, DEU)). 10 to 12-weeks-old male and female Balb/cJ mice were orally dosed with 200 µl LA for a total of $1x10^9$ CFU of WT LA, GAD80, GAD81, GAD82, or GAD83 delivered. An additional group of mice were dosed with 200 µl of dosing buffer only. Mice were dosed on three sequential days, every other week for 12 weeks. Prior to the first day of dosing, samples were collected for antibody analysis. Serum was collected by tail vein bleed and fecal supernatant collected following centrifugation of fecal samples homogenized in PBS plus 1X protease inhibitor (ProteaseArrest, G Biosciences, St. Louis, MO, USA). All samples were held at -80°C until analysis.

Two weeks following the final oral LA dose, mice were gavaged one additional time and then euthanized. The spleen, Peyer's patches (PP), mesenteric lymph node (MLN), and colon were collected in RPMI supplemented with glutamine, HEPES, penicillin, and streptomycin. Tissues were processed into single cell suspensions. PP and spleen were mechanically disrupted using a GentleMACS dissociator (Miltenyi Biotec, Auburn, CA, USA) and MLN mechanically disrupted by mashing through a 100 µm cell strainer. The colon was processed based on the method described by Stoeker et al. (97). Briefly, the colon

had the fat/mesentery removed by careful dissection, tissues were suspended in PBS with 1 mM dithiothreitol (DTT) and 5 mM ethylenediaminetetraacetic acid (EDTA), and lumens gently brushed to remove debris and mucus. Using scissors, the tissues were cut into less than 1 mm pieces which were suspended in culture media (RPMI supplemented with 10% FBS, glutamine, HEPES, 2-mercaptoethanol, sodium pyruvate, essential and non-essential amino acids, penicillin, and streptomycin) plus 125 µg/ml Liberase TM (Sigma-Aldrich, Darmstadt, DEU) and 100 µg/ml DNase I (Sigma-Aldrich, Darmstadt, DEU) followed by agitation using a GentleMACS dissociator. Tissues were incubated at 37°C for 30 min with gentle rocking. Suspensions were filtered and cells isolated by Percoll gradient.

All processed samples were filtered and live cells counted using a Cellometer Auto200 (Nexcelom Bioscience, Lawrence MA, USA). Cells were stored on ice in culture media until ELISPOT plate set-up and flow analysis.

2.3.2.6: VP8pep Antigen Specific ELISPOT

24 hours prior to tissue collection and processing, ELISPOT plates (MultiScreen Filter Plates, EMD Millipore, Burlington, MA, USA) were prepared according to the manufacturer's recommendations, coated with 10 µg/ml anti-IgA antibody (ELISpot^{Plus} Kit, Mabtech, Nacka Strand, SWE), and incubated at 4˚C overnight. On the day of tissue collection and processing, plates were washed with PBS and blocked with culture medium for at least 1 hour at 37˚C. Cell suspensions from spleen, PP, MLN, and colon in culture media were added to wells in duplicate. Spleen and MLN were added at 250,000 cells/well and cells from the colon and PP were plated at 100,000 cells/well. Plates were incubated at 37˚C and 5% CO_2 for 18 hours. Following incubation, cells were discarded, wells washed with PBS + 0.05% Tween20 (PBST), and 100 µl/ml of VP8-biotin peptide (MASLIYRQLL-biotin, Bio-Synthesis Inc., Lewisville, TX, USA) at 1 µg/ml added to wells and incubated for 2 hours at room temperature. Wells were washed with PBST and then 100 µL/well of Streptavidin-HRP (Thermo Scientific, Rockford, IL, USA) was added and incubated for 1 hour at room temperature. Wells were washed 3x with PBST and then 3x with PBS and 100 µL/well of 0.44 µm filtered room temperature TMB for ELISPOT (Mabtech, Nacka Strand, SWE) added. Plates were incubated

for 10 minutes at room temperature and the reaction stopped by washing wells with ultrapure water. Plates were dried overnight, and spots counted using Cellular Technology Limited Immunospot analyzer and software (Cleveland, OH, USA).

50,000 cells from the spleen, PP, MLN, and colon on the day of isolation were washed with staining buffer plus 1 mM EDTA, blocked with anti-mouse CD16/32 (Biolegend), and labeled with a cocktail of 7-AAD viability staining solution (Biolegend), FITC anti-mouse CD45 (Biolegend), and Pacific Blue anti-mouse CD19 (Biolegend). Flow cytometry was performed using a Gallios flow cytometer (Beckman Coulter, Indianapolis, IN, USA). Analysis was performed using FlowJo software (Ashland, OR, USA). Gates were set using fluorescence minus one (FMO) controls after gating for live cells. $CD45^{+}CD19^{+}$ B cell percentages determined from flow cytometry analysis were used to calculate the VP8pep-specific IgA secreting cells per $1x10^{6}$ B cells based on the following calculation:

$$\text{spots per well} * \left(\frac{(1 * 10^{6})}{\text{cells per well} * \%\ \text{B cells determined by flow cytometry}}\right)$$

2.3.2.7: VP8pep Antigen Specific Serum and Fecal Supernatant ELISA

Nunc MaxiSorp 96-well plates (Rochester, NY, USA) were coated overnight with 1 µg/ml of VP8pep (MASLIYRQLLC, Genscript, Piscataway, NJ, USA) in 1x PBS. The next day, wells were blocked with 1% bovine serum albumin (BSA) in PBS for 1 hour at room temperature, washed with PBST, and then 100 µl serum or fecal supernatant serially diluted in sample diluent (PBST plus 1% BSA) added. Serum samples started at a dilution of 1:50 and fecal samples started at a dilution of 1:25. Plates were incubated with samples for 2 hours at room temperature, washed with PBST, and 100 µl anti-mouse IgG-HRP (serum) (Cell Signaling, Beverly, MA, USA) or anti-mouse IgA-HRP (fecal supernatant) (Bethyl, Montgomery, TX, USA) in sample diluent added and incubated for 1 hour at room temperature. Wells were washed with PBST and 100 µl SureBlue Reserve TMB (Seracare, Milford, MA, USA) added for 15 min. Colorimetric reaction was stopped with 1N HCl and the absorbance measured at 450 nm – 570 nm on a plate reader.

Endpoint titers were determined using samples collected prior to LA dosing as negative controls. Titer cut offs were calculated as follows:

$$\text{Average Absorbance of Negative Samples} + \text{Standard Deviation} * 95\% \text{ Confidence Level Multiplier}$$

Where the 95% confidence level multiplier was determined from the chart published by Frey et al. (162). Titers were considered positive if the sample value was greater than the calculated cut off.

2.3.2.8: Quantitative Real-Time PCR Cytokine Evaluation

Isolated MLN and PP cells that were not used for ELISPOT analysis (between $1x10^6$ and $1x10^7$ live cells) were washed once with cold 1x PBS, centrifuged, and the pellet frozen at -80°C. RNA was extracted using the Quick-RNA MiniPrep extraction kit (Zymo Research, Irvine, CA, USA) based on the manufacturers recommended protocol. RNA concentrations were determined using the Qubit RNA Broad-Range Assay Kit (Invitrogen, Waltham, MA, USA). RNA was diluted to 5 ng/ul and frozen at -20°C until qRT-PCR assay.

The qRT-PCR assay was run in skirted 96-well PCR plates (Bio-Rad, Hercules, CA, USA) using Luna Universal Probe One-Step RT-qPCR SuperMix (New England Biolabs, Ipswich, MA, USA). MLN and PP extracted RNA was evaluated for expression of the cytokines TGF-β, aldh1a1 (retinaldehyde dehydrogenase 1), aldh1a2 (retinaldehyde dehydrogenase 2), tnfnf13b (B cell activating factor (BAFF)), IL-21, IL-6 and the housekeeping genes HRPT and B2m using primer pairs and probes predesigned by Integrated DNA Technologies (Coralville, IA, USA). Primer pairs and probes are reported in Table 2.5. Primer efficiencies ranged from 93-107%. All samples were randomized and run in duplicate with a pooled interplate control sample. Additionally, the SPUD assay was performed on each sample to screen for the presence of inhibitors (191). Plates were run on BioRad CFX96 Touch Real-Time PCR Detection System and results analyzed using BioRad CFX Maestro Software.

Cytokines were normalized to averages of the housekeeping genes HPRT and B2m. Fold change in cytokine expression was determined by calculating the Ct compared to the dosing buffer only mouse group and then transformed using log2.

Table 2.5. Cytokine primer pairs and probe sequences.

Gene	Primer Sequences	Probe Sequence
HPRT Exon: 6-7	5'-AAC AAA GTC TGG CCT GTA TCC-3' 5'-CCC CAA AAT GGT TAA GGT TGC-3'	5'-/56-FAM/CTT GCT GGT/ZEN/GAA AAG GAC CTC TCG GAA/3IABkFQ/-3'
B2m Exon: 1-2	5'-GGG TGG AAC TGT GTT ACG TAG-3' 5'-TGG TCT TTC TGG TGC TTG TC-3'	5'-/56-FAM/CCG GAG AAT/ZEN/GGG AAG CCG AAC ATA C/3IABkFQ/-3'
TGFb1 Exon: 1-2	5'-CCG AAT GTC TGA CGT ATT GAA GA-3' 5'-GCG GAC TAC TAT GCT AAA GAG G-3'	5'-/5HEX/ATA GAT GGCZEN/GTT GTT GCG GTC CA/3IABkFQ/-3'
Tnfsf13b Exon: 6-7	5'-TCA TCT CCT TCT TCC AGC CT-3' 5'-GAC CCT GTT CCG ATG TAT TCA G-3'	5'-/56-FAM/ACA CTG CCC/ZEN/AAC AAT TCC TGC TAC T/3IABkFQ/-3'
Aldh1a1 Exon: 11-13	5'-ACC CAG TTC TCT TCC ATT TCC-3' 5'-CAT CAC TGT GTC ATC TGC TCT-3'	5'-/56-FAM/ACA CTG CCC/ZEN/AAC AAT TCC TGC TAC T/3IABkFQ/-3'
Aldh1a2 Exon: 8-9	5'-CAC TGG CCT TGG TTG AAG A-3' 5'-GAA GTA ACC TGA AGA GAG TGA CC-3'	5'-/5HEX/AGA TGC TGA/ZEN/CTT GGA CTA CGC TGT G/3IABkFQ/-3'
IL21 Exon: 1-3	5'-GGT TTG ATG GCT TGA GTT TGG-3' 5'-TGA CTT GGA TCC TGA ACT TCT ATC-3'	5'-/5HEX/TGC TCA CAG/ZEN/TGC CCC TTT ACA TCT T/3IABkFQ/-3'
IL6 Exon: 4-5	5'-TCC TTA GCC ACT CCT TCT GT-3' 5'-AGC CAG AGT CCT TCA GAG A-3'	5'-/56-FAM/AGT TAA CCC/ZEN/ACA CCA CCC CAG C/3IABkFQ/-3'

2.2.2.9: Statistics

Significant differences between groups were determined by one-way ANOVA followed by an uncorrected Dunn's multiple comparisons test (Kruskal-Wallis test) using GraphPad Prism 8.1.0 for windows (GraphPad software, San Diego, CA, USA). Correlation calculations were also performed using GraphPad Prism.

2.3.3: Results

2.3.3.1: LA VP8pep Strain Construction

The RV VP8 N-terminal 10 amino acid peptide (MASLIYRQLL) was selected for LA vaccine development based on its identification as a neutralizing epitope against the human RV Wa strain following fine mapping studies of linear neutralizing epitopes from VP8 (187). VP8 sequence analysis of four type A RV (Human Wa, Human Venezuela, Simian Agent 11, and Murine) identified these 10 N-terminal AA as

conserved, making it an excellent epitope for evaluation in a mouse model of rotavirus vaccination and infection (Figure 2.7).

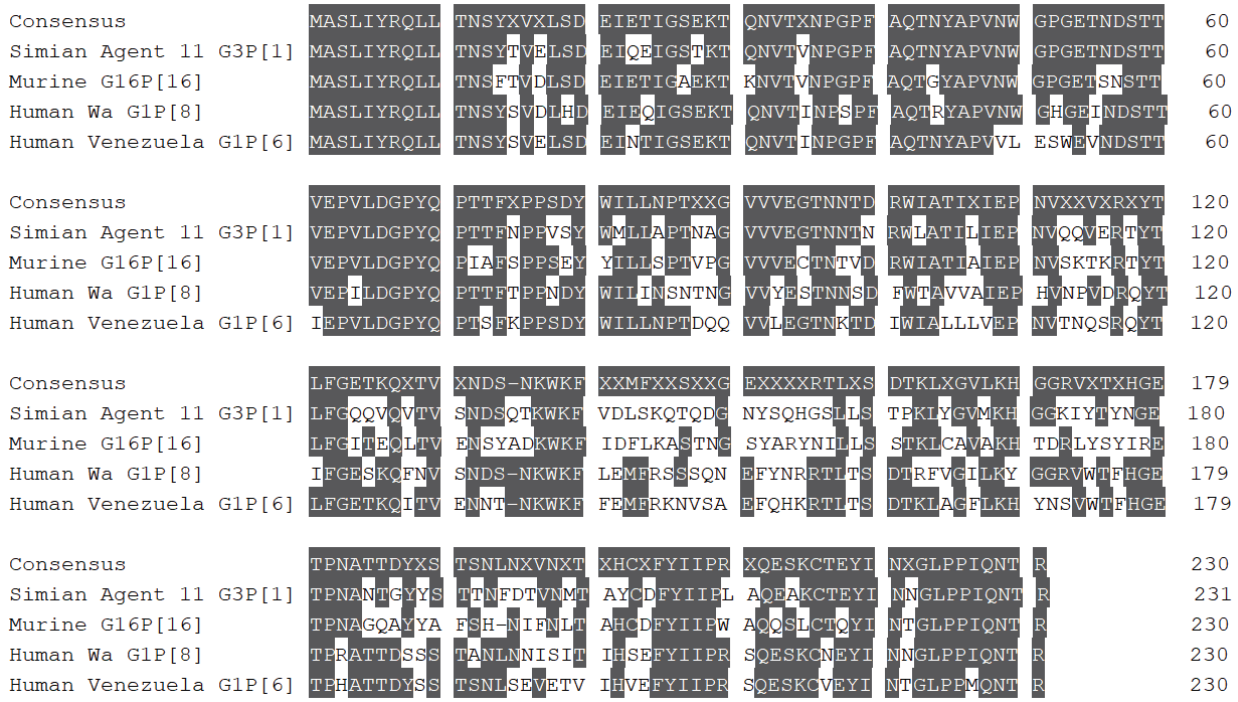

Figure 2.7. Rotavirus A VP8 sequence alignment. Protein alignment of the VP8 trypsin cleavage fragment of VP4 from two human, a murine, and a simian type A rotavirus. Highlighted amino acids are conserved. Protein sequence similarities range from 52.8-67.4%. The N terminal 10 amino acids have been found to be a neutralizing epitope and have a conserved protein sequence among type A rotaviruses. Uniport Knowledgebase (UniPortKB): Murine: Q83440; Human WA G1P[8]: P11193; Human Venezuela G1P[6]: P11197; Simian agent 11: P0C6Y9. Sequence alignment performed by Geneious Prime V11.03+7 (Auckland, NZ).

The 10 N-terminal AA from peptide VP8 (VP8pep) was inserted into the LA SlpA protein as previously described by Kajikawa et al. utilizing the LA NCFM Δupp double-crossover method (Figure 2.1) (47, 136). LA surface expression of VP8pep was confirmed by flow cytometry using an antibody specifically raised against the VP8pep sequence by Genscript. Flow cytometry showed robust surface expression of the VP8pep on the LA surface of 100% of bacteria with no cross reaction to WT LA (Figure 2.8A). Adjuvant strains were created by transformation of VP8pep-expressing LA with plasmids for surface

expression of *Salmonella spp.* FliC or *E. coli* FimH or secretion of the mouse IL-1β cytokine. Surface expression of FliC (GAD82) and FimH (GAD83) were confirmed by flow cytometry which detected the proteins on greater than 95% of LA containing the expression plasmid (Figure 2.8 B and C). Mouse IL-1β secretion was confirmed by anti-IL-1β ELISA on bacterial culture supernatants. Overnight growth culture supernatants were measured at 187 ng/ml for LA GAD81 compared to 0 ng/ml for GAD80. All developed VP8pep expressing LA strains are summarized in Table 2.1.

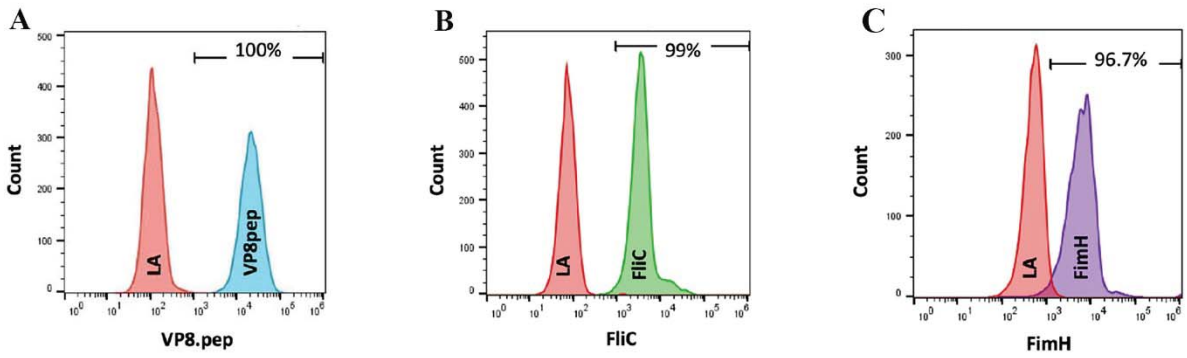

Figure 2.8. LA surface expression of VP8 10 amino acid peptide (VP8pep) (A), *Salmonella* spp. FliC (B), and *E. coli* FimH (C). LA surface expression was assessed by flow cytometry using anti-VP8pep, anti-FliC, and anti-FimH antibodies (Table 2.4). All strains showed greater than 95% expression when compared to WT LA (LA) only.

2.3.3.2: Immune Response to LA-VP8pep Oral Dosing

Female and male Balb/cJ mice were orally dosed six times over 12 weeks with WT LA, GAD80, GAD81, GAD82, GAD83, or dosing buffer only. Serum and fecal supernatants were collected for anti-VP8 IgG and IgA responses to vaccination assessed by ELISA. Induction of VP8pep-specific IgA-producing B cells was determined by ELISPOT performed on single cell suspensions isolated from the spleen, MLN, PP, and colon. We found that there was significantly elevated serum anti-VP8pep IgG for GAD80 and GAD83 compared to mice dosed with buffer only (Figure 2.9A). GAD82 had significantly elevated fecal IgA than mice dosed with LA WT or GAD81 (Figure 2.9B). The presence of anti-VP8pep antibodies in the serum and feces of buffer and WT LA groups was unexpected.

ELISPOT did not identify VP8pep-specific IgA B cells in the spleen, MLN, or PP for any of the treatment groups. There was significant increase in colonic VP8pep-specific IgA B cells in mice dosed with GAD80, GAD82, and GAD83 compared to dosing buffer and WT LA dosed mice (Figure 2.9C). GAD81 dosed mice also had increased VP8pep-specific IgA B cells but these results were not significant. The ELISPOT results show that all vaccine strains were able to induce specific immune responses to VP8pep.

None of the ELISA or ELISPOT results showed significantly increased immune response to vaccination between GAD80 and adjuvanted vaccine strains. Average fecal IgA responses and number of colonic VP8pep-specific IgA B cells were increased for GAD82 and GAD83 compared to GAD80 suggesting that the adjuvants may have increased individual titers or specific B cell numbers compared to GAD80. All mice in the GAD80 group had detectable anti-VP8 IgA fecal titers consistent with 100% response to vaccination in this group.

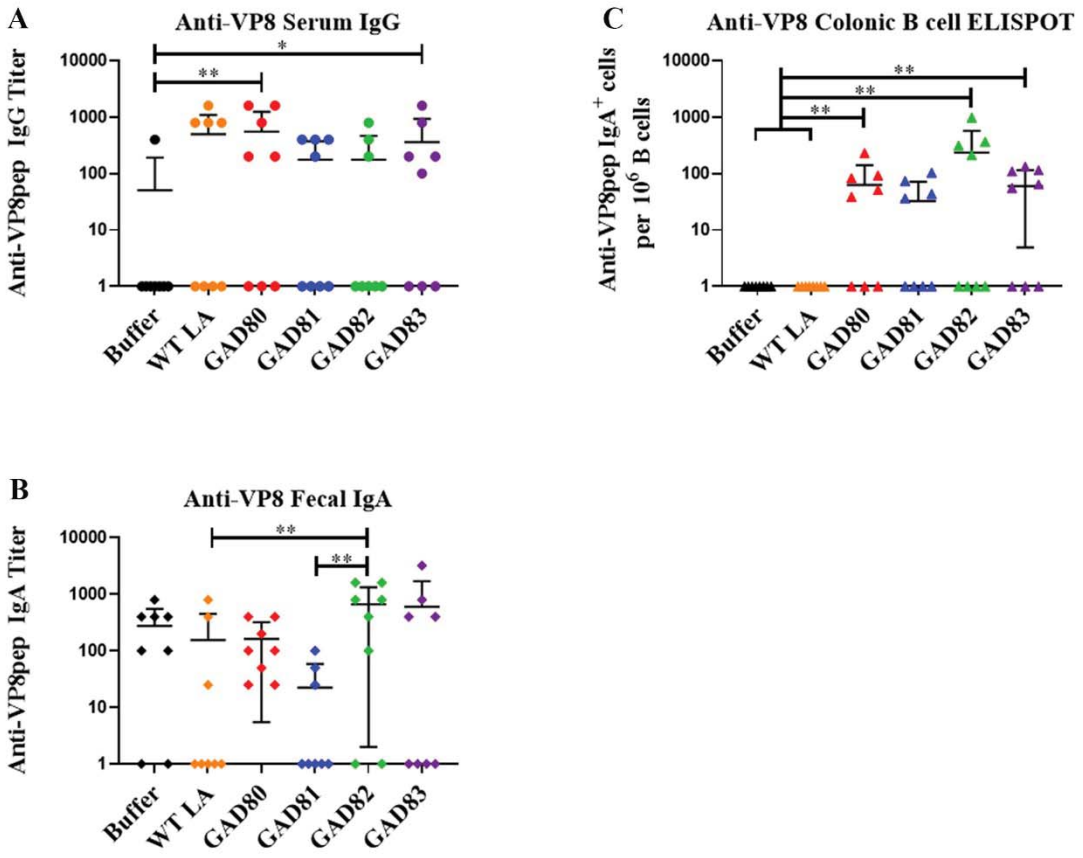

Figure 2.9. VP8pep-specific immune response following oral dosing. Anti-VP8pep end point serum IgG (A), fecal IgA (B), and VP8pep-specific IgA colonic B cells (C) in Balb/cJ mice after 6 oral doses of dosing buffer, WT LA, GAD80, GAD81, GAD82, or GAD83. GAD80, GAD83, and GAD82 had significantly elevated IgG or IgA antibody responses as measured by ELISA and increased VP8pep-specific IgA B cells isolated from the colon compared to mice who had been dosed with either buffer or WT LA only. These results confirm an immune response to the VP8 10 AA peptide embedded within the LA surface layer protein. *$p<0.1$ and **$p<0.05$ based on a Kruskal-Wallis one-way ANOVA. Y-axis shown in anti-log.
WT LA: wild type *Lactobacillus acidophilus*

2.3.3.3: Cytokine Expression

To evaluate the effects the LA vaccine and adjuvants had on cytokines important for IgA class switch and secretion, we measured the mRNA levels of selected cytokines in the MLN and PPs. Cytokines evaluated included: TGF-β, Tnfnf13b (BAFF), aladh1a1 (retinaldehyde dehydrogenase 1), aladh1a2 (retinaldehyde dehydrogenase 2), IL-6, and IL-21. Cytokine levels were measured 18 hours after delivery

of the final vaccine dose and are reported as fold change compared to mice gavaged with dosing buffer only (Figure 2.10 A and B).

Significant differences were observed for all adjuvanted vaccine strains compared to GAD80. The cytokine fold change was the most striking in the PP. GAD82 and GAD83 had significantly decreased levels of TGF-β and IL-21 than GAD80 and GAD81 in the PP. Similar significant decreases in IL-21 were found in the MLN. In both the PP and MLN, GAD82 and GAD83 had significantly elevated levels of retinaldehyde dehydrogenase 1 (aldh1a1). GAD82 had elevated BAFF in the PP and GAD81 had significantly elevated IL-6 in both the PP and MLN.

Using a nonparametric Spearman correlation, no association was found between serum or fecal antibody responses and cytokine levels.

A **Peyer's Patch**

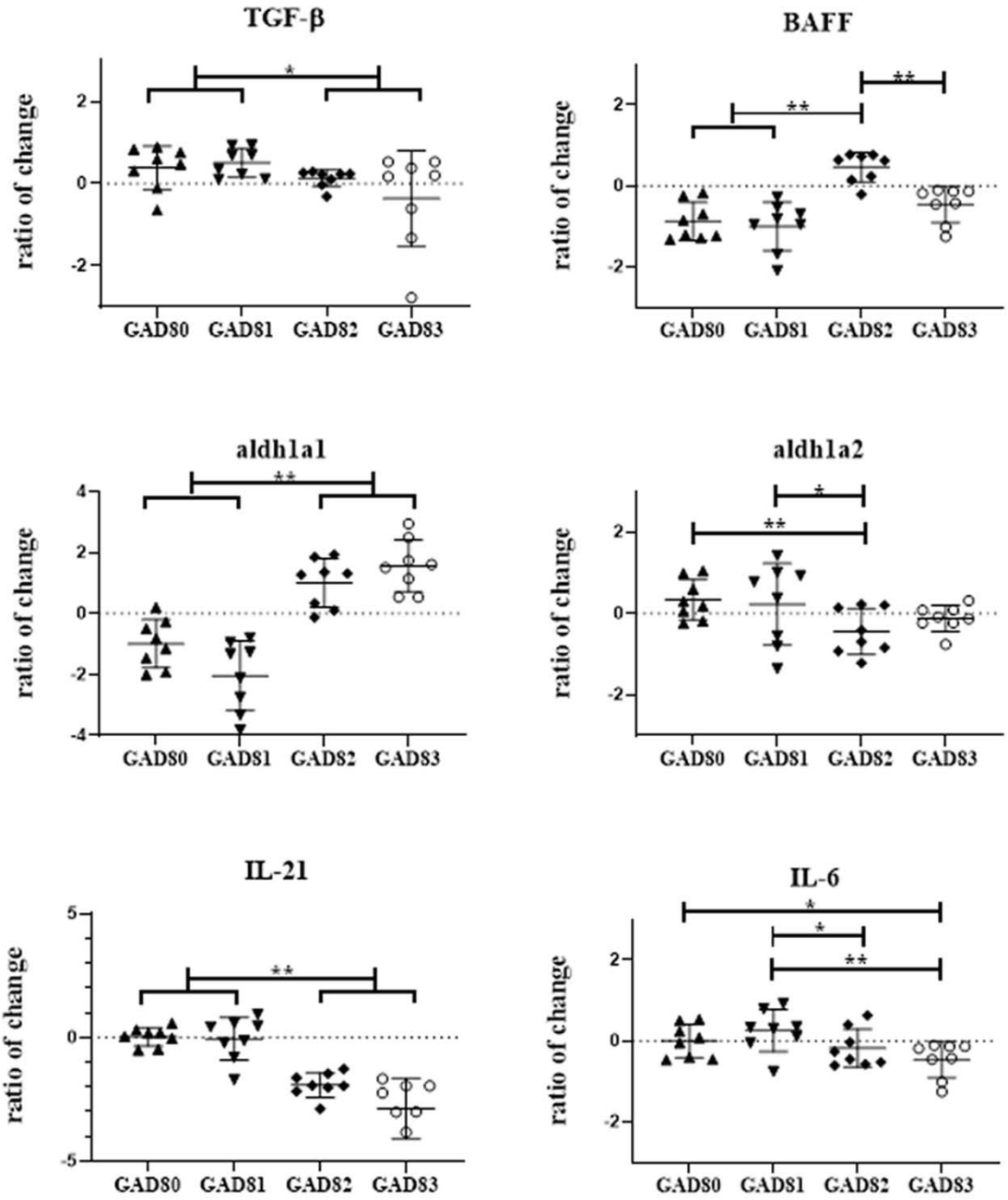

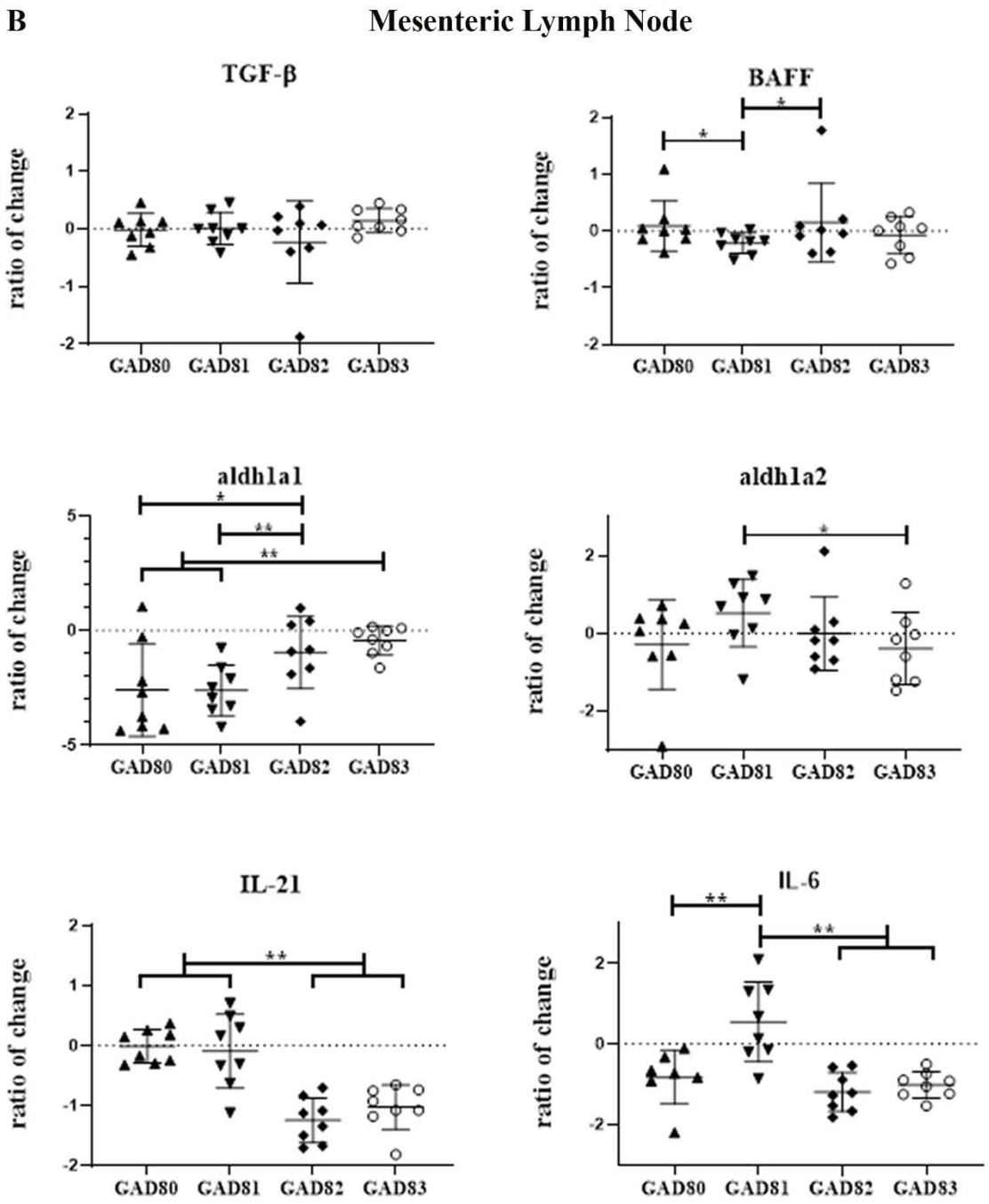

Figure 2.10. Peyer's patch and mesenteric lymph node cytokine expression following oral dosing. PP (A) and MLN (B) cytokine fold change compared to mice gavaged with dosing buffer only. There were significant differences in cytokine changes for all LA strains. *p<0.1 and **p<0.05 based on a Kruskal-Wallis one-way ANOVA. Y axis shown in Log_2

2.3.4: Discussion

The development of the next generation of rotavirus vaccines is key to preventing death and diarrheal illness in at-risk children. The lack of vaccine efficacy in many developing counties leaves these children susceptible even in the face of large vaccination campaigns. Decreasing rotavirus diarrheal episodes is also essential as diarrhea may predispose to malnutrition and stunting which can have negative effects on cognitive development and health (192, 193). There has been a call for methods that move away from attenuated live vaccines and research into new rotavirus vaccination methods are an active area of investigation. Subunit and parentally delivered vaccines are being evaluated with some candidates currently in clinical trials (194). Parenteral vaccines are of interest as there are many excellent adjuvant options and their use would avoid the differences in the gastrointestinal tract that may influence the immune response in non-responder children. The importance of IgA in preventing rotavirus infection and disease cannot be overlooked and, unfortunately, these parenteral vaccine strategies are unable to induce a robust IgA response. Development of oral vaccine vectors is essential.

Here we show the potential of LA to act as a subunit vaccine vector against rotavirus. LA was amenable to SlpA insertion of a 10 AA neutralizing epitope from the VP8 RV capsid protein that has been shown to induce neutralizing antibodies (187). Oral vaccination of LA-VP8pep in mice with and without mucosal adjuvants resulted in increased serum and mucosal anti-VP8pep antibodies and IgA-secreting colonic B cells.

The ELISPOT results (Figure 2.9C) clearly show significantly increased numbers of anti-VP8pep IgA-secreting B cells compared to mice orally dosed with buffer or WT LA. The ELISA results (Figure 2.9 A and B) were confounded by positive serum and fecal supernatant antibody titers in the buffer and WT LA group. A reason for the “positive” titer results in these two groups is unknown and possible explanations include: cross/poly-reactive antibodies, exposure to LA vaccine strains (GAD80-83) through animal handling and cage changes, or exposure to rotavirus in the mouse facility. Experiments to screen the dosing buffer delivered group for anti-SlpA antibody titers (which would signify LA exposure) and to evaluate the antibody responses to other rotavirus proteins (such as the immunogenic capsid protein VP6) are of interest.

The mice are confirmed rotavirus-exposure negative upon purchase from the vendor and sentinels in our facility routinely test negative for anti-rotavirus antibody making exposure to rotavirus during the vaccination experiment unlikely. Unintended exposure to LA-VP8pep or facility contamination with rotavirus are unlikely but if occurring would be important to control moving forward with future vaccine experiments. We hypothesize that polyreactive antibodies are the likely source of the positive titer results observed in the dosing buffer and WT LA mouse groups. Polyreactive antibodies have been found at higher abundance in Balb/c mice (155). Future studies to evaluate the antibody response to vaccination through in vitro virus neutralization assays and/or in vivo rotavirus challenge studies would help to determine if the antibody titers measured in all groups are polyreactive or a protective antibody response induced by the GAD80-83 vaccine strains.

In addition to evaluating the immune response to vaccination, we further investigated the in vivo effects of LA and adjuvants on immune activation at sites of mucosal IgA induction, namely, the MLN and PP. Differences in cytokine fold change (Figure 2.10 A and B) between the LA dosing groups confirms that immune responses are altered by adjuvants. A direct correlation between cytokine fold change and IgG or IgA responses could not be identified. This is likely because of the complex interaction of immune cells and cytokines responsible for B cell class switching and IgA secretion. Regardless, the differences we observed in the MLN and PP confirm biologic activity of our LA vaccine strain and adjuvants.

Understanding the cytokine responses to our LA-vaccine strains is complicated. TGF-β, BAFF, IL-21, and IL-6 were selected for evaluation because of their importance in B cell IgA class switching and IgA secretion (195). TGF-β plays an important role in controlling inflammation by inhibiting pro-inflammatory signaling and has been shown to increase IgA isotype class switching in B cells (196, 197). LA has been shown to increase TGF-β expression in mice (198). TGF-β can act in concert with IL-21 to increase IgA class switching in the PPs (199). IL-21 is also important for induction of IgA to the microbiota and reducing pro-inflammatory responses (200, 201). FimH (GAD83) and FliC (GAD82) both had significant decreases in TGF-β and IL-21 indicating an increased pro-inflammatory response in the PP and MLN compared to GAD80 and GAD81. How the decrease in TGF-β and IL-21 effects IgA section or induction of IgA B cells

is unclear as there was no decrease in measured IgA responses by ELISA or ELISPOT. It is interesting that GAD81 did not cause similar changes in TGF-β and IL-21 as it is a pro-inflammatory cytokine; this may be related to the timing of sample collection following LA oral delivery. GAD81 did induce a significant increase in IL-6 in both the PP and MLN which we have previously shown in vitro (47).

As reported in section 2.2.3.2, there is increased dendritic cell (DC) trafficking of adjuvanted LA to the MLN which made a DC-specific enzyme especially interesting to evaluate. Retinaldehyde dehydrogenase (aladh1a1 and aladh1a2) is primarily produced by DCs and acts to convert retinal to retinoic acid (RA), important in the induction of the mucosal homing integrin α4β7 and CCR9 on T and B cells (202). DCs in the PP express aladh1a1 while MLN DCs have been found to express aladh1a2 (202). Both FimH (GAD83) and FliC (GAD82) induced significant changes in aladh1a1 in the PP. TLRs can induce retinaldehyde dehydrogenase suggesting a possible mechanism for FimH and FliC aladh1a1 induction (203). Further identification of adjuvants and characterization of immune responses to LA-adjuvant combinations may allow for engineering of a LA vector that can induce specific immune responses.

In conclusion, stable high expression of the neutralizing rotavirus peptide, VP8pep, in the LA surface layer protein, SlpA, is possible. LA oral vaccination in mice was well tolerated and resulted in increased anti-VP8pep systemic and local antibodies as well as colonic IgA B cells. The ability to induce antibodies via oral delivery and modulate the immune response through various adjuvant strategies makes LA attractive for development as a next generation rotavirus vaccine.

2.4: Conclusion

LA has the potential to be a powerful oral vaccine vector. It can be genetically manipulated to express various neutralizing epitopes within the surface layer protein, SlpA, and to secrete or surface-display protein adjuvants. Sections 2.2 and 2.3 report the immune response in mice to an orally delivered LA vaccine against HIV-1 or rotavirus. Additionally, multiple LA adjuvant strategies were utilized, and their mechanism of action evaluated. LA expressing peptides from the neutralizing viral epitopes HIV-1 MPER and RV VP8pep were able to induce measurable systemic and local antibody responses and peptide-specific IgA B cells at the site of immune induction. In the case of LA-MPER, these peptide-specific IgA B cells could be detected at mucosal sites distant from vaccination.

Mechanistic studies evaluating LA uptake, trafficking, and cytokine responses in PP and MLN confirm that LA is taken up and trafficked to sites of immune induction and that LA +/- adjuvants can alter immune simulating cytokine responses. Taken together LA is a heat-stable and easily delivered vaccine platform that can stability express protective pathogen epitopes at high levels. It is rapidly taken up into sites of mucosal immune induction and can generate immune responses that can be manipulated by the addition of various adjuvant strategies. Further work is necessary to evaluate the neutralizing ability of induced antibodies, protection from infection, and immune response to combination adjuvant strategies. These studies are underway.

CHAPTER 3: NUTRITIONAL SUPPLEMENTATION WITH RICE BRAN DECREASES EPISODES OF DIARRHEA, INCREASES FECAL MICROBIOME α-DIVERSITY, AND STABILIZES TOTAL FECAL SECRETORY IGA IN 6- TO 12-MONTH-OLD MALIAN INFANTS

3.1: Introduction

Diarrheal disease is the second leading cause of death and major causative factor of malnutrition in children under the age of five worldwide (204). Low- and middle-income countries, especially in sub-Saharan Africa and south-central Asia, are disproportionately affected (205). Causes of diarrhea include acute and chronic infections, malnutrition, as well as food and water contamination. Malnutrition predisposes to decreased epithelial barrier function and microbial dysbiosis that can increase the risk of diarrhea and worsen malnutrition condition by decreasing food energy intake and intestinal absorption of nutrients (206, 207). Malnutrition-associated decreases in anthropometric growth of children can have lifelong health and cognitive implications (208).

An additional health burden to children at risk for malnutrition is the subclinical condition called environmental enteric dysfunction (EED), which is characterized by increased inflammation and permeability of the small intestine. EED contributes to under/malnutrition and has been associated with decreased response to vaccination in some studies resulting in increased risk of preventable disease (209, 210). While the cause of EED is not fully elucidated, many of the associated factors are the same as those that cause diarrhea such as malnutrition, enteric pathogens, and microbial dysbiosis (211, 212).

Rice is a major source of calories worldwide with production in over 114 counties. The Food and Agriculture Organization (FAO) of the United Nations predicted the 2018 global output of rice paddy to be 769.9 million tons with 510.6 million tons milled (213). One of the major by-products of rice milling is rice bran (8-12%) which is used as animal feed or treated as waste (214, 215). Rice bran includes many bioactive components that have positive health benefits and anti-inflammatory effects (215-217). While rice bran is readily available and underutilized in countries that mill rice, interest in rice bran as a prebiotic and food

supplement has been increasing and further study of the health effects in human populations are necessary. Recently we published the findings of a longitudinal phase I study of infants from Nicaragua and Mali who were supplemented with rice bran as a dietary intervention for healthy children at risk for malnutrition, diarrhea, and EED (218). Daily rice bran ingestion was found to be safe and well tolerated by infants 6 to 12 months of age. In addition, rice bran ingestion decreased diarrheal incidence in children from Mali, decreased the gut leakage protein Alpha-1 antitrypsin (AAT) in children from Nicaragua, and improved weight and length for age z-scores. These results indicated that dietary rice bran consumption in low- and middle-income countries could be an effective intervention against malnutrition and stunting.

To further assess the effects of rice bran ingestion on the intestinal mucosa and local immune system, we have measured the concentration of the predominant humoral antibody at mucosal surfaces, secretory IgA (sIgA). sIgA helps to protect the mucosa from pathogens, regulates mucosal inflammation and tolerance, and plays an important role in modulating the intestinal microbiome (219, 220). Alterations in sIgA have been found in undernourished and malnourished children and in fecal samples of adults with inflammatory bowel diseases such as Crohn's disease and ulcerative colitis suggesting that sIgA may play a role in disease pathogenesis (221, 222). Total fecal sIgA concentrations in the context of EED risk and disease progression, to the authors knowledge, have not been studied.

The purpose of this study is to evaluate the fecal sIgA concentrations and the association of sIgA with fecal EED markers neopterin, myeloperoxidase, calprotectin, and alpha-1 antitrypsin and the fecal microbiome in Malian infants with and without daily rice bran supplementation to the diet.

3.2: Materials and Methods

3.2.1: Study Design and Sample Collection

This 6-month, phase 1, infant rice bran intervention study has been previously described (218). The clinical trial registrations are (NCT02557373 and NCT02557373). Briefly, heat-stabilized rice bran was fed (1 to 5 g rice bran per day depending on age of the participant) to weaning infants from León, Nicaragua

and Dioro, Mali, West Africa. Fifty healthy (defined for the purpose of this study as infants with no previous incidences of diarrhea, antibiotic usage, known allergies, or immune altering conditions) infants were enrolled for each country and randomized into control (no rice bran intervention) and rice bran groups. The required ethical reviews and approvals were completed as provided by the Internal Review Board (IRB) of the Colorado State University Research Integrity and the Compliance Review office (protocol ID# 14-5233 H Nicaragua, 15-5744 H Mali). The Mali intervention was approved by the Institut National de Recherche en Santé Publique (National Institute of Research in Public Health, FWA 00000892) and registered at clinicaltrial.gov as (NCT02557373) on 23 September 2015. Ethical review and approvals for the Nicaraguan intervention was provided by the IRBs of the Universidad Nacional Autónoma de Nicaragua – León, University of North Carolina at Chapel Hill, and Virginia Polytechnic Institute and State University. This review and approval were registered at clinicaltrial.gov on 26 November 2105 as (NCT02615886). All participants' parent's/guardian's informed consent was obtained prior to the start of the trial.

The rice bran was provided by the United States Department of Agriculture-Agricultural Research Service (USDA-ARS) Dale Bumpers National Rice Research Center and packaged by Western Innovations, Inc. (Denver, CO, USA). Each infant was given a 2-week supply and daily compliance was reported by the parent/guardian. In Nicaragua a member of the study team visited each infant's home weekly while in Mali a community health worker had a daily. Questionnaires were used to evaluate health events, antibiotic treatment, food history, and other domestic information (example: mother's education, animals present at home, drinking water source, etc). The results of these questionnaires were published by Zambrana et al. (218). Two members of the Mali control group withdrew from participation.

Fecal samples were collected for analysis at 6, 8, and 12 months of age for the Nicaragua control group and monthly for the remaining participants. Additionally, fecal samples were collected if there was a reported incidence of diarrhea. The fecal samples were collected from diapers and processed by adding Phosphate Buffered Saline (PBS) with 1% glycerol (1 part fecal sample to 19 parts PBS/glycerol). Samples were homogenized via vortex and centrifuged at 3000 RPM to separate out debris. Samples were frozen at -80°C until evaluation.

3.2.2: Stool Environment Enteric Dysfunction Marker Analysis

The biomarkers evaluated to assess for gastrointestinal inflammation and epithelial leakage include neopterin (NEO), myeloperoxidase (MPO), calprotective (CAL), and alpha-1 antitrypsin (AAT). All tests were run on the processed stool samples and elevated via Enzyme-Linked-Immunosorbant-Assay (ELISA) as described by Zambrana et al. (218). Briefly, the collected stool samples from months 6, 8, 10, and 12 months were centrifuged to remove debris and supernatant used for ELISA using commercially available kits as follows: CAL was determined at a 1:360 dilution (Eagle Biosciences, Nashua, NH, USA), NEO was determined at 1:100 dilution (GenWay Biotech Inc, San Diego, CA, USA), MPO was determined at 1:500 dilution (Immundiagnostik AG, Bensheim, DEU), and AAT determined at 1:12,500 dilution (Immuchrom GMBH, Heppenheim, DEU). All samples were run in triplicate and concentrations calculated using standards run on each plate.

3.2.3: Total Fecal sIgA ELISA

Total fecal sIgA was measured via ELISA based on a previously published method (223). Frozen processed fecal samples were defrosted and commercially available ProteaseArrest protease inhibitor cocktail (G-biosciences, St. Louis, MO) was added at the manufacturers recommended concentration. Samples were homogenized 3 times and then centrifuged at 12,000 PRM. Supernatants were collected and each sample was run in duplicate at a starting dilution of 1:500-1000 in sample buffer (1% bovine serum albumin (BSA) in PBS and 0.05% Tween20) followed by eleven 1:2 dilutions in sample buffer. Samples were incubated for 2 hours at room temperature on Greiner Bio-One high binding microplates (Monroe, NC) coated overnight with mouse anti-secretory component (IgA) clone GA-1 (Sigma-Aldrich, St. Louis, MO) in carbonate buffer pH 9.6 and blocked with 1% BSA in PBS for 1 hour at room temperature. After sample incubation, plates were washed 5 times with PBS + 0.05% Tween20 and antibody binding was detected by biotin mouse anti-human IgA1/IgA2 (BD Pharmingen, Franklin Lakes, NJ) diluted in sample buffer followed by incubation for 30 minutes at room temperature with streptavidin-conjugated horseradish

peroxidase (Thermo Scientific, Rockford, IL) diluted in sample buffer. After washing 7 times with PBS + 0.05% Tween20, plates were incubated with SureBlue Reserve TMB Peroxidase Substrate (SeraCare, Milford, MA). The color development was stopped with 1N HCl and the absorbance measured at 450 nm – 570 nm background on a plate reader. Total fecal sIgA was calculated based on a standard curve (0 to 100 ng/ml) of purified human IgA from colostrum (Sigma-Aldrich St. Louis, MO) run on each plate. Fecal sIgA concentration was calculated by averaging the dilution factors that fell within the range of the standard curve.

3.2.4: Fecal Total sIgA and EED Marker Statistical Analysis

Statistical analysis for evaluation of total fecal sIgA and for EED markers over time and between countries was performed using SAS 9.4 (Cary, NC, USA). For total sIgA analysis, a mixed model analysis was done separately for each country using log transformed IgA (to satisfy model assumptions) as the response. Fixed effects included Group and Age plus Group*Age interaction. Subjects were included as random effect to account for repeated measures. Dunnett adjusted pairwise comparisons were used to compare downstream timepoints versus 6 months. Correlation between sIgA and diarrhea was determined using a mixed logistic regression separately for each country. EED marker comparison between countries was performed using a Welch-Satterthwaite t-test and Wilcoxon rank-sum test. EED score analysis between rice bran and control groups was performed by one-way ANOVA followed by an uncorrected Dunn's multiple comparisons test (Kruskal-Wallis test) and within the rice bran or control group performed by one-way ANOVA following followed by Fisher's LSD test performed using GraphPad Prism 8.1.0 for windows (GraphPad software, San Diego, CA, USA).

3.2.5: Metataxonomics Sample Processing, Sequencing, Analysis, and Statistical Analysis

Infant stool samples were processed as described by Zambrana et al. (218). Briefly, DNA was extracted from frozen fecal samples for 16S microbial analysis using a MoBio PowerSoil Kit (Solana Beach, CA, USA). PCR amplification of amplicons was performed with Fischer Hot Start Master Mix

(Fisher Scientific, Waltham, MA, USA) and EMP standard protocols (224-228). DNA was purified using magnetic beads, samples pooled and quantified using Kapa Kit (Kapa Biosystems, Wilmington, MA, USA), and run on Illumina-MiSeq with the Illumina V2 500 cycle kit (San Diego, CA, USA).

A total of 7,248,191 raw single-end FASTQ formatted forward sequence reads represented by 326 samples were imported to the Quantitative Insights Into Microbial Ecology 2 (QIIME 2) (229). The amplicon sequence variant (ASV) absolute abundances were compiled into a table for each sample was inferred from reads using the Divisive Amplicon Denoising Algorithm 2 (DADA2) pipeline (230). Taxonomic identities for ASV representative sequences were assigned with Naïve Bayes classifiers independently trained on 99% OTU reference collections bound by the 515F/806R (Parada/Aprill) primer pair and trimmed to 248bp extracted from either Greengenes 13_8 (231) or SILVA 132 (232) marker gene databases. Alpha diversity metrics, Chao1 and Shannon's Index were computed using QIIME 2 as described by Zambrana et al (218). The raw ASV table, representative sequences, taxonomy tables, and alpha diversity tables were exported from QIIME 2 for further processing in R (233). A master table comprised of ASV representative sequences, full and truncated taxonomic lineages, and raw absolute abundances for all ASVs within all samples was constructed using base R in combination with package dplyr. Potential contaminant ASVs assigned by either database as chloroplast, mitochondria, eukaryote, or unassigned kingdom were removed from the master table. Any samples exhibiting excess of 1% relative abundance of contaminants and any biological samples with total absolute ASV abundance fewer than 999 were removed from the master table. The processed master table was subset as needed to retain the appropriate samples for each of the analyses presented here. Samples analyzed after processing included 321 biological samples. A previously described approach (234) was followed to construct a midpoint rooted phylogenetic tree from ASV representative sequences using R packages Biostrings, DECIPHER, phangorn, and ape. The phylogenetic relatedness of microbial communities were compared using three UniFrac distance metrics: generalized (235), unweighted (236), and weighted (236). UniFrac distance matrices were computed using R package GUniFrac and ordinated with principal coordinates analysis (PCoA) using R packages ape, dplyr, ggplot2, and ggpubr. Comparisons of phylogenetic-independent microbiota composition (i.e.

composition of ASVs) proceeded using the compositional data analysis paradigm (237). Zero counts for ASVs were imputed using the count zero multiplicative (CZM) method from R package zCompositions followed by applying the centered log-ratio (clr) transformation with log base 2. The relationships between samples were visualized through principal components analysis (PCA) using R packages dplyr, ggbiplot, ggplot2, and ggpubr. Differential abundance testing at the phylum, family, lowest assignment, and ASV levels was conducted with ALDEx2 (238) from Bioconductor suite (239). For a given differentially abundant ASV or taxon, $\log_2$ fold differences between groups were visualized using packages dplyr, ggplot2, and ggpubr. Sequence reads were curated from the NCBI SRA under accession number SRP159269 and BioProject PRJNA488807 from the previous publication (218).

Pairwise comparisons of alpha diversity across groups were performed using the non-parametric Wilcoxon rank-sum test (240) with the resultant *P*-values adjusted for multiple comparisons using the Benjamani-Hochberg (BH) procedure (241). Non-parametric testing was performed after the results of Shapiro-Wilk normality testing (242) indicated non-normal distributions. Non-parametric permutational analysis of variance (PERMANOVA) (243) from the R package vegan was utilized to detect differences between groups in phylogenetic relatedness of microbial communities with the three UniFrac distance metrics referenced above and similarities in ASV composition using the Aitchison distance metric (244). ALDEx2 testing was performed as follows: 1000 Monte Carlo (MC) instances of the Dirichlet distribution for each sample were generated from the respective subset tables containing absolute abundance data; the clr transformation was then applied over each MC instance; *P*-values were produced using the non-parametric Wilcoxon rank-sum test (240), also called the Mann-Whitney *U* test (245), to compare each ASV/taxon's clr abundance values between the specified two groups; *P*-values were adjusted for multiple comparisons using the Benjamani-Hochberg (BH) procedure (241) resulting in adjusted *P*-values (henceforth referred to as BH-*P*); *P*-values and BH-*P*-values for each ASV/taxon were averaged across all MC instances to yield expected *P*-values and expected BH-*P*-values. Any ASV/taxon with an expected BH-*P*-value less than 0.1 was deemed significant. The package BiocParallel from the Bioconductor suite

was used to execute ALDEx2 functions using multi-core processing to drastically reduce computational time (246).

MetagenomeSeq was utilized to compare the log fold change between the different treatments (247). Data were first normalized using cumulative sum scaling (CSS) (247). Taxa analyzed were those that included at least one sequence read within at least 10 of the samples observed to guard against sparsity. We used the zero inflated Gaussian model for the analysis and completed and all against all contrast comparisons utilizing. Log-fold-changes were compared utilizing empirical Bayes' moderated t values calculated utilizing the function eBayes and using false-discovery-rate (FDR) adjusted p-values. Log-fold-changes were considered significant if larger than 2 and associated with a p-value less than 0.01. Correlation between OTUs and total fecal sIgA concentrations were determined by a nonparametric Spearman Correlation without correction for multiple testing.

3.3: Results

3.3.1: Total Fecal sIgA and EED Marker Concentrations at 6 Months of Age for Nicaraguan and Malian Infants

Fifty 6-month-old infants from Nicaragua and fifty 6-month-old infants from Mali were enrolled and randomly assigned to control or daily rice bran intervention groups. Infants had fecal samples collected at each month except for the Nicaragua control cohort where the fecal samples were collected only at months 6, 8, and 12. Within each country, the two subgroups of infants (control and rice bran) had similar socio-economic factors (218). Environmental and household factors such as maternal education, drinking water sources, livestock-domestic animals, and vaccination were markedly different between the two countries.

To determine the differences between Mali and Nicaragua infants' mucosal environment, total fecal sIgA, MPO, NEO, CAL, and AAT were evaluated for all infants at the time of enrollment (prior to rice bran dietary intervention). MPO, CAL, and NEO are markers of inflammation. MPO and CAL are released

from neutrophils and NEO is an indicator of Th1 cell activity as it is released from macrophages and dendritic cells (DC) following IFN-ɣ secretion from T cells. AAT is normally present in serum and in instances of increased intestinal permeability is lost into the GI lumen. All have been identified as fecal biomarkers associated with EED (248, 249).

The 6-month-old infants from Mali had significantly elevated total fecal sIgA concentration compared to the Nicaraguan children (Figure 3.1A). Additionally, the inflammatory markers MPO and AAT were significantly elevated in the infants from Mali suggesting elevated levels of neutrophil degranulation and epithelial leakage in these children compared to the Nicaraguan infants (Figure 3.1B). NEO was significantly higher in Nicaraguan infants. The significance of the lower levels of NEO in Malian infants when compared to Nicaragua is unknown and may be due to global variation noted in the utility of the markers from other larger studies spanning multiple countries (250). There were no significant differences detected in CAL concentrations between Malian and Nicargian infants at 6 months of age. Over the course of the six-month study, children from Mali had higher number of diarrhea episodes reported than those from Nicaragua (28 versus 9). The increased fecal sampling in the control group, increased incidence of diarrhea, and higher total fecal sIgA concentrations made the Mali cohort well suited for investigation of rice bran effects on the intestinal mucosal immune response over time.

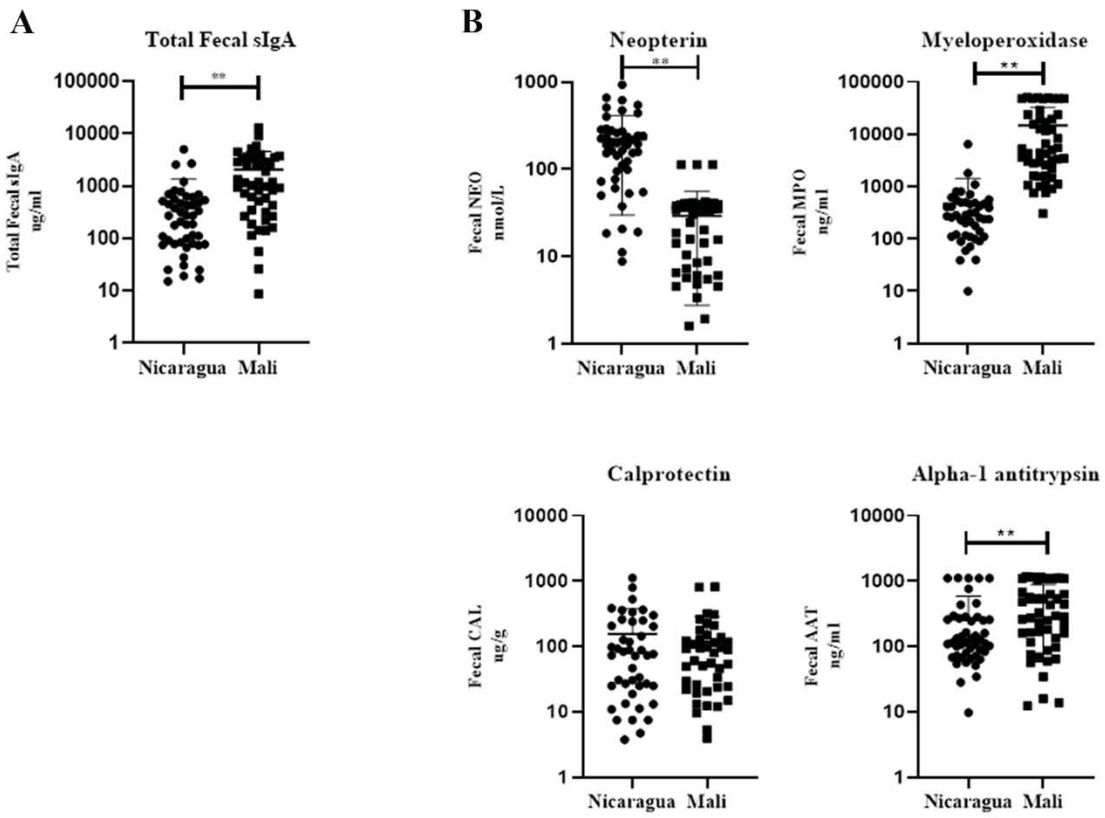

Figure 3.1. Comparison of total fecal sIgA and EED marker concentrations for Nicaraguan and Malian 6-month-old infants. (A) 6-month-old Malian infants had significantly higher concentrations of total fecal sIgA than the Nicaraguan infants. (B) 6-month-old Malian infants had significantly increased concentrations of fecal MPO and AAT and decreased concentrations of NEO than Nicaraguan infants. $^{**}p < 0.05$. Y axis is $\log_{10}$ scale.
EED: environmental enteric dysfunction; sIgA: secretory IgA; NEO: neopterin; MPO: myeloperoxidase; AAT: alpha-1antitrypsin; CAL: calprotectin

3.3.2: Effects of Rice Bran Ingestion on Total Fecal sIgA, EED Scores, and Diarrheal Episodes in Malian Infants Over Time

To evaluate the changes in total fecal sIgA in Malian infants over time in response to daily rice bran ingestion, total fecal sIgA concentrations were measured by ELISA. Figure 3.2A shows that the total fecal sIgA for the control cohort was significantly increased at months 9, 10, and 11 from 6 months of age. There were no significant differences between the control and rice bran groups from 6 to 12 months. The

control group had increased incidence of diarrhea compared to the rice bran group (20 versus 8) (Figure 3.2C). Incidence of diarrhea had a weak positive association with total fecal sIgA concentration (Table 3.1).

To determine the effect that rice bran ingestion had on risk for EED, we calculated EED scores for the control group and rice bran group based on the 4-component score index described by Becker-Dreps et al. (251). In the rice bran participants, there was a significant decrease in EED scores from 6 to 12 months with a generalized decrease in EED score averages over the entire study. In the control group, EED scores between 8 and 12 months and 10 and 12 months were significantly decreased with the EED score averages increasing at 8 and 10 months before decreasing at 12 months of age (Figure 3.2B). There were no significant differences between the control and rice bran groups. No correlation was detected between fecal sIgA concentration and the EED score. There was a positive correlation between total fecal sIgA concentration and NEO and ATT (Table 3.1).

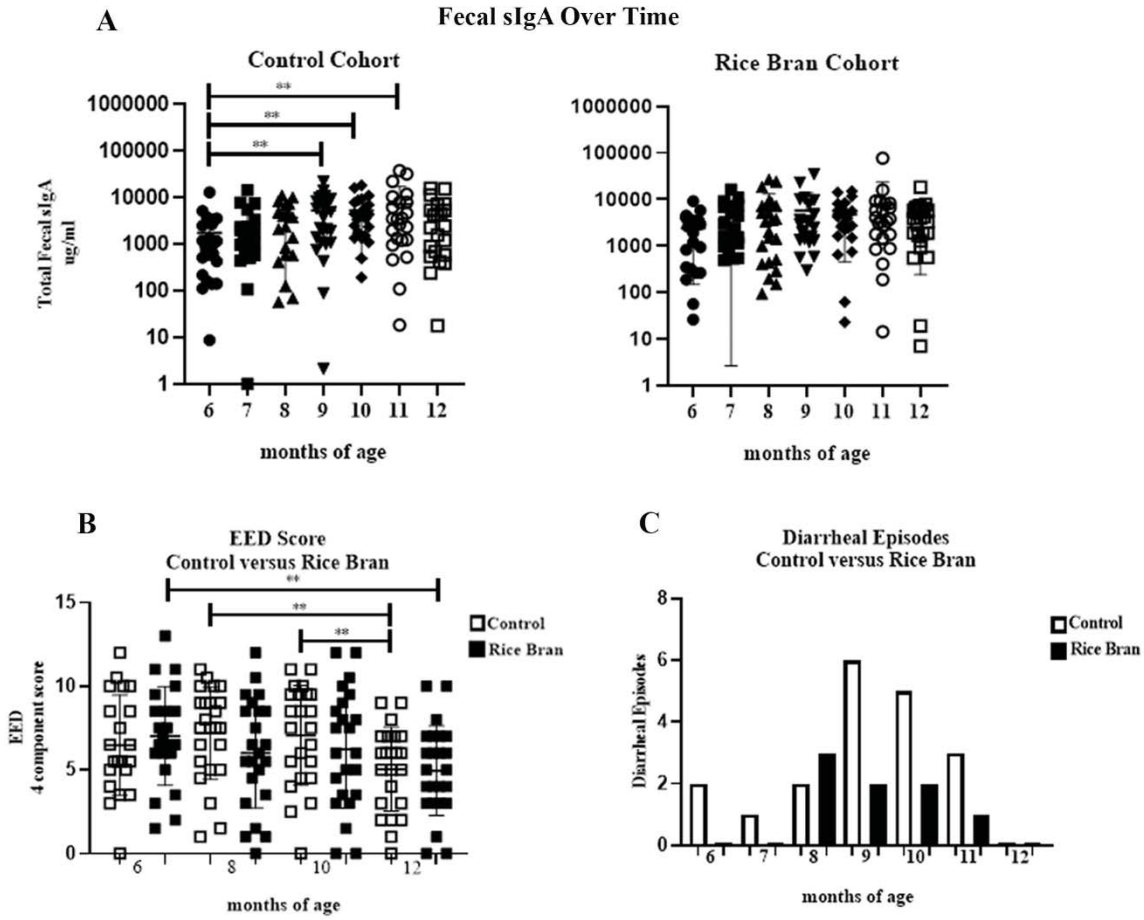

Figure 3.2. Total fecal sIgA concentration, EED score, and diarrheal episodes over time in Malian infants with daily rice bran ingestion versus age matched controls. (A) The Mali control cohort had significant increases in total fecal sIgA concentration at 9, 10, and 11 months compared to 6 months of age. There were no significant differences between the rice bran cohort total fecal sIgA concentrations for any time points. There were no significant differences between the total fecal sIgA concentrations in the rice bran and control groups. (B) 4-component EED scores were calculated at 6, 8, 10, and 12 months of age for all individuals in the control and rice bran groups. There was a significant decrease in EED scores from 6 to 12 months for the rice bran cohort and from 8 and 10 to 12 months for the control group. (C) Diarrheal episodes from 6 to 12 months of age between the control and rice bran groups. There were an increased number of diarrheal episodes for the control groups (20 diarrheal episodes) compared to the rice bran group (8 diarrheal episodes). ** $p < 0.05$.
sIgA: secretory IgA; EED: environmental enteric dysfunction

Table 3.1. Total fecal sIgA correlation with episodes of diarrhea, markers of EED (neopterin (NEO) and alpha-1 antitrypsin (AAT)), and α-diversity indexes.

	sIgA correlation	P value
Diarrheal episodes	0.23	0.068
NEO	0.33	< 0.01
AAT	0.47	< 0.01
Shannon diversity index		
Control group	0.21	< 0.01
Rice bran group	-0.02	0.808
All individuals	0.109	0.056
Chao1 diversity index		
Control group	0.129	0.024
Rice bran group	0.02	0.808
All individuals	0.08	0.158

3.3.3: Effects of Rice Bran Ingestion on Microbiome Diversity and Composition Over Time

Diarrheal episodes and malnutrition have been associated with an immature microbiome in infants and children (252). Over time microbiome α-diversity, a measure of bacterial species richness, increases in infants and young children (253). While α-diversity is not a direct measure of the maturity of the microbiome, it is known to decrease with incidence of diarrhea and certain disease states (254). As shown in Figure 3.2 A and B, there were increases in the total sIgA fecal concentration and EED scores between 8-11 months of age in the control infants that were not observed in the rice bran cohort. These alterations coincided appear to occur with the increased incidence of diarrhea in the control infants (Figure 3.2 C). To evaluate changes that to the microbiome during this time frame, we assessed two measurements of α-diversity, Shannon diversity and chao1, for both the control and rice bran infants at 9, 10, and 11 months of age compared to the start of the study (6 months of age). As expected, age was the strongest driver of increased α-diversity indexes, yet notably in the rice bran cohort, both the Shannon diversity and chao1 were significantly increased (from 6 months of age) at 9 months when compared to 10 months of age in the control group (Figure 3.3). There were no differences in α-diversity between the rice bran and control groups at 6, 9, 10, or 11 months of age. These results support that the rice bran cohort progressed one month earlier to a more diverse and possibly matured microbiome when compared to the control group.

Additionally, there was a significant correlation between both the Shannon diversity and chao1 indices and total sIgA concentrations for the control infants that was not found for the rice bran cohort (Table 3.1).

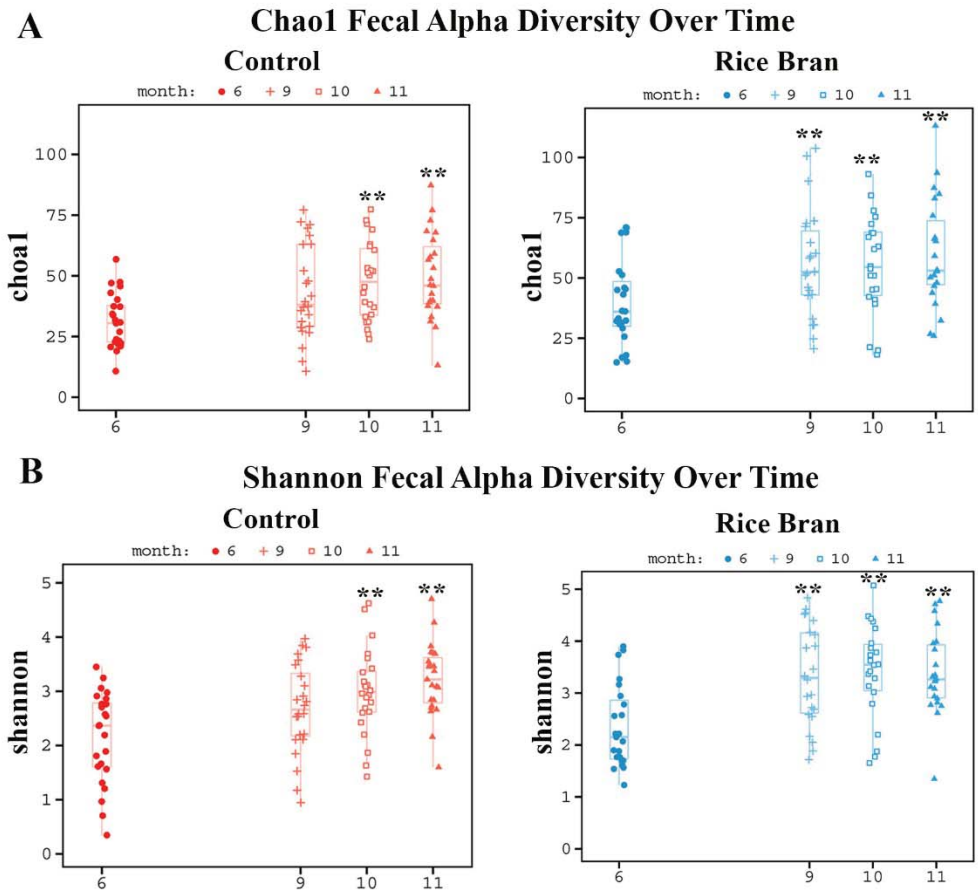

Figure 3.3. Gut microbiota α-diversity for the control and rice bran cohorts over time. Fecal microbiome chao1 (A) and Shannon diversity (B) for the control and rice bran groups at months 6, 9, 10, and 11 months of age. In the rice bran group, there is a significant increase in α-diversity at months 9, 10, and 11 months of age compared to 6 months of age. In the control group, there is a significant difference in α-diversity at months 10 and 11 compared to 6 months of age. ** $p < 0.05$ compared to 6 months of age.

Comparison of the microbiota between the control and rice bran groups at 6, 9, 10, and 11 months of age identified numerous significant differences at the genus and species taxonomic level. Figure 3.4 shows fold changes for select operational taxonomic units (OTU) between the two cohorts (all OTUs

identified as being significantly different between the rice bran and the control group are reported in Supplemental Figure 3.1). There were few significant differences between the control and rice bran groups at 6 months of age (9 OTUs). Over time, rice bran ingestion resulted in a generalized increase in the number of OTUs compared to the control cohort. Association between total fecal sIgA concentration and the OTUs identified as significantly different between the control and rice bran groups at 6, 9, 10, and 11 months of age were evaluated by a nonparametric Spearman correlation. In the control group at 9, 10, and 11 months of age, OTUs more often had a positive association with total fecal sIgA concentrations while the rice bran cohort OTUs were more likely to have a negative association (Supplemental figure 3.2). The significance of these correlations is unknown. No bacterial genera or species were associated with total fecal sIgA concentrations over multiple time points or between the two cohorts.

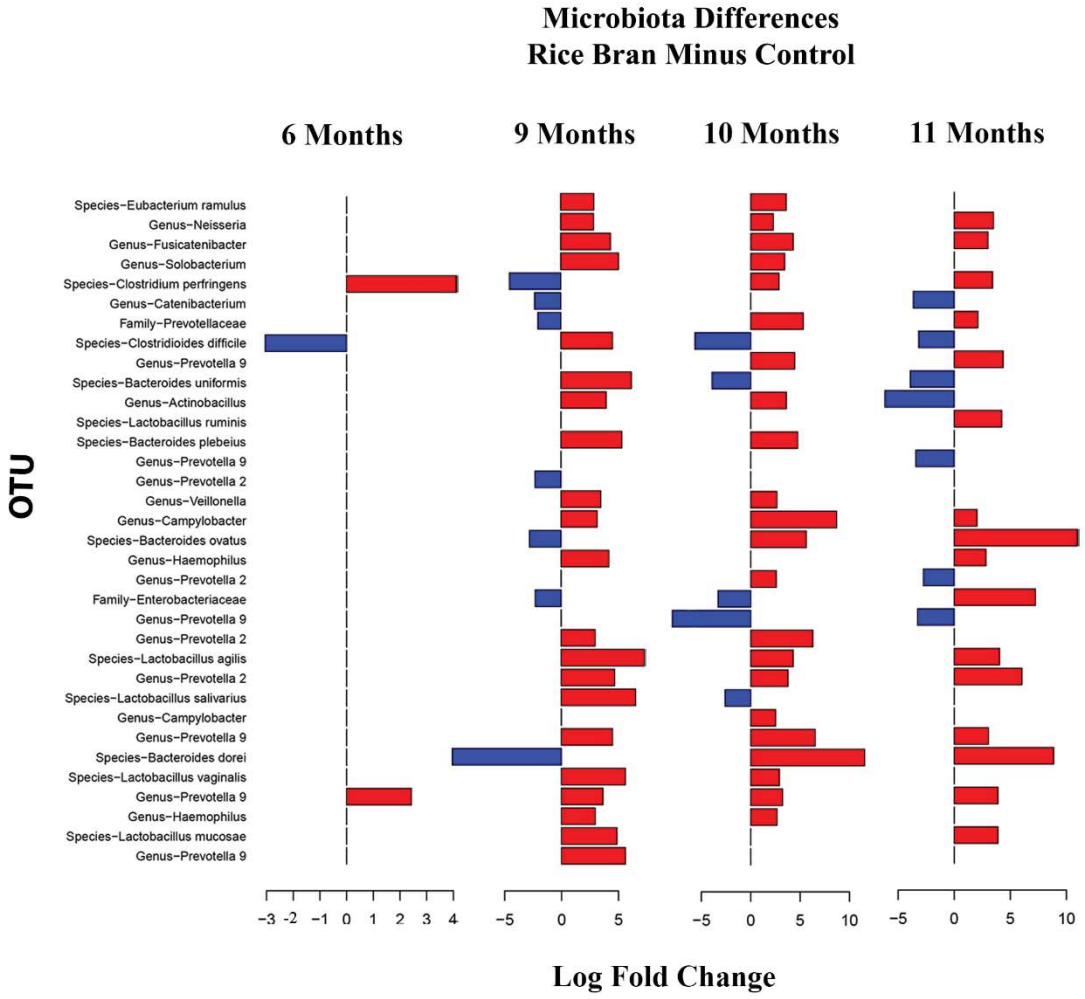

Figure 3.4. Log-fold microbiota differences between control and rice bran groups at 6, 9, 10, and 11 months of age. Red bars indicate the OTU is increased in rice bran group and blue bars indicate the OTU is increased in the control group. Changes were considered significant if the log-fold change was larger than 2 with a p-value < 0.01. Selection of 34 genus and species (out of 122 identified as significant shown in Supplemental Figure 3.1) that showed similar trends over time.

3.4: Discussion and Conclusions

In Mali, food security and malnutrition are major concerns with stunting and wasting affecting 30.4% and 13.5% of children under the age of 5 respectively (255). Most of the population in Mali relies on agriculture for their livelihoods with production of rice averaging between 4.5 tons to 6 tons/hectares in irrigated areas. The Malian government has ongoing irrigation projects with the goal of increasing reliable

water access to stabilize rice growth and extend the growing season (256). Implementation of a rice bran supplementation program in addition to irrigation programs that would increase rice production could have a great impact on the country's food security. The ingestion of rice bran by infants could result in long-term health benefits by decreasing diarrhea and EED which are major causes of malnutrition and stunting.

Here we show the gut mucosal immune benefits of rice bran nutritional supplementation in a cohort of healthy Malian infants. Rice bran ingestion resulted in decreased incidence of diarrhea, decreased EED scores over time, stabilization of total fecal sIgA concentrations, and earlier age onset for increased microbiome α-diversity. This study showed that sIgA concentration was associated with the EED biomarkers NEO and AAT, Shannon diversity and choa1 α-diversity indexes in the control group, and diarrhea episodes. The association of sIgA with NEO, AAT, and diarrhea suggests that total sIgA may be elevated after pathogen exposure and/or increased intestinal inflammation and barrier dysfunction.

Fecal sIgA concentrations in health and disease are poorly understood. The clinical significance of the stabilization of fecal sIgA concentrations and the association of total fecal sIgA concentrations with fecal biomarkers of EED and diarrhea is unknown. The increased fecal sIgA in the control group is different from what has been reported in gnotobiotic piglets and conventional laboratory mice where rice bran ingestion increased total fecal sIgA levels (257, 258). We hypothesize that this difference between the Malian infants and laboratory animals is due to the limited microbiome in gnotobiotic animals and lack of chronic environmental enteric pathogen exposures in controlled laboratory environments. Total fecal sIgA concentrations in individuals with or at risk for EED have not been previously published. IgA concentrations in the EED context are more often studied in response to oral vaccines where there is generally a decreased IgA response to vaccination (251, 259). There is a single study by Campbell et al. evaluating serum IgA and fecal EED biomarkers; no association between IgA and NEO, MPO, or AAT was reported (260). This contrasts with our findings and was not surprising given that fecal sIgA and serum IgA do not often correlate (261).

The role of sIgA in maintaining mucosal homeostasis may explain the positive correlation between NEO and for AAT. In mice predisposed to colitis, sIgA increases as a compensatory mechanism to

increased epithelial permeability (262). In instances of decreased mucosal barrier function, increased sIgA can help to restore the barrier by coating bacteria, which decreases local inflammation and maintains IL-10, an important cytokine for epithelial regeneration and integrity (263). Given AAT is a measurement of epithelial permeability, it is possible that as AAT levels increase, sIgA could also increase to restore mucosal barrier integrity. No direct influence of NEO on IgA can be found in the literature. NEO is released from macrophages and DCs in response to T cell secretion of IFN-γ. IFN-γ can also increase epithelial expression of the poly-Ig receptor responsible for IgA secretion into the intestinal lumen (264). The correlation between NEO and sIgA may be due to upstream regulation by IFN-γ. The association of sIgA with AAT and NEO suggests that the elevation of sIgA in the control cohort is an attempt to restore the mucosal barrier in response to increased inflammation and/or permeability.

The microbiome is an important factor in human health and disease (265), and changes from birth while maturing into an adult-like composition around 2-5 years of age. The gut microbiota educates the mucosal immune system which in turn helps to shape the microbiome balance (266, 267). Many allergic and intestinal inflammatory diseases as well as EED and malnutrition have been found to be associated with an altered microbiome composition. Infant microbiome maturation involves increases in α-diversity (253, 268). In our cohort, we found that age was also the strongest predictor of the microbiome α-diversity. The rice bran cohort's α-diversity increased one month earlier than the control group suggesting a delayed maturation or regression in the control children. Diarrhea has been associated with decreases in α-diversity and regression in microbiome maturation (254, 269). The control infants had more episodes of diarrhea which may be responsible for their delayed α-diversity increase. Total fecal sIgA concentration was associated with both Shannon diversity and chao1 in the control group but not for the rice bran. Why this association is occurring in the control group only is unknown but may be related to the microbiota differences between the two groups over time and their specific interaction with the mucosal immune system and sIgA induction.

Evaluation of OTUs between the control and rice bran groups identified several bacterial genera and species that differed between the two cohorts. Similar to what was observed by Zambrana et al. at 8

and 12 months, there were increases in species of *Lactobacilli spp*., *Veillonella spp*., and *Campylobacter spp*. (218). Additionally, we found significant fold changes in bacterial species that have been associated with dysbiosis and chronic disease including *Fusicatenibacter spp*., *Prevotella spp*., *Bacteroides spp*., and *Ruminococcus spp*. (270-272). These findings are observational and additional functional studies are required to fully understand how these microbe alterations are affecting the mucosal environment. Additionally, we found numerous OTUs that were associated with increases in total fecal sIgA concentrations in the control group. The correlations were not consistent between age groups or with the rice bran cohort. The interaction of the microbiome with the mucosal immune system is complex, involving not only direct interaction but metabolite influence. Further evaluation of metabolites between the two cohorts and associated with OTUs may help to understand the correlation between total fecal sIgA and specific bacteria.

In conclusion, rice bran is a well-tolerated and promising novel nutritional supplement that positively affects mucosal health, microbiome diversity, and decreases episodes of diarrhea in children. Long term, population based investigations of rice bran intake in children are needed to investigate the level of impact these intestinal environment changes can have on malnutrition and stunting between ages 2-5 years old. Rice is a massive nutritional staple in much of the world making rice bran readily available and sustainable for implementation into a nutritional program. In Mali, where programs to increase irrigation and rice production are already underway, utilization of rice bran could have an even greater effect on combating food insecurity and malnutrition.

CHAPTER 4: CONCLUDING REMARKS AND FUTURE DIRECTIONS

4.1: Concluding Remarks

Protecting the mucosa from pathogens is essential for preventing infection and disease from numerous bacteria and viruses. Here we present methods for increasing mucosal health and inducing pathogen specific immunity using pre and probiotics.

As reviewed in Chapter 1, mucosal vaccine development has been difficult with approved mucosal vaccines utilizing attenuated-live or heat-killed pathogens. There is a need for alternative mucosal vaccine strategies, especially oral vaccines due to their ease of administration. The gastrointestinal (GI) track possesses many innate defenses such as gastric acid, bile, peristalsis, mucus, and the commensal microbiome that make delivery of antigens and adjuvants to sites of mucosal immune induction especially challenging. Additionally, alterations in the GI environment, such as dysbiosis, presence of enteric pathogens, inflammatory conditions, and presence of maternal antibody in breastfed infants can result in unpredictable responses to oral vaccines.

The microbiome is recognized as a natural adjuvant to oral vaccines through its interaction with the mucosal immune system via pattern recognition receptors and metabolites (273). Identifying the microbiome composition that is “ideal” for oral vaccine response is an active area of investigation. Results from these studies have been difficult to interpret and implement due to the complex interaction between the microbiome, immune system, nutritional status, and diet. For example, evaluation of immune response to oral attenuated-live rotavirus vaccines in children from Ghana, Pakistan, and Amsterdam have found conflicting results between the presence of various gram negative bacteria and vaccine response that are speculated to be related to differences in immune activation by LPS from various bacteria genera (274, 275). Additionally, the vaccine response may be related to the type of vaccine used indicating that microbe adjuvant effects are not one size fits all (276).

Altering the microbiome though antibiotics and pre and probiotics have been shown to change the response to oral vaccines in addition to increasing mucosal barrier function and providing protection from

pathogens and diarrheal illness. We show in Chapter 3 that ingestion of the prebiotic rice bran can decrease diarrheal episodes, stabilize total fecal sIgA levels, increase microbiome α-diversity, and decrease EED scores. The protective effects of rice bran are likely a combination of metabolites and increases in microbes that influence mucosal health or decrease pathogens by niche exclusion. Studies have shown that rice bran can protect against *Salmonella spp.* colonization, decrease norovirus and rotavirus infection, and increase antibody response to rotavirus vaccination (257, 277, 278). Rice bran effects on vaccine response was not evaluated here but is of interest considering the increased immune response previously observed to human rotavirus vaccines in gnotobiotic pigs.

Utilization of the lactic acid bacteria *L. acidophilus* (LA) as a vaccine vector provides a mechanism to both supply the benefits of a probiotic for immune health and stimulate an adaptive immune response to protective antigens. Proof of concept has been shown for the use of lactic acid bacteria as oral vaccine vectors (reviewed in Chapter 1). In Chapter 2, we furthered our development of the LA oral vaccine platform by creating new LA constructs against the mucosal pathogens HIV-1 and rotavirus and evaluated the *E. coli* type I pilus protein FimH as a LA vaccine adjuvant. The addition of FimH increased serum IgG and mucosal IgA antibodies in addition to mucosal IgA secreting B cells against the HIV-1 neutralizing epitope MPER. Immune responses to the LA-rotavirus vaccine demonstrates that a LA vector could be an alternative to the current live-attenuated rotavirus vaccines. Whether a LA vaccine could induce protective immune responses in the face of an altered mucosal environment is unknown, but modification of LA with multiple adjuvant strategies may create a vaccine that has similar performance regardless of the microbiome or inflammatory state of the mucosa.

4.2: Future Directions

The ability of pre and probiotics to enhance mucosal health and immune response to vaccination has been established but few studies have investigated the mechanisms behind these changes. A better understanding of how mucosal health, dysbiosis, inflammation and vaccine response are related is needed

to develop effective vaccine strategies and treatments/supplements that help standardize mucosal vaccine responses.

We have shown that rice bran ingestion can affect the microbiome composition, markers of EED, and sIgA concentrations. The study presented in Chapter 3 was performed in healthy children. Rice bran effects on mucosal health, microbiome composition, and the immune system in children with dysbiosis, stunting, and/or environmental enteric dysfunction is unknown. Evaluating the effects of rice bran ingestion in unhealthy children is an important next step. Additionally, responses to oral vaccination were not studied in this cohort of children as most were not vaccinated. It would be interesting and important to include measurements of immune response to oral vaccination in future studies. Increases in vaccine response secondary to rice bran ingestion would have important health implications in developing and low-income countries where there is the most variation in vaccine efficacy.

There is much work necessary in continuing to develop LA as a mucosal vaccine platform. It is essential for us to understand the viral protection conferred by our LA vaccines. Rotavirus neutralization assays and in vivo challenge studies are currently underway. Evaluation of other metrics of immune induction by LA vaccination such as T cell subsets, LA uptake, and APC activation would provide valuable information about the type of response induced by the vaccine. We are currently developing multiple LA vaccines with various combinations of rotavirus capsid proteins and adjuvants. Additionally, we are developing and evaluating multiple antigen/adjuvant display strategies that will allow us to select the most capable vaccine. We are currently utilizing three adjuvant strategies: IL-1β, FliC, and FimH. Further mechanistic studies of these adjuvants individually and in combination are also necessary.

The true test of the LA-vaccine platform will be its ability to induce immune responses in individuals where other oral vaccine strategies have failed. The decreased immune response in some populations to the currently available attenuated-live vaccines provides an excellent model for evaluating the performance of our LA platform. To date, no lactic acid bacterial vaccine has been evaluated in animal models or individuals with an altered microbiome or EED. Studies measuring the induction of protective

immune responses in different mucosal environments and continued evaluation of antigen and adjuvant combinations will allow for development of LA as a powerful mucosal vaccine platform.

REFERENCES

1. Markowiak P, Slizewska K. Effects of Probiotics, Prebiotics, and Synbiotics on Human Health. Nutrients. 2017;9(9).
2. Gallo A, Passaro G, Gasbarrini A, Landolfi R, Montalto M. Modulation of microbiota as treatment for intestinal inflammatory disorders: An uptodate. World J Gastroenterol. 2016;22(32):7186-202.
3. Boirivant M, Strober W. The mechanism of action of probiotics. Curr Opin Gastroenterol. 2007;23(6):679-92.
4. Holmgren J, Czerkinsky C. Mucosal immunity and vaccines. Nat Med. 2005;11(4 Suppl):S45-53.
5. Neutra MR, Kozlowski PA. Mucosal vaccines: the promise and the challenge. Nat Rev Immunol. 2006;6(2):148-58.
6. Kim SH, Jang YS. The development of mucosal vaccines for both mucosal and systemic immune induction and the roles played by adjuvants. Clin Exp Vaccine Res. 2017;6(1):15-21.
7. Zimmermann P, Curtis N. The influence of the intestinal microbiome on vaccine responses. Vaccine. 2018;36(30):4433-9.
8. Boyaka PN. Inducing Mucosal IgA: A Challenge for Vaccine Adjuvants and Delivery Systems. J Immunol. 2017;199(1):9-16.
9. Zimmermann P, Curtis N. The influence of probiotics on vaccine responses - A systematic review. Vaccine. 2018;36(2):207-13.
10. Wells JM, Mercenier A. Mucosal delivery of therapeutic and prophylactic molecules using lactic acid bacteria. Nat Rev Microbiol. 2008;6(5):349-62.
11. LeCureux JS, Dean GA. Lactobacillus Mucosal Vaccine Vectors: Immune Responses against Bacterial and Viral Antigens. mSphere. 2018;3(3).
12. Rosales-Mendoza S, Angulo C, Meza B. Food-Grade Organisms as Vaccine Biofactories and Oral Delivery Vehicles. Trends Biotechnol. 2016;34(2):124-36.
13. Gupta RK, Siber GR. Adjuvants for human vaccines--current status, problems and future prospects. Vaccine. 1995;13(14):1263-76.
14. Tregoning JS, Russell RF, Kinnear E. Adjuvanted influenza vaccines. Hum Vaccin Immunother. 2018;14(3):550-64.
15. Akira S, Uematsu S, Takeuchi O. Pathogen recognition and innate immunity. Cell. 2006;124(4):783-801.
16. Girardin SE, Boneca IG, Viala J, Chamaillard M, Labigne A, Thomas G, et al. Nod2 is a general sensor of peptidoglycan through muramyl dipeptide (MDP) detection. J Biol Chem. 2003;278(11):8869-72.
17. Smits HH, Engering A, van der Kleij D, de Jong EC, Schipper K, van Capel TM, et al. Selective probiotic bacteria induce IL-10-producing regulatory T cells in vitro by modulating dendritic cell function through dendritic cell-specific intercellular adhesion molecule 3-grabbing nonintegrin. J Allergy Clin Immunol. 2005;115(6):1260-7.
18. Konstantinov SR, Smidt H, de Vos WM, Bruijns SC, Singh SK, Valence F, et al. S layer protein A of Lactobacillus acidophilus NCFM regulates immature dendritic cell and T cell functions. Proc Natl Acad Sci U S A. 2008;105(49):19474-9.

19. Kawashima T, Ikari N, Watanabe Y, Kubota Y, Yoshio S, Kanto T, et al. Double-Stranded RNA Derived from Lactic Acid Bacteria Augments Th1 Immunity via Interferon-beta from Human Dendritic Cells. Front Immunol. 2018;9:27.
20. Ren Y, Pan H, Pan B, Bu W. Identification and functional characterization of three TLR signaling pathway genes in Cyclina sinensis. Fish Shellfish Immunol. 2016;50:150-9.
21. Jounai K, Ikado K, Sugimura T, Ano Y, Braun J, Fujiwara D. Spherical lactic acid bacteria activate plasmacytoid dendritic cells immunomodulatory function via TLR9-dependent crosstalk with myeloid dendritic cells. PLoS One. 2012;7(4):e32588.
22. Christensen HR, Frokiaer H, Pestka JJ. Lactobacilli differentially modulate expression of cytokines and maturation surface markers in murine dendritic cells. J Immunol. 2002;168(1):171-8.
23. Hart AL, Lammers K, Brigidi P, Vitali B, Rizzello F, Gionchetti P, et al. Modulation of human dendritic cell phenotype and function by probiotic bacteria. Gut. 2004;53(11):1602-9.
24. Lebeer S, Vanderleyden J, De Keersmaecker SC. Genes and molecules of lactobacilli supporting probiotic action. Microbiol Mol Biol Rev. 2008;72(4):728-64, Table of Contents.
25. Yanagihara S, Kanaya T, Fukuda S, Nakato G, Hanazato M, Wu XR, et al. Uromodulin-SlpA binding dictates Lactobacillus acidophilus uptake by intestinal epithelial M cells. Int Immunol. 2017;29(8):357-63.
26. Mercier-Bonin M, Chapot-Chartier MP. Surface Proteins of Lactococcus lactis: Bacterial Resources for Muco-adhesion in the Gastrointestinal Tract. Front Microbiol. 2017;8:2247.
27. Otte JM, Podolsky DK. Functional modulation of enterocytes by gram-positive and gram-negative microorganisms. Am J Physiol Gastrointest Liver Physiol. 2004;286(4):G613-26.
28. Schlee M, Harder J, Koten B, Stange EF, Wehkamp J, Fellermann K. Probiotic lactobacilli and VSL#3 induce enterocyte beta-defensin 2. Clin Exp Immunol. 2008;151(3):528-35.
29. Perdigon G, Maldonado Galdeano C, Valdez JC, Medici M. Interaction of lactic acid bacteria with the gut immune system. Eur J Clin Nutr. 2002;56 Suppl 4:S21-6.
30. Yam KK, Pouliot P, N'Diaye M M, Fournier S, Olivier M, Cousineau B. Innate inflammatory responses to the Gram-positive bacterium Lactococcus lactis. Vaccine. 2008;26(22):2689-99.
31. Bermudez-Humaran LG, Cortes-Perez NG, Lefevre F, Guimaraes V, Rabot S, Alcocer-Gonzalez JM, et al. A novel mucosal vaccine based on live Lactococci expressing E7 antigen and IL-12 induces systemic and mucosal immune responses and protects mice against human papillomavirus type 16-induced tumors. J Immunol. 2005;175(11):7297-302.
32. Kalina WV, Mohamadzadeh M. Lactobacilli as natural enhancer of cellular immune response. Discov Med. 2005;5(26):199-203.
33. Bermudez-Humaran LG. Lactococcus lactis as a live vector for mucosal delivery of therapeutic proteins. Hum Vaccin. 2009;5(4):264-7.
34. Bermudez-Humaran LG, Kharrat P, Chatel JM, Langella P. Lactococci and lactobacilli as mucosal delivery vectors for therapeutic proteins and DNA vaccines. Microb Cell Fact. 2011;10 Suppl 1:S4.
35. Rhee JH, Lee SE, Kim SY. Mucosal vaccine adjuvants update. Clin Exp Vaccine Res. 2012;1(1):50-63.
36. Freytag LC, Clements JD. Mucosal adjuvants. Vaccine. 2005;23(15):1804-13.
37. Jiang B, Li Z, Ou B, Duan Q, Zhu G. Targeting ideal oral vaccine vectors based on probiotics: a systematical view. Appl Microbiol Biotechnol. 2019;103(10):3941-53.

38. Li Y, Li X, Liu H, Zhuang S, Yang J, Zhang F. Intranasal immunization with recombinant Lactococci carrying human papillomavirus E7 protein and mouse interleukin-12 DNA induces E7-specific antitumor effects in C57BL/6 mice. Oncol Lett. 2014;7(2):576-82.
39. Watford WT, Moriguchi M, Morinobu A, O'Shea JJ. The biology of IL-12: coordinating innate and adaptive immune responses. Cytokine Growth Factor Rev. 2003;14(5):361-8.
40. Dinarello CA. Overview of the IL-1 family in innate inflammation and acquired immunity. Immunol Rev. 2018;281(1):8-27.
41. Conos SA, Lawlor KE, Vaux DL, Vince JE, Lindqvist LM. Cell death is not essential for caspase-1-mediated interleukin-1beta activation and secretion. Cell Death Differ. 2016;23(11):1827-38.
42. Boucher D, Monteleone M, Coll RC, Chen KW, Ross CM, Teo JL, et al. Caspase-1 self-cleavage is an intrinsic mechanism to terminate inflammasome activity. J Exp Med. 2018;215(3):827-40.
43. Staats HF, Ennis FA, Jr. IL-1 is an effective adjuvant for mucosal and systemic immune responses when coadministered with protein immunogens. J Immunol. 1999;162(10):6141-7.
44. Antoni G, Presentini R, Perin F, Tagliabue A, Ghiara P, Censini S, et al. A short synthetic peptide fragment of human interleukin 1 with immunostimulatory but not inflammatory activity. J Immunol. 1986;137(10):3201-4.
45. Shornick LP, De Togni P, Mariathasan S, Goellner J, Strauss-Schoenberger J, Karr RW, et al. Mice deficient in IL-1beta manifest impaired contact hypersensitivity to trinitrochlorobenzone. J Exp Med. 1996;183(4):1427-36.
46. Kajikawa A, Masuda K, Katoh M, Igimi S. Adjuvant effects for oral immunization provided by recombinant Lactobacillus casei secreting biologically active murine interleukin-1{beta}. Clin Vaccine Immunol. 2010;17(1):43-8.
47. Kajikawa A, Zhang L, LaVoy A, Bumgardner S, Klaenhammer TR, Dean GA. Mucosal Immunogenicity of Genetically Modified Lactobacillus acidophilus Expressing an HIV-1 Epitope within the Surface Layer Protein. PLoS One. 2015;10(10):e0141713.
48. Abbas AK, Trotta E, D RS, Marson A, Bluestone JA. Revisiting IL-2: Biology and therapeutic prospects. Sci Immunol. 2018;3(25).
49. Kandasamy M, Selvakumari Jayasurya A, Moochhala S, Huat Bay B, Kun Lee Y, Mahendran R. Lactobacillus rhamnosus GG secreting an antigen and Interleukin-2 translocates across the gastrointestinal tract and induces an antigen specific immune response. Microbiol Immunol. 2011;55(10):704-14.
50. Santiago AF, Fernandes RM, Santos BP, Assis FA, Oliveira RP, Carvalho CR, et al. Role of mesenteric lymph nodes and aging in secretory IgA production in mice. Cell Immunol. 2008;253(1-2):5-10.
51. Mishra J, Waters CM, Kumar N. Molecular mechanism of interleukin-2-induced mucosal homeostasis. Am J Physiol Cell Physiol. 2012;302(5):C735-47.
52. Brynskov J, Tvede N, Andersen CB, Vilien M. Increased concentrations of interleukin 1 beta, interleukin-2, and soluble interleukin-2 receptors in endoscopical mucosal biopsy specimens with active inflammatory bowel disease. Gut. 1992;33(1):55-8.
53. Pullman WE, Doe WF. IL-2 production by intestinal lamina propria cells in normal inflamed and cancer-bearing colons. Clin Exp Immunol. 1992;88(1):132-7.
54. Cortes-Perez NG, Lefevre F, Corthier G, Adel-Patient K, Langella P, Bermudez-Humaran LG. Influence of the route of immunization and the nature of the bacterial vector on

immunogenicity of mucosal vaccines based on lactic acid bacteria. Vaccine. 2007;25(36):6581-8.
55. Hugentobler F, Di Roberto RB, Gillard J, Cousineau B. Oral immunization using live Lactococcus lactis co-expressing LACK and IL-12 protects BALB/c mice against Leishmania major infection. Vaccine. 2012;30(39):5726-32.
56. Hugentobler F, Yam KK, Gillard J, Mahbuba R, Olivier M, Cousineau B. Immunization against Leishmania major infection using LACK- and IL-12-expressing Lactococcus lactis induces delay in footpad swelling. PLoS One. 2012;7(2):e30945.
57. Mustafa AD, Kalyanasundram J, Sabidi S, Song AA, Abdullah M, Abdul Rahim R, et al. Proof of concept in utilizing in-trans surface display system of Lactobacillus plantarum as mucosal tuberculosis vaccine via oral administration in mice. BMC Biotechnol. 2018;18(1):63.
58. Szatraj K, Szczepankowska AK, Saczynska V, Florys K, Gromadzka B, Lepek K, et al. Expression of avian influenza haemagglutinin (H5) and chicken interleukin 2 (chIL-2) under control of the ptcB promoter in Lactococcus lactis. Acta Biochim Pol. 2014;61(3):609-14.
59. Chang SY, Ko HJ, Kweon MN. Mucosal dendritic cells shape mucosal immunity. Exp Mol Med. 2014;46:e84.
60. Curiel TJ, Morris C, Brumlik M, Landry SJ, Finstad K, Nelson A, et al. Peptides identified through phage display direct immunogenic antigen to dendritic cells. J Immunol. 2004;172(12):7425-31.
61. Yang WT, Yang GL, Shi SH, Liu YY, Huang HB, Jiang YL, et al. Protection of chickens against H9N2 avian influenza virus challenge with recombinant Lactobacillus plantarum expressing conserved antigens. Appl Microbiol Biotechnol. 2017;101(11):4593-603.
62. Hou X, Jiang X, Jiang Y, Tang L, Xu Y, Qiao X, et al. Oral Immunization against PEDV with Recombinant Lactobacillus casei Expressing Dendritic Cell-Targeting Peptide Fusing COE Protein of PEDV in Piglets. Viruses. 2018;10(3).
63. Yao XY, Yuan MM, Li DJ. Molecular adjuvant C3d3 improved the anti-hCGbeta humoral immune response in vaginal inoculation with live recombinant Lactobacillus expressing hCGbeta-C3d3 fusion protein. Vaccine. 2007;25(32):6129-39.
64. Michon C, Kuczkowska K, Langella P, Eijsink VG, Mathiesen G, Chatel JM. Surface display of an anti-DEC-205 single chain Fv fragment in Lactobacillus plantarum increases internalization and plasmid transfer to dendritic cells in vitro and in vivo. Microb Cell Fact. 2015;14:95.
65. Yang WT, Yang GL, Wang Q, Huang HB, Jiang YL, Shi CW, et al. Protective efficacy of Fc targeting conserved influenza virus M2e antigen expressed by Lactobacillus plantarum. Antiviral Res. 2017;138:9-21.
66. Roopenian DC, Akilesh S. FcRn: the neonatal Fc receptor comes of age. Nat Rev Immunol. 2007;7(9):715-25.
67. Mohamadzadeh M, Duong T, Sandwick SJ, Hoover T, Klaenhammer TR. Dendritic cell targeting of Bacillus anthracis protective antigen expressed by Lactobacillus acidophilus protects mice from lethal challenge. Proc Natl Acad Sci U S A. 2009;106(11):4331-6.
68. Mohamadzadeh M, Durmaz E, Zadeh M, Pakanati KC, Gramarossa M, Cohran V, et al. Targeted expression of anthrax protective antigen by Lactobacillus gasseri as an anthrax vaccine. Future Microbiol. 2010;5(8):1289-96.
69. Jiang Y, Hu J, Guo Y, Yang W, Ye L, Shi C, et al. Construction and immunological evaluation of recombinant Lactobacillus plantarum expressing HN of Newcastle disease virus and DC- targeting peptide fusion protein. J Biotechnol. 2015;216:82-9.

70. Shi SH, Yang WT, Yang GL, Zhang XK, Liu YY, Zhang LJ, et al. Lactobacillus plantarum vaccine vector expressing hemagglutinin provides protection against H9N2 challenge infection. Virus Res. 2016;211:46-57.
71. Yang WT, Shi SH, Yang GL, Jiang YL, Zhao L, Li Y, et al. Cross-protective efficacy of dendritic cells targeting conserved influenza virus antigen expressed by Lactobacillus plantarum. Sci Rep. 2016;6:39665.
72. Wang X, Wang L, Huang X, Ma S, Yu M, Shi W, et al. Oral Delivery of Probiotics Expressing Dendritic Cell-Targeting Peptide Fused with Porcine Epidemic Diarrhea Virus COE Antigen: A Promising Vaccine Strategy against PEDV. Viruses. 2017;9(11).
73. Yang G, Jiang Y, Tong P, Li C, Yang W, Hu J, et al. Alleviation of enterotoxigenic Escherichia coli challenge by recombinant Lactobacillus plantarum expressing a FaeG- and DC-targeting peptide fusion protein. Benef Microbes. 2017;8(3):379-91.
74. Yang G, Yao J, Yang W, Jiang Y, Du J, Huang H, et al. Construction and immunological evaluation of recombinant Lactobacillus plantarum expressing SO7 of Eimeria tenella fusion DC-targeting peptide. Vet Parasitol. 2017;236:7-13.
75. Sahay B, Colliou N, Zadeh M, Ge Y, Gong M, Owen JL, et al. Dual-route targeted vaccine protects efficiently against botulinum neurotoxin A complex. Vaccine. 2018;36(1):155-64.
76. Huang KY, Yang GL, Jin YB, Liu J, Chen HL, Wang PB, et al. Construction and immunogenicity analysis of Lactobacillus plantarum expressing a porcine epidemic diarrhea virus S gene fused to a DC-targeting peptide. Virus Res. 2018;247:84-93.
77. Ma S, Wang L, Huang X, Wang X, Chen S, Shi W, et al. Oral recombinant Lactobacillus vaccine targeting the intestinal microfold cells and dendritic cells for delivering the core neutralizing epitope of porcine epidemic diarrhea virus. Microb Cell Fact. 2018;17(1):20.
78. Wang Y, Feng B, Niu C, Jia S, Sun C, Wang Z, et al. Dendritic Cell Targeting of Bovine Viral Diarrhea Virus E2 Protein Expressed by Lactobacillus casei Effectively Induces Antigen-Specific Immune Responses via Oral Vaccination. Viruses. 2019;11(6).
79. Liang S, Hajishengallis G. Heat-labile enterotoxins as adjuvants or anti-inflammatory agents. Immunol Invest. 2010;39(4-5):449-67.
80. Petrovsky N. Comparative Safety of Vaccine Adjuvants: A Summary of Current Evidence and Future Needs. Drug Saf. 2015;38(11):1059-74.
81. Hajishengallis G, Arce S, Gockel CM, Connell TD, Russell MW. Immunomodulation with enterotoxins for the generation of secretory immunity or tolerance: applications for oral infections. J Dent Res. 2005;84(12):1104-16.
82. Agren L, Lowenadler B, Lycke N. A novel concept in mucosal adjuvanticity: the CTA1-DD adjuvant is a B cell-targeted fusion protein that incorporates the enzymatically active cholera toxin A1 subunit. Immunol Cell Biol. 1998;76(3):280-7.
83. Agren L, Sverremark E, Ekman L, Schon K, Lowenadler B, Fernandez C, et al. The ADP-ribosylating CTA1-DD adjuvant enhances T cell-dependent and independent responses by direct action on B cells involving anti-apoptotic Bcl-2- and germinal center-promoting effects. J Immunol. 2000;164(12):6276-86.
84. Lei H, Sheng Z, Ding Q, Chen J, Wei X, Lam DM, et al. Evaluation of oral immunization with recombinant avian influenza virus HA1 displayed on the Lactococcus lactis surface and combined with the mucosal adjuvant cholera toxin subunit B. Clin Vaccine Immunol. 2011;18(7):1046-51.

85. Chowdhury MY, Li R, Kim JH, Park ME, Kim TH, Pathinayake P, et al. Mucosal vaccination with recombinant Lactobacillus casei-displayed CTA1-conjugated consensus matrix protein-2 (sM2) induces broad protection against divergent influenza subtypes in BALB/c mice. PLoS One. 2014;9(4):e94051.
86. Li R, Chowdhury MY, Kim JH, Kim TH, Pathinayake P, Koo WS, et al. Mucosally administered Lactobacillus surface-displayed influenza antigens (sM2 and HA2) with cholera toxin subunit A1 (CTA1) Induce broadly protective immune responses against divergent influenza subtypes. Vet Microbiol. 2015;179(3-4):250-63.
87. Ge JW, Liu DQ, Li YJ. Construction of recombinant lactobacilli expressing the core neutralizing epitope (COE) of porcine epidemic diarrhea virus and a fusion protein consisting of COE and Escherichia coli heat-labile enterotoxin B, and comparison of the immune responses by orogastric immunization. Can J Microbiol. 2012;58(11):1258-67.
88. Jiang Y, Yang G, Wang Q, Wang Z, Yang W, Gu W, et al. Molecular mechanisms underlying protection against H9N2 influenza virus challenge in mice by recombinant Lactobacillus plantarum with surface displayed HA2-LTB. J Biotechnol. 2017;259:6-14.
89. Mutsch M, Zhou W, Rhodes P, Bopp M, Chen RT, Linder T, et al. Use of the inactivated intranasal influenza vaccine and the risk of Bell's palsy in Switzerland. N Engl J Med. 2004;350(9):896-903.
90. Colombi D, Oliveira ML, Campos IB, Monedero V, Perez-Martinez G, Ho PL. Haemagglutination induced by Bordetella pertussis filamentous haemagglutinin adhesin (FHA) is inhibited by antibodies produced against FHA(430-873) fragment expressed in Lactobacillus casei. Curr Microbiol. 2006;53(6):462-6.
91. Okuno T, Kashige N, Satho T, Irie K, Hiramatsu Y, Sharmin T, et al. Expression and secretion of cholera toxin B subunit in lactobacilli. Biol Pharm Bull. 2013;36(6):952-8.
92. Qiao X, Li G, Wang X, Li X, Liu M, Li Y. Recombinant porcine rotavirus VP4 and VP4-LTB expressed in Lactobacillus casei induced mucosal and systemic antibody responses in mice. BMC Microbiol. 2009;9:249.
93. Yu M, Qi R, Chen C, Yin J, Ma S, Shi W, et al. Immunogenicity of recombinant Lactobacillus casei-expressing F4 (K88) fimbrial adhesin FaeG in conjunction with a heat-labile enterotoxin A (LTAK63) and heat-labile enterotoxin B (LTB) of enterotoxigenic Escherichia coli as an oral adjuvant in mice. J Appl Microbiol. 2017;122(2):506-15.
94. Miao EA, Alpuche-Aranda CM, Dors M, Clark AE, Bader MW, Miller SI, et al. Cytoplasmic flagellin activates caspase-1 and secretion of interleukin 1beta via Ipaf. Nat Immunol. 2006;7(6):569-75.
95. Cui B, Liu X, Fang Y, Zhou P, Zhang Y, Wang Y. Flagellin as a vaccine adjuvant. Expert Rev Vaccines. 2018;17(4):335-49.
96. Kajikawa A, Zhang L, Long J, Nordone S, Stoeker L, LaVoy A, et al. Construction and immunological evaluation of dual cell surface display of HIV-1 gag and Salmonella enterica serovar Typhimurium FliC in Lactobacillus acidophilus for vaccine delivery. Clin Vaccine Immunol. 2012;19(9):1374-81.
97. Stoeker L, Nordone S, Gunderson S, Zhang L, Kajikawa A, LaVoy A, et al. Assessment of Lactobacillus gasseri as a candidate oral vaccine vector. Clin Vaccine Immunol. 2011;18(11):1834-44.
98. Kajikawa A, Igimi S. Innate and acquired immune responses induced by recombinant Lactobacillus casei displaying flagellin-fusion antigen on the cell-surface. Vaccine. 2010;28(19):3409-15.

99. Hong SH, Byun YH, Nguyen CT, Kim SY, Seong BL, Park S, et al. Intranasal administration of a flagellin-adjuvanted inactivated influenza vaccine enhances mucosal immune responses to protect mice against lethal infection. Vaccine. 2012;30(2):466-74.
100. Fazeli A, Bruce C, Anumba DO. Characterization of Toll-like receptors in the female reproductive tract in humans. Hum Reprod. 2005;20(5):1372-8.
101. Guimaraes VD, Gabriel JE, Lefevre F, Cabanes D, Gruss A, Cossart P, et al. Internalin-expressing Lactococcus lactis is able to invade small intestine of guinea pigs and deliver DNA into mammalian epithelial cells. Microbes Infect. 2005;7(5-6):836-44.
102. de Azevedo M, Karczewski J, Lefevre F, Azevedo V, Miyoshi A, Wells JM, et al. In vitro and in vivo characterization of DNA delivery using recombinant Lactococcus lactis expressing a mutated form of L. monocytogenes Internalin A. BMC Microbiol. 2012;12:299.
103. Pontes D, Innocentin S, Del Carmen S, Almeida JF, Leblanc JG, de Moreno de Leblanc A, et al. Production of Fibronectin Binding Protein A at the surface of Lactococcus lactis increases plasmid transfer in vitro and in vivo. PLoS One. 2012;7(9):e44892.
104. Pontes D, Azevedo M, Innocentin S, Blugeon S, Lefevre F, Azevedo V, et al. Immune response elicited by DNA vaccination using Lactococcus lactis is modified by the production of surface exposed pathogenic protein. PLoS One. 2014;9(1):e84509.
105. Mancha-Agresti P, de Castro CP, Dos Santos JSC, Araujo MA, Pereira VB, LeBlanc JG, et al. Recombinant Invasive Lactococcus lactis Carrying a DNA Vaccine Coding the Ag85A Antigen Increases INF-gamma, IL-6, and TNF-alpha Cytokines after Intranasal Immunization. Front Microbiol. 2017;8:1263.
106. Gaillard JL, Berche P, Frehel C, Gouin E, Cossart P. Entry of L. monocytogenes into cells is mediated by internalin, a repeat protein reminiscent of surface antigens from gram-positive cocci. Cell. 1991;65(7):1127-41.
107. Innocentin S, Guimaraes V, Miyoshi A, Azevedo V, Langella P, Chatel JM, et al. Lactococcus lactis expressing either Staphylococcus aureus fibronectin-binding protein A or Listeria monocytogenes internalin A can efficiently internalize and deliver DNA in human epithelial cells. Appl Environ Microbiol. 2009;75(14):4870-8.
108. Jiang X, Yu M, Qiao X, Liu M, Tang L, Jiang Y, et al. Up-regulation of MDP and tuftsin gene expression in Th1 and Th17 cells as an adjuvant for an oral Lactobacillus casei vaccine against anti-transmissible gastroenteritis virus. Appl Microbiol Biotechnol. 2014;98(19):8301-12.
109. Vasquez AE, Manzo RA, Soto DA, Barrientos MJ, Maldonado AE, Mosqueira M, et al. Oral administration of recombinant Neisseria meningitidis PorA genetically fused to H. pylori HpaA antigen increases antibody levels in mouse serum, suggesting that PorA behaves as a putative adjuvant. Hum Vaccin Immunother. 2015;11(3):776-88.
110. Quintana I, Espariz M, Villar SR, Gonzalez FB, Pacini MF, Cabrera G, et al. Genetic Engineering of Lactococcus lactis Co-producing Antigen and the Mucosal Adjuvant 3' 5'- cyclic di Adenosine Monophosphate (c-di-AMP) as a Design Strategy to Develop a Mucosal Vaccine Prototype. Front Microbiol. 2018;9:2100.
111. Wang W, Song Y, Liu L, Zhang Y, Wang T, Zhang W, et al. Neutralizing-antibody-mediated protection of chickens against infectious bursal disease via one-time vaccination with inactivated recombinant Lactococcus lactis expressing a fusion protein constructed from the RCK protein of Salmonella enterica and VP2 of infectious bursal disease virus. Microb Cell Fact. 2019;18(1):21.

112. Wardowska A, Dzierzbicka K, Menderska A, Trzonkowski P. New conjugates of tuftsin and muramyl dipeptide as stimulators of human monocyte-derived dendritic cells. Protein Pept Lett. 2013;20(2):200-4.
113. Skrnjug I, Rueckert C, Libanova R, Lienenklaus S, Weiss S, Guzman CA. The mucosal adjuvant cyclic di-AMP exerts immune stimulatory effects on dendritic cells and macrophages. PLoS One. 2014;9(4):e95728.
114. Heffernan EJ, Reed S, Hackett J, Fierer J, Roudier C, Guiney D. Mechanism of resistance to complement-mediated killing of bacteria encoded by the Salmonella typhimurium virulence plasmid gene rck. J Clin Invest. 1992;90(3):953-64.
115. Rosselin M, Virlogeux-Payant I, Roy C, Bottreau E, Sizaret PY, Mijouin L, et al. Rck of Salmonella enterica, subspecies enterica serovar enteritidis, mediates zipper-like internalization. Cell Res. 2010;20(6):647-64.
116. Taguchi A, Kawana K, Yokoyama T, Adachi K, Yamashita A, Tomio K, et al. Adjuvant effect of Japanese herbal medicines on the mucosal type 1 immune responses to human papillomavirus (HPV) E7 in mice immunized orally with Lactobacillus-based therapeutic HPV vaccine in a synergistic manner. Vaccine. 2012;30(36):5368-72.
117. Kim JI, Park TE, Maharjan S, Li HS, Lee HB, Kim IS, et al. Soluble RANKL expression in Lactococcus lactis and investigation of its potential as an oral vaccine adjuvant. BMC Immunol. 2015;16:71.
118. Xu YG, Guan XT, Liu ZM, Tian CY, Cui LC. Immunogenicity in Swine of Orally Administered Recombinant Lactobacillus plantarum Expressing Classical Swine Fever Virus E2 Protein in Conjunction with Thymosin alpha-1 as an Adjuvant. Appl Environ Microbiol. 2015;81(11):3745-52.
119. Underwood JR, Chivers M, Dang TT, Licciardi PV. Stimulation of tetanus toxoid-specific immune responses by a traditional Chinese herbal medicine. Vaccine. 2009;27(47):6634-41.
120. Kiyohara H, Nagai T, Munakata K, Nonaka K, Hanawa T, Kim SJ, et al. Stimulating effect of Japanese herbal (kampo) medicine, hochuekkito on upper respiratory mucosal immune system. Evid Based Complement Alternat Med. 2006;3(4):459-67.
121. Wang M, Gao Z, Zhang Z, Pan L, Zhang Y. Roles of M cells in infection and mucosal vaccines. Hum Vaccin Immunother. 2014;10(12):3544-51.
122. Jiang YF, Ma ZH, Zhao PW, Pan Y, Liu YY, Feng JY, et al. Effect of thymosin-alpha(1) on T-helper 1 cell and T-helper 2 cell cytokine synthesis in patients with hepatitis B virus e antigen-positive chronic hepatitis B. J Int Med Res. 2010;38(6):2053-62.
123. Li CL, Zhang T, Saibara T, Nemoto Y, Ono M, Akisawa N, et al. Thymosin alpha1 accelerates restoration of T cell-mediated neutralizing antibody response in immunocompromised hosts. Int Immunopharmacol. 2002;2(1):39-46.
124. Gerritse K, Posno M, Schellekens MM, Boersma WJ, Claassen E. Oral administration of TNP-Lactobacillus conjugates in mice: a model for evaluation of mucosal and systemic immune responses and memory formation elicited by transformed lactobacilli. Res Microbiol. 1990;141(7-8):955-62.
125. Marteau P, Rambaud JC. Potential of using lactic acid bacteria for therapy and immunomodulation in man. FEMS Microbiol Rev. 1993;12(1-3):207-20.
126. Takahashi K, Orito N, Tokunoh N, Inoue N. Current issues regarding the application of recombinant lactic acid bacteria to mucosal vaccine carriers. Appl Microbiol Biotechnol. 2019;103(15):5947-55.

127. Apostolico Jde S, Lunardelli VA, Coirada FC, Boscardin SB, Rosa DS. Adjuvants: Classification, Modus Operandi, and Licensing. J Immunol Res. 2016;2016:1459394.
128. Edelman R. Vaccine adjuvants. Rev Infect Dis. 1980;2(3):370-83.
129. Umesaki Y, Setoyama H. Structure of the intestinal flora responsible for development of the gut immune system in a rodent model. Microbes Infect. 2000;2(11):1343-51.
130. Hardy H, Harris J, Lyon E, Beal J, Foey AD. Probiotics, prebiotics and immunomodulation of gut mucosal defences: homeostasis and immunopathology. Nutrients. 2013;5(6):1869-912.
131. Stout E, Klaenhammer T, Barrangou R. CRISPR-Cas Technologies and Applications in Food Bacteria. Annu Rev Food Sci Technol. 2017;8:413-37.
132. van Pijkeren JP, Barrangou R. Genome Editing of Food-Grade Lactobacilli To Develop Therapeutic Probiotics. Microbiol Spectr. 2017;5(5).
133. Matsuguchi T, Takagi A, Matsuzaki T, Nagaoka M, Ishikawa K, Yokokura T, et al. Lipoteichoic acids from Lactobacillus strains elicit strong tumor necrosis factor alpha-inducing activities in macrophages through Toll-like receptor 2. Clinical and diagnostic laboratory immunology. 2003;10(2):259-66.
134. Zeuthen LH, Fink LN, Frokiaer H. Toll-like receptor 2 and nucleotide-binding oligomerization domain-2 play divergent roles in the recognition of gut-derived lactobacilli and bifidobacteria in dendritic cells. Immunology. 2008;124(4):489-502.
135. Sanders ME, Klaenhammer TR. Invited review: the scientific basis of Lactobacillus acidophilus NCFM functionality as a probiotic. J Dairy Sci. 2001;84(2):319-31.
136. Douglas GL, Goh YJ, Klaenhammer TR. Integrative food grade expression system for lactic acid bacteria. Methods Mol Biol. 2011;765:373-87.
137. Wang Z, Yu Q, Gao J, Yang Q. Mucosal and systemic immune responses induced by recombinant Lactobacillus spp. expressing the hemagglutinin of the avian influenza virus H5N1. Clin Vaccine Immunol. 2012;19(2):174-9.
138. Moeini H, Rahim RA, Omar AR, Shafee N, Yusoff K. Lactobacillus acidophilus as a live vehicle for oral immunization against chicken anemia virus. Appl Microbiol Biotechnol. 2011;90(1):77-88.
139. Hongying F, Xianbo W, Fang Y, Yang B, Beiguo L. Oral immunization with recombinant Lactobacillus acidophilus expressing the adhesin Hp0410 of Helicobacter pylori induces mucosal and systemic immune responses. Clin Vaccine Immunol. 2014;21(2):126-32.
140. O'Flaherty S, Klaenhammer TR. Multivalent Chromosomal Expression of the Clostridium botulinum Serotype A Neurotoxin Heavy-Chain Antigen and the Bacillus anthracis Protective Antigen in Lactobacillus acidophilus. Appl Environ Microbiol. 2016;82(20):6091-101.
141. Lin R, Zhang Y, Long B, Li Y, Wu Y, Duan S, et al. Oral Immunization with Recombinant Lactobacillus acidophilus Expressing espA-Tir-M Confers Protection against Enterohemorrhagic Escherichia coli O157:H7 Challenge in Mice. Front Microbiol. 2017;8:417.
142. Chu H, Kang S, Ha S, Cho K, Park SM, Han KH, et al. Lactobacillus acidophilus expressing recombinant K99 adhesive fimbriae has an inhibitory effect on adhesion of enterotoxigenic Escherichia coli. Microbiol Immunol. 2005;49(11):941-8.
143. Zhu LF, Long BG, Luo J, Jiang R, Fang HY. [Construction of a recombinant Lactobacillus acidophilus expressing high levels of Helicobacter pylori adhesin Hp0410]. Nan Fang Yi Ke Da Xue Xue Bao. 2010;30(2):334-7.

144. Corthesy B, Boris S, Isler P, Grangette C, Mercenier A. Oral immunization of mice with lactic acid bacteria producing Helicobacter pylori urease B subunit partially protects against challenge with Helicobacter felis. J Infect Dis. 2005;192(8):1441-9.
145. Goh YJ, Azcarate-Peril MA, O'Flaherty S, Durmaz E, Valence F, Jardin J, et al. Development and application of a upp-based counterselective gene replacement system for the study of the S-layer protein SlpX of Lactobacillus acidophilus NCFM. Appl Environ Microbiol. 2009;75(10):3093-105.
146. Kajikawa A, Nordone SK, Zhang L, Stoeker LL, LaVoy AS, Klaenhammer TR, et al. Dissimilar properties of two recombinant Lactobacillus acidophilus strains displaying Salmonella FliC with different anchoring motifs. Appl Environ Microbiol. 2011;77(18):6587-96.
147. Bumgardner SA, Zhang L, LaVoy AS, Andre B, Frank CB, Kajikawa A, et al. Nod2 is required for antigen-specific humoral responses against antigens orally delivered using a recombinant Lactobacillus vaccine platform. PLoS One. 2018;13(5):e0196950.
148. Crooks ET, Moore PL, Richman D, Robinson J, Crooks JA, Franti M, et al. Characterizing anti-HIV monoclonal antibodies and immune sera by defining the mechanism of neutralization. Hum Antibodies. 2005;14(3-4):101-13.
149. Mehandru S, Wrin T, Galovich J, Stiegler G, Vcelar B, Hurley A, et al. Neutralization profiles of newly transmitted human immunodeficiency virus type 1 by monoclonal antibodies 2G12, 2F5, and 4E10. J Virol. 2004;78(24):14039-42.
150. Stiegler G, Kunert R, Purtscher M, Wolbank S, Voglauer R, Steindl F, et al. A potent cross-clade neutralizing human monoclonal antibody against a novel epitope on gp41 of human immunodeficiency virus type 1. AIDS Res Hum Retroviruses. 2001;17(18):1757-65.
151. LeCureux J DL, Kajikawa A, LaVoy A, Vilander A, Zhang L, and Dean G. Antigen-specific immune induction by a recombinant Lactobacillus acidophilus oral vaccine is T-cell dependent and enhanced by co-expression of adjuvants. In preparation.
152. Bien J, Sokolova O, Bozko P. Role of Uropathogenic Escherichia coli Virulence Factors in Development of Urinary Tract Infection and Kidney Damage. Int J Nephrol. 2012;2012:681473.
153. Hase K, Kawano K, Nochi T, Pontes GS, Fukuda S, Ebisawa M, et al. Uptake through glycoprotein 2 of FimH(+) bacteria by M cells initiates mucosal immune response. Nature. 2009;462(7270):226-30.
154. Azizi A, Kumar A, Diaz-Mitoma F, Mestecky J. Enhancing oral vaccine potency by targeting intestinal M cells. PLoS Pathog. 2010;6(11):e1001147.
155. Fransen F, Zagato E, Mazzini E, Fosso B, Manzari C, El Aidy S, et al. BALB/c and C57BL/6 Mice Differ in Polyreactive IgA Abundance, which Impacts the Generation of Antigen-Specific IgA and Microbiota Diversity. Immunity. 2015;43(3):527-40.
156. Martinoli C, Chiavelli A, Rescigno M. Entry route of Salmonella typhimurium directs the type of induced immune response. Immunity. 2007;27(6):975-84.
157. Mossman KL, Mian MF, Lauzon NM, Gyles CL, Lichty B, Mackenzie R, et al. Cutting edge: FimH adhesin of type 1 fimbriae is a novel TLR4 ligand. J Immunol. 2008;181(10):6702-6.
158. Baorto DM, Gao Z, Malaviya R, Dustin ML, van der Merwe A, Lublin DM, et al. Survival of FimH-expressing enterobacteria in macrophages relies on glycolipid traffic. Nature. 1997;389(6651):636-9.

159. Fan X, Yue Y, Xiong S. Incorporation of a bi-functional protein FimH enhances the immunoprotection of chitosan-pVP1 vaccine against coxsackievirus B3-induced myocarditis. Antiviral Res. 2017;140:121-32.
160. Walker DC, Aoyama K, Klaenhammer TR. Electrotransformation of lactobacillus acidophilus group A1. FEMS Microbiol Lett. 1996;138(2-3):233-7.
161. Fukuda S, Hase K, Ohno H. Application of a mouse ligated Peyer's patch intestinal loop assay to evaluate bacterial uptake by M cells. J Vis Exp. 2011(58).
162. Frey A, Di Canzio J, Zurakowski D. A statistically defined endpoint titer determination method for immunoassays. J Immunol Methods. 1998;221(1-2):35-41.
163. Choudhury D, Thompson A, Stojanoff V, Langermann S, Pinkner J, Hultgren SJ, et al. X-ray structure of the FimC-FimH chaperone-adhesin complex from uropathogenic Escherichia coli. Science. 1999;285(5430):1061-6.
164. Schembri MA, Hasman H, Klemm P. Expression and purification of the mannose recognition domain of the FimH adhesin. FEMS Microbiol Lett. 2000;188(2):147-51.
165. Cerovic V, Bain CC, Mowat AM, Milling SW. Intestinal macrophages and dendritic cells: what's the difference? Trends Immunol. 2014;35(6):270-7.
166. Tamoutounour S, Henri S, Lelouard H, de Bovis B, de Haar C, van der Woude CJ, et al. CD64 distinguishes macrophages from dendritic cells in the gut and reveals the Th1-inducing role of mesenteric lymph node macrophages during colitis. Eur J Immunol. 2012;42(12):3150-66.
167. Mora JR, von Andrian UH. Differentiation and homing of IgA-secreting cells. Mucosal Immunol. 2008;1(2):96-109.
168. Miquel-Clopes A, Bentley EG, Stewart JP, Carding SR. Mucosal vaccines and technology. Clin Exp Immunol. 2019;196(2):205-14.
169. Watkins JD, Sholukh AM, Mukhtar MM, Siddappa NB, Lakhashe SK, Kim M, et al. Anti-HIV IgA isotypes: differential virion capture and inhibition of transcytosis are linked to prevention of mucosal R5 SHIV transmission. AIDS. 2013;27(9):F13-20.
170. Tomaras GD, Ferrari G, Shen X, Alam SM, Liao HX, Pollara J, et al. Vaccine-induced plasma IgA specific for the C1 region of the HIV-1 envelope blocks binding and effector function of IgG. Proc Natl Acad Sci U S A. 2013;110(22):9019-24.
171. Fischer H, Yamamoto M, Akira S, Beutler B, Svanborg C. Mechanism of pathogen-specific TLR4 activation in the mucosa: fimbriae, recognition receptors and adaptor protein selection. Eur J Immunol. 2006;36(2):267-77.
172. Habibi M, Asadi Karam MR, Bouzari S. In silico Study of Toll-Like Receptor 4 Binding Site of FimH from Uropathogenic Escherichia coli. Journal of Medical Microbiology and Infectious Diseases. 2014;2(1):35-9.
173. Wardlaw T, Salama P, Brocklehurst C, Chopra M, Mason E. Diarrhoea: why children are still dying and what can be done. Lancet. 2010;375(9718):870-2.
174. Rotavirus vaccines WHO position paper: January 2013 - Recommendations. Vaccine. 2013;31(52):6170-1.
175. O'Ryan M. Rotavirus Vaccines: a story of success with challenges ahead. F1000Res. 2017;6:1517.
176. Burnett E, Parashar U, Tate J. Rotavirus Vaccines: Effectiveness, Safety, and Future Directions. Paediatr Drugs. 2018;20(3):223-33.

177. Steele AD, Victor JC, Carey ME, Tate JE, Atherly DE, Pecenka C, et al. Experiences with rotavirus vaccines: can we improve rotavirus vaccine impact in developing countries? Hum Vaccin Immunother. 2019;15(6):1215-27.
178. Saif L, Yuan L, Ward L, To T. Comparative studies of the pathogenesis, antibody immune responses, and homologous protection to porcine and human rotaviruses in gnotobiotic piglets. Adv Exp Med Biol. 1997;412:397-403.
179. Offit PA, Clark HF. Protection against rotavirus-induced gastroenteritis in a murine model by passively acquired gastrointestinal but not circulating antibodies. J Virol. 1985;54(1):58-64.
180. Burns JW, Siadat-Pajouh M, Krishnaney AA, Greenberg HB. Protective effect of rotavirus VP6-specific IgA monoclonal antibodies that lack neutralizing activity. Science. 1996;272(5258):104-7.
181. Feng N, Lawton JA, Gilbert J, Kuklin N, Vo P, Prasad BV, et al. Inhibition of rotavirus replication by a non-neutralizing, rotavirus VP6-specific IgA mAb. J Clin Invest. 2002;109(9):1203-13.
182. Corthesy B, Benureau Y, Perrier C, Fourgeux C, Parez N, Greenberg H, et al. Rotavirus anti-VP6 secretory immunoglobulin A contributes to protection via intracellular neutralization but not via immune exclusion. J Virol. 2006;80(21):10692-9.
183. Blutt SE, Miller AD, Salmon SL, Metzger DW, Conner ME. IgA is important for clearance and critical for protection from rotavirus infection. Mucosal Immunol. 2012;5(6):712-9.
184. Isolauri E, Joensuu J, Suomalainen H, Luomala M, Vesikari T. Improved immunogenicity of oral D x RRV reassortant rotavirus vaccine by Lactobacillus casei GG. Vaccine. 1995;13(3):310-2.
185. Liu F, Wen K, Li G, Yang X, Kocher J, Bui T, et al. Dual functions of Lactobacillus acidophilus NCFM as protection against rotavirus diarrhea. J Pediatr Gastroenterol Nutr. 2014;58(2):169-76.
186. Zhang W, Azevedo MS, Wen K, Gonzalez A, Saif LJ, Li G, et al. Probiotic Lactobacillus acidophilus enhances the immunogenicity of an oral rotavirus vaccine in gnotobiotic pigs. Vaccine. 2008;26(29-30):3655-61.
187. Kovacs-Nolan J, Yoo D, Mine Y. Fine mapping of sequential neutralization epitopes on the subunit protein VP8 of human rotavirus. Biochem J. 2003;376(Pt 1):269-75.
188. Kovacs-Nolan J, Mine Y. Tandem copies of a human rotavirus VP8 epitope can induce specific neutralizing antibodies in BALB/c mice. Biochim Biophys Acta. 2006;1760(12):1884-93.
189. Giammarioli AM, Mackow ER, Fiore L, Greenberg HB, Ruggeri FM. Production and characterization of murine IgA monoclonal antibodies to the surface antigens of rhesus rotavirus. Virology. 1996;225(1):97-110.
190. Clarke E, Desselberger U. Correlates of protection against human rotavirus disease and the factors influencing protection in low-income settings. Mucosal Immunol. 2015;8(1):1-17.
191. Nolan T, Hands RE, Ogunkolade W, Bustin SA. SPUD: a quantitative PCR assay for the detection of inhibitors in nucleic acid preparations. Anal Biochem. 2006;351(2):308-10.
192. Pinkerton R, Oria RB, Lima AA, Rogawski ET, Oria MO, Patrick PD, et al. Early Childhood Diarrhea Predicts Cognitive Delays in Later Childhood Independently of Malnutrition. Am J Trop Med Hyg. 2016;95(5):1004-10.

193. Guerrant RL, DeBoer MD, Moore SR, Scharf RJ, Lima AA. The impoverished gut--a triple burden of diarrhoea, stunting and chronic disease. Nat Rev Gastroenterol Hepatol. 2013;10(4):220-9.
194. Burke RM, Tate JE, Kirkwood CD, Steele AD, Parashar UD. Current and new rotavirus vaccines. Curr Opin Infect Dis. 2019;32(5):435-44.
195. Cerutti A. The regulation of IgA class switching. Nat Rev Immunol. 2008;8(6):421-34.
196. Ehrhardt RO, Strober W, Harriman GR. Effect of transforming growth factor (TGF)-beta 1 on IgA isotype expression. TGF-beta 1 induces a small increase in sIgA+ B cells regardless of the method of B cell activation. J Immunol. 1992;148(12):3830-6.
197. Konkel JE, Chen W. Balancing acts: the role of TGF-beta in the mucosal immune system. Trends Mol Med. 2011;17(11):668-76.
198. Chen CC, Louie S, Shi HN, Walker WA. Preinoculation with the probiotic Lactobacillus acidophilus early in life effectively inhibits murine Citrobacter rodentium colitis. Pediatr Res. 2005;58(6):1185-91.
199. Seo GY, Youn J, Kim PH. IL-21 ensures TGF-beta 1-induced IgA isotype expression in mouse Peyer's patches. J Leukoc Biol. 2009;85(5):744-50.
200. Cao AT, Yao S, Gong B, Nurieva RI, Elson CO, Cong Y. Interleukin (IL)-21 promotes intestinal IgA response to microbiota. Mucosal Immunol. 2015;8(5):1072-82.
201. Li SN, Wang W, Fu SP, Wang JF, Liu HM, Xie SS, et al. IL-21 modulates release of proinflammatory cytokines in LPS-stimulated macrophages through distinct signaling pathways. Mediators Inflamm. 2013;2013:548073.
202. Iwata M, Hirakiyama A, Eshima Y, Kagechika H, Kato C, Song SY. Retinoic acid imprints gut-homing specificity on T cells. Immunity. 2004;21(4):527-38.
203. Pino-Lagos K, Guo Y, Noelle RJ. Retinoic acid: a key player in immunity. Biofactors. 2010;36(6):430-6.
204. Diarrhoeal disease: WHO; 2017 [updated 2 May 2017. Available from: https://www.who.int/en/news-room/fact-sheets/detail/diarrhoeal-disease.
205. Bhutta ZA, Salam RA. Global nutrition epidemiology and trends. Ann Nutr Metab. 2012;61 Suppl 1:19-27.
206. Brown KH. Diarrhea and malnutrition. J Nutr. 2003;133(1):328S-32S.
207. Walson JL, Berkley JA. The impact of malnutrition on childhood infections. Curr Opin Infect Dis. 2018;31(3):231-6.
208. Black RE, Allen LH, Bhutta ZA, Caulfield LE, de Onis M, Ezzati M, et al. Maternal and child undernutrition: global and regional exposures and health consequences. Lancet. 2008;371(9608):243-60.
209. Humphrey JH. Child undernutrition, tropical enteropathy, toilets, and handwashing. Lancet. 2009;374(9694):1032-5.
210. Church JA, Parker EP, Kosek MN, Kang G, Grassly NC, Kelly P, et al. Exploring the relationship between environmental enteric dysfunction and oral vaccine responses. Future Microbiol. 2018;13:1055-70.
211. Crane RJ, Jones KD, Berkley JA. Environmental enteric dysfunction: an overview. Food Nutr Bull. 2015;36(1 Suppl):S76-87.
212. Louis-Auguste J, Kelly P. Tropical Enteropathies. Curr Gastroenterol Rep. 2017;19(7):29.

213. FAO Rice Market Monitor (RMM): Food and Agricultur Organization of the United Nation; [Available from: http://www.fao.org/economic/est/publications/rice-publications/rice-market-monitor-rmm/en/.
214. Sharif MK, Butt MS, Anjum FM, Khan SH. Rice bran: a novel functional ingredient. Crit Rev Food Sci Nutr. 2014;54(6):807-16.
215. Zarei I, Luna E, Leach JE, McClung A, Vilchez S, Koita O, et al. Comparative Rice Bran Metabolomics across Diverse Cultivars and Functional Rice Gene(-)Bran Metabolite Relationships. Metabolites. 2018;8(4).
216. Zarei I, Brown DG, Nealon NJ, Ryan EP. Rice Bran Metabolome Contains Amino Acids, Vitamins & Cofactors, and Phytochemicals with Medicinal and Nutritional Properties. Rice (N Y). 2017;10(1):24.
217. Ryan EP. Bioactive food components and health properties of rice bran. J Am Vet Med Assoc. 2011;238(5):593-600.
218. Zambrana LE, McKeen S, Ibrahim H, Zarei I, Borresen EC, Doumbia L, et al. Rice bran supplementation modulates growth, microbiota and metabolome in weaning infants: a clinical trial in Nicaragua and Mali. Sci Rep. 2019;9(1):13919.
219. de Sousa-Pereira P, Woof JM. IgA: Structure, Function, and Developability. Antibodies (Basel). 2019;8(4).
220. Corthesy B. Multi-faceted functions of secretory IgA at mucosal surfaces. Front Immunol. 2013;4:185.
221. Rytter MJ, Kolte L, Briend A, Friis H, Christensen VB. The immune system in children with malnutrition--a systematic review. PLoS One. 2014;9(8):e105017.
222. Lehmann T, Schallert K, Vilchez-Vargas R, Benndorf D, Puttker S, Sydor S, et al. Metaproteomics of fecal samples of Crohn's disease and Ulcerative Colitis. J Proteomics. 2019;201:93-103.
223. Scholtens PA, Alliet P, Raes M, Alles MS, Kroes H, Boehm G, et al. Fecal secretory immunoglobulin A is increased in healthy infants who receive a formula with short-chain galacto-oligosaccharides and long-chain fructo-oligosaccharides. J Nutr. 2008;138(6):1141-7.
224. Apprill A, McNally S, Parsons R, Weber L. Minor revision to V4 region SSU rRNA 806R gene primer greatly increases detection of SAR11 bacterioplankton. Aquat Microb Ecol. 2015;75(2):129-37.
225. Caporaso JG, Lauber CL, Walters WA, Berg-Lyons D, Huntley J, Fierer N, et al. Ultra-high-throughput microbial community analysis on the Illumina HiSeq and MiSeq platforms. ISME J. 2012;6(8):1621-4.
226. Caporaso JG, Lauber CL, Walters WA, Berg-Lyons D, Lozupone CA, Turnbaugh PJ, et al. Global patterns of 16S rRNA diversity at a depth of millions of sequences per sample. Proc Natl Acad Sci U S A. 2011;108 Suppl 1:4516-22.
227. Walters W, Hyde ER, Berg-Lyons D, Ackermann G, Humphrey G, Parada A, et al. Improved Bacterial 16S rRNA Gene (V4 and V4-5) and Fungal Internal Transcribed Spacer Marker Gene Primers for Microbial Community Surveys. mSystems. 2016;1(1).
228. Parada AE, Needham DM, Fuhrman JA. Every base matters: assessing small subunit rRNA primers for marine microbiomes with mock communities, time series and global field samples. Environ Microbiol. 2016;18(5):1403-14.
229. Bolyen E, Rideout JR, Dillon MR, Bokulich NA, Abnet CC, Al-Ghalith GA, et al. Reproducible, interactive, scalable and extensible microbiome data science using QIIME 2. Nature Biotechnology. 2019.

230. Callahan BJ, McMurdie PJ, Rosen MJ, Han AW, Johnson AJ, Holmes SP. DADA2: High-resolution sample inference from Illumina amplicon data. Nature methods. 2016;13(7):581-3.
231. DeSantis TZ, Hugenholtz P, Larsen N, Rojas M, Brodie EL, Keller K, et al. Greengenes, a chimera-checked 16S rRNA gene database and workbench compatible with ARB. Applied and environmental microbiology. 2006;72(7):5069-72.
232. Quast C, Pruesse E, Yilmaz P, Gerken J, Schweer T, Yarza P, et al. The SILVA ribosomal RNA gene database project: improved data processing and web-based tools. Nucleic acids research. 2013;41(Database issue):D590-6.
233. Team RC. R: A language and environment for statistical computing. R Foundation for Statistical Computing, Vienna, Austria; 2019.
234. Callahan BJ, Sankaran K, Fukuyama JA, McMurdie PJ, Holmes SP. Bioconductor Workflow for Microbiome Data Analysis: from raw reads to community analyses. F1000Res. 2016;5:1492.
235. Chen J, Bittinger K, Charlson ES, Hoffmann C, Lewis J, Wu GD, et al. Associating microbiome composition with environmental covariates using generalized UniFrac distances. Bioinformatics. 2012;28(16):2106-13.
236. Lozupone C, Lladser ME, Knights D, Stombaugh J, Knight R. UniFrac: an effective distance metric for microbial community comparison. The ISME journal. 2011;5(2):169-72.
237. Gloor GB, Macklaim JM, Pawlowsky-Glahn V, Egozcue JJ. Microbiome Datasets Are Compositional: And This Is Not Optional. Frontiers in microbiology. 2017;8:2224.
238. Fernandes AD, Macklaim JM, Linn TG, Reid G, Gloor GB. ANOVA-like differential expression (ALDEx) analysis for mixed population RNA-Seq. PloS one. 2013;8(7):e67019-e.
239. Gentleman RC, Carey VJ, Bates DM, Bolstad B, Dettling M, Dudoit S, et al. Bioconductor: open software development for computational biology and bioinformatics. Genome biology. 2004;5(10):R80.
240. Wilcoxon F. Individual Comparisons by Ranking Methods. Biometrics Bulletin. 1945;1(6):80-3.
241. Benjamini Y, Hochberg Y. Controlling the False Discovery Rate: A Practical and Powerful Approach to Multiple Testing. Journal of the Royal Statistical Society Series B (Methodological). 1995;57(1):289-300.
242. Shapiro SS, Wilk MB. An analysis of variance test for normality (complete samples). Biometrika. 1965;52(3-4):591-611.
243. Anderson MJ. A new method for non-parametric multivariate analysis of variance. Austral Ecology. 2001;26(1):32-46.
244. Aitchison J, Barceló-Vidal C, Martín-Fernández JA, Pawlowsky-Glahn V. Logratio Analysis and Compositional Distance. Mathematical Geology. 2000;32(3):271-5.
245. Mann HB, Whitney DR. On a Test of Whether one of Two Random Variables is Stochastically Larger than the Other. The Annals of Mathematical Statistics. 1947;18(1):50-60.
246. Morgan M, Obenchain V, Lang M, Thompson R, Turaga N. BiocParallel: Bioconductor facilities for parallel evaluation. 2019.
247. Paulson J. MetagenomeSeq: statistical analysis for sparse high-throughput sequenceing. BioconductorJp. 2014:1-20.
248. Kosek M, Haque R, Lima A, Babji S, Shrestha S, Qureshi S, et al. Fecal markers of intestinal inflammation and permeability associated with the subsequent acquisition of linear growth deficits in infants. Am J Trop Med Hyg. 2013;88(2):390-6.

249. George CM, Oldja L, Biswas S, Perin J, Lee GO, Kosek M, et al. Geophagy is associated with environmental enteropathy and stunting in children in rural Bangladesh. Am J Trop Med Hyg. 2015;92(6):1117-24.
250. Malnutrition and Enteric Disease Study (MAL-ED): NIH Fogarty International Center; 2018 [updated 2018 January 26. Available from: https://www.fic.nih.gov/About/Staff/Pages/mal-ed.aspx.
251. Becker-Dreps S, Vilchez S, Bucardo F, Twitchell E, Choi WS, Hudgens MG, et al. The Association Between Fecal Biomarkers of Environmental Enteropathy and Rotavirus Vaccine Response in Nicaraguan Infants. Pediatr Infect Dis J. 2017;36(4):412-6.
252. Subramanian S, Huq S, Yatsunenko T, Haque R, Mahfuz M, Alam MA, et al. Persistent gut microbiota immaturity in malnourished Bangladeshi children. Nature. 2014;510(7505):417-21.
253. Backhed F, Roswall J, Peng Y, Feng Q, Jia H, Kovatcheva-Datchary P, et al. Dynamics and Stabilization of the Human Gut Microbiome during the First Year of Life. Cell Host Microbe. 2015;17(6):852.
254. Reese AT, Dunn RR. Drivers of Microbiome Biodiversity: A Review of General Rules, Feces, and Ignorance. mBio. 2018;9(4).
255. Mali Nutritional Prolife: Development Initiatives Poverty Research Ltd; [Available from: https://globalnutritionreport.org/resources/nutrition-profiles/africa/western-africa/mali/.
256. Mali Small-Scale Irrigation Project 2016 [Available from: https://www.usaid.gov/sites/default/files/documents/1860/USAID_AEG_-_KfW_Irrigation_Fact_Sheet_-_FTF_-_Nov_16_FINAL.pdf.
257. Yang X, Twitchell E, Li G, Wen K, Weiss M, Kocher J, et al. High protective efficacy of rice bran against human rotavirus diarrhea via enhancing probiotic growth, gut barrier function, and innate immunity. Sci Rep. 2015;5:15004.
258. Henderson AJ, Kumar A, Barnett B, Dow SW, Ryan EP. Consumption of rice bran increases mucosal immunoglobulin A concentrations and numbers of intestinal Lactobacillus spp. J Med Food. 2012;15(5):469-75.
259. Naylor C, Lu M, Haque R, Mondal D, Buonomo E, Nayak U, et al. Environmental Enteropathy, Oral Vaccine Failure and Growth Faltering in Infants in Bangladesh. EBioMedicine. 2015;2(11):1759-66.
260. Campbell RK, Schulze KJ, Shaikh S, Mehra S, Ali H, Wu L, et al. Biomarkers of Environmental Enteric Dysfunction Among Children in Rural Bangladesh. J Pediatr Gastroenterol Nutr. 2017;65(1):40-6.
261. Externest D, Meckelein B, Schmidt MA, Frey A. Correlations between antibody immune responses at different mucosal effector sites are controlled by antigen type and dosage. Infect Immun. 2000;68(7):3830-9.
262. Khounlotham M, Kim W, Peatman E, Nava P, Medina-Contreras O, Addis C, et al. Compromised intestinal epithelial barrier induces adaptive immune compensation that protects from colitis. Immunity. 2012;37(3):563-73.
263. Boullier S, Tanguy M, Kadaoui KA, Caubet C, Sansonetti P, Corthesy B, et al. Secretory IgA-mediated neutralization of Shigella flexneri prevents intestinal tissue destruction by down-regulating inflammatory circuits. J Immunol. 2009;183(9):5879-85.
264. Sollid LM, Kvale D, Brandtzaeg P, Markussen G, Thorsby E. Interferon-gamma enhances expression of secretory component, the epithelial receptor for polymeric immunoglobulins. J Immunol. 1987;138(12):4303-6.

265. Clemente JC, Ursell LK, Parfrey LW, Knight R. The impact of the gut microbiota on human health: an integrative view. Cell. 2012;148(6):1258-70.
266. Robertson RC, Manges AR, Finlay BB, Prendergast AJ. The Human Microbiome and Child Growth - First 1000 Days and Beyond. Trends Microbiol. 2019;27(2):131-47.
267. Dzidic M, Boix-Amoros A, Selma-Royo M, Mira A, Collado MC. Gut Microbiota and Mucosal Immunity in the Neonate. Med Sci (Basel). 2018;6(3).
268. Yatsunenko T, Rey FE, Manary MJ, Trehan I, Dominguez-Bello MG, Contreras M, et al. Human gut microbiome viewed across age and geography. Nature. 2012;486(7402):222-7.
269. Kieser S, Sarker SA, Sakwinska O, Foata F, Sultana S, Khan Z, et al. Bangladeshi children with acute diarrhoea show faecal microbiomes with increased Streptococcus abundance, irrespective of diarrhoea aetiology. Environ Microbiol. 2018;20(6):2256-69.
270. Takeshita K, Mizuno S, Mikami Y, Sujino T, Saigusa K, Matsuoka K, et al. A Single Species of Clostridium Subcluster XIVa Decreased in Ulcerative Colitis Patients. Inflamm Bowel Dis. 2016;22(12):2802-10.
271. Precup G, Vodnar DC. Gut Prevotella as a possible biomarker of diet and its eubiotic versus dysbiotic roles: a comprehensive literature review. Br J Nutr. 2019;122(2):131-40.
272. Wilkins LJ, Monga M, Miller AW. Defining Dysbiosis for a Cluster of Chronic Diseases. Sci Rep. 2019;9(1):12918.
273. Pabst O, Hornef M. Gut microbiota: a natural adjuvant for vaccination. Immunity. 2014;41(3):349-51.
274. Harris V, Ali A, Fuentes S, Korpela K, Kazi M, Tate J, et al. Rotavirus vaccine response correlates with the infant gut microbiota composition in Pakistan. Gut Microbes. 2017:1-9.
275. Harris VC, Armah G, Fuentes S, Korpela KE, Parashar U, Victor JC, et al. Significant Correlation Between the Infant Gut Microbiome and Rotavirus Vaccine Response in Rural Ghana. J Infect Dis. 2017;215(1):34-41.
276. Oh JZ, Ravindran R, Chassaing B, Carvalho FA, Maddur MS, Bower M, et al. TLR5-mediated sensing of gut microbiota is necessary for antibody responses to seasonal influenza vaccination. Immunity. 2014;41(3):478-92.
277. Kumar A, Henderson A, Forster GM, Goodyear AW, Weir TL, Leach JE, et al. Dietary rice bran promotes resistance to Salmonella enterica serovar Typhimurium colonization in mice. BMC Microbiol. 2012;12:71.
278. Lei S, Ramesh A, Twitchell E, Wen K, Bui T, Weiss M, et al. High Protective Efficacy of Probiotics and Rice Bran against Human Norovirus Infection and Diarrhea in Gnotobiotic Pigs. Front Microbiol. 2016;7:1699.

APPENDIX

Chapter 3 Supplemental Figures

Supplemental Figure 3.1. Log-fold OTU differences between treatment groups extended from Figure 3.4. Log-fold differences determined by metagenomeSeq for rice bran minus control group at 6, 9, 10, and 11 months of age for all genus and species shown to have a log-fold difference greater than 2 with a p-value < 0.01. Red bars indicate increase in the rice bran groups and blue bars indicate increased in the control group.

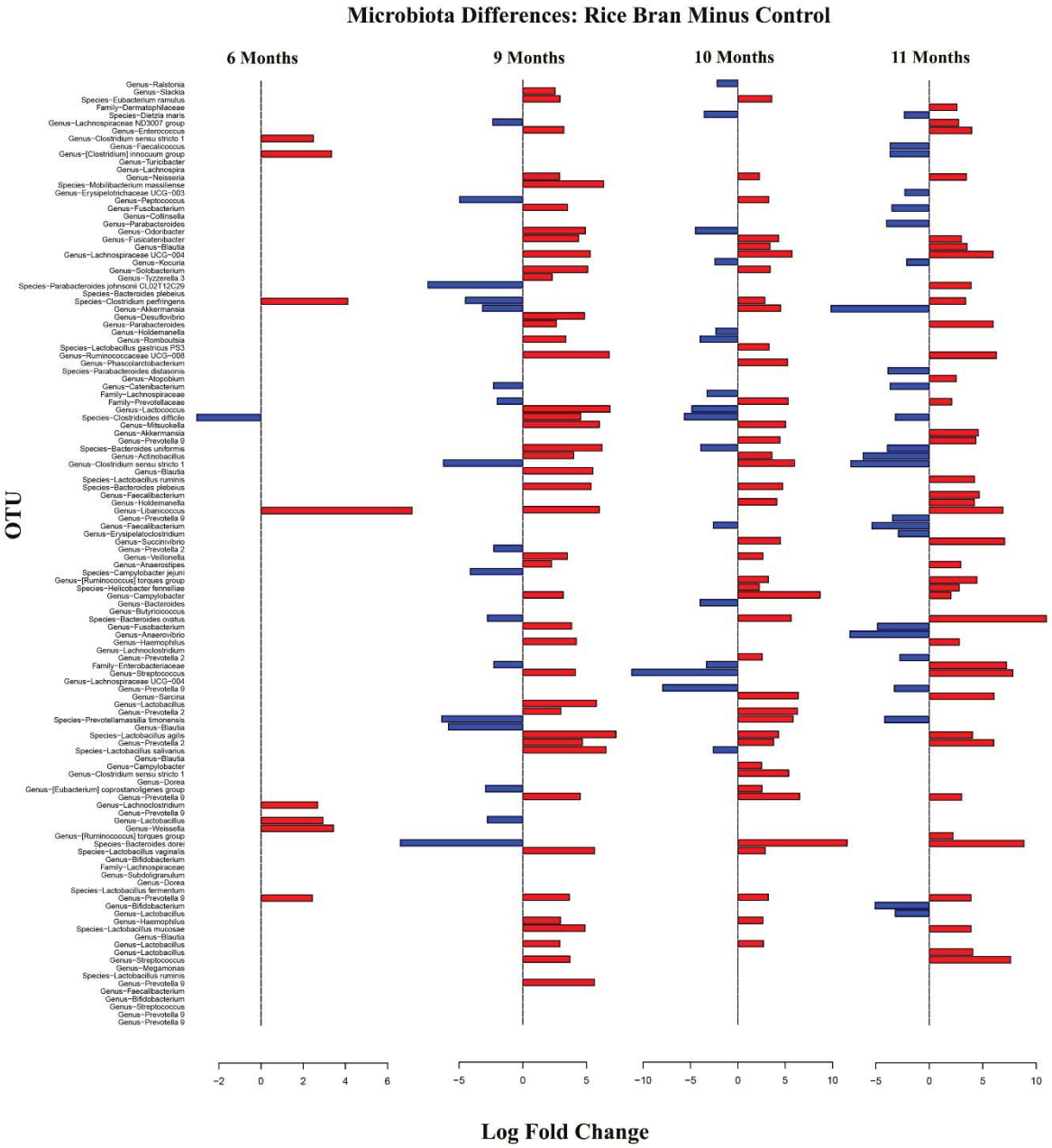

Supplemental Figure 3.2. Correlation between total fecal sIgA concentration and microbiota for control and rice bran groups at 6, 9, 10, and 11 months of age. Spearman correlation between total fecal sIgA concentration and the OTUs identified in Supplemental Figure 3.1 for the control (A) and rice bran cohorts (B). Red (positive correlation) and blue (negative correlation) bars are significant ($p < 0.05$).

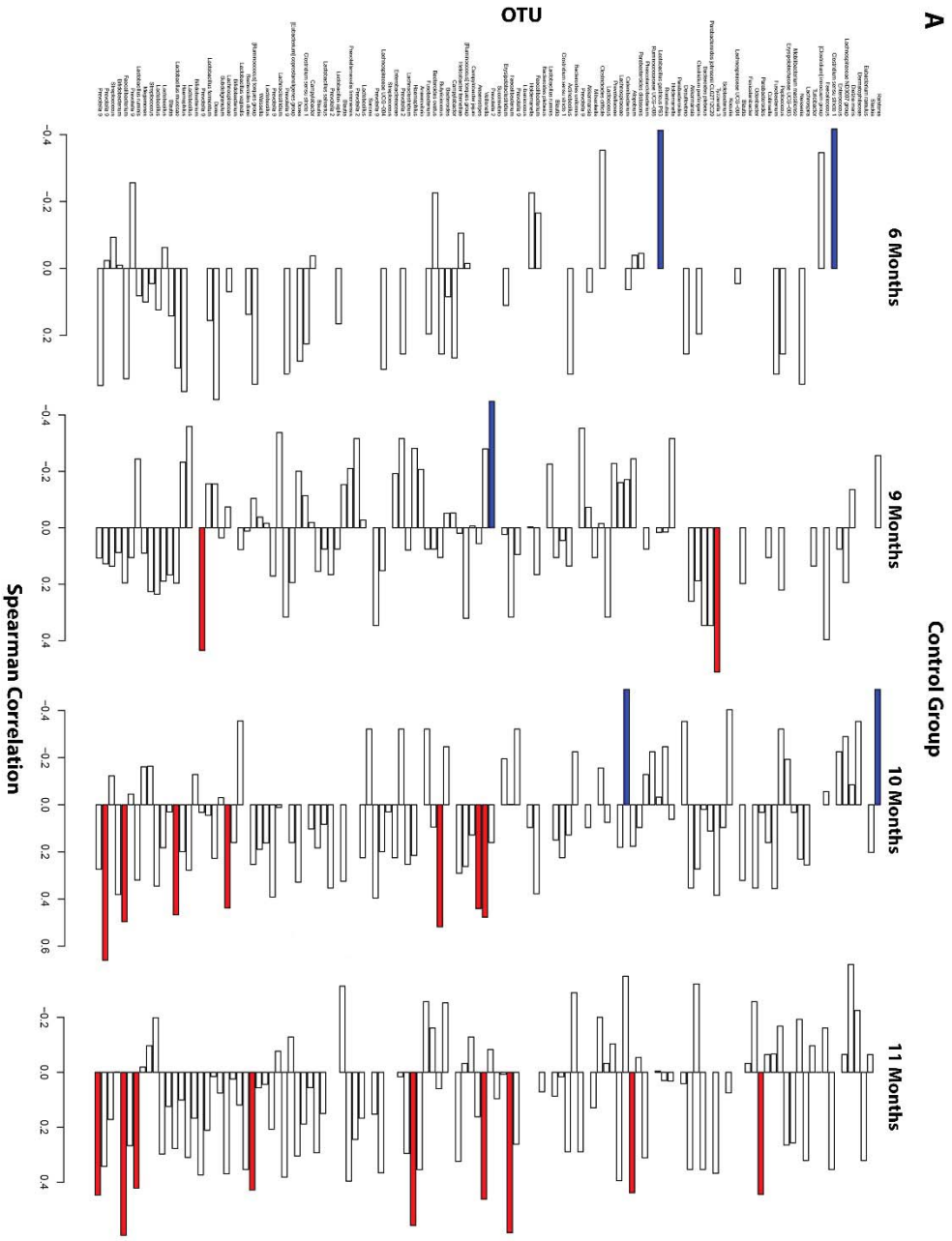

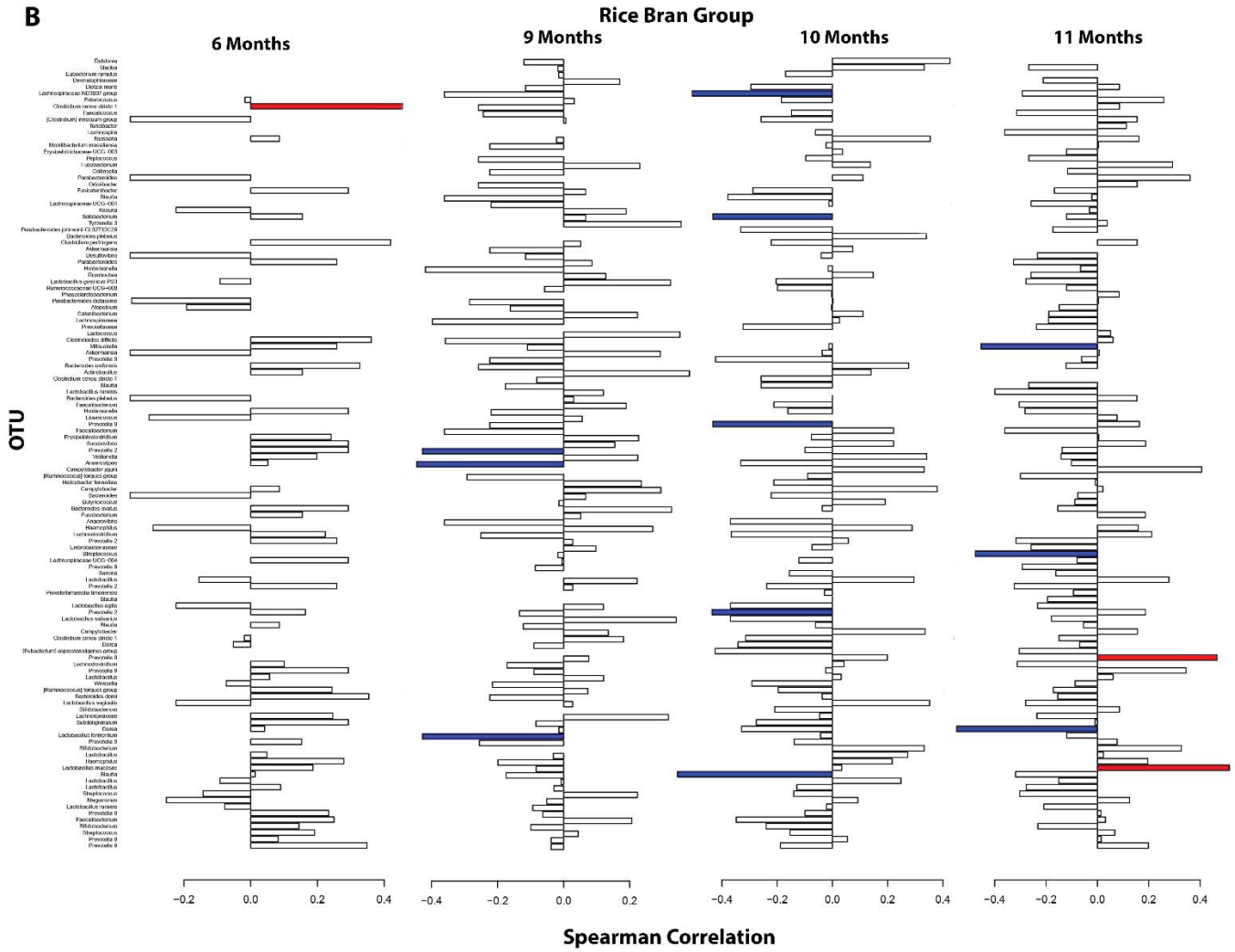
B
Rice Bran Group
6 Months
9 Months
10 Months
11 Months
OTU
−0.2
0.0
0.2
0.4
−0.4
−0.2
0.0
0.2
−0.4
−0.2
0.0
0.2
0.4
−0.4
−0.2
0.0
0.2
0.4
Spearman Correlation